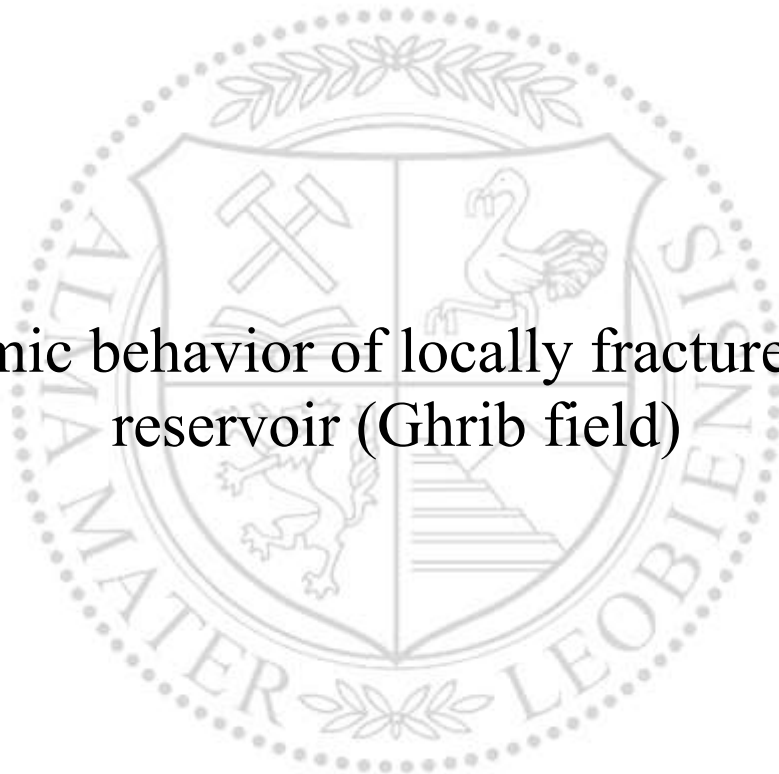




Chair of Reservoir Engineering

Master's Thesis

Dynamic behavior of locally fractured tight
reservoir (Ghrib field)



Hela Bouabdelli, BSc

February 2019

This thesis is dedicated to my family, who has been a constant source of support and encouragement during the challenges of study and life.

AFFIDAVIT

I declare on oath that I wrote this thesis independently, did not use other than the specified sources and aids, and did not otherwise use any unauthorized aids.

I declare that I have read, understood, and complied with the guidelines of the senate of the Montanuniversität Leoben for "Good Scientific Practice".

Furthermore, I declare that the electronic and printed version of the submitted thesis are identical, both, formally and with regard to content.

Date 08.03.2019



Signature Author
Hela, Bouabdelli
Matriculation Number: 01435477

Acknowledgements

The completion of this thesis could not have been possible without the participation and assistance of so many people whose names may not all be enumerated. Their contributions are sincerely appreciated and gratefully acknowledged.

However, i would like to express my deep appreciation and indebtedness particularly to:

My advisors Mr Foued Alzahou, Mr Mohamed Ali khiari and the entire reservoir engineering department within Mazarine Energy BV for their support, kind and understanding spirit during my work .I would like to express my very great appreciation to Prof. Holger Ott and Prof. Siroos Azizmohammadi for their valuable suggestions. Their willingness to give their time so generously has been very much appreciated.

To all relatives, friends and others who in one way or another shared their support, morally, either financially or physically, thank you. I will be forever grateful for your love.

Abstract

The definition of commercially and technically feasible development strategy is one of the major tasks of the reservoir engineering analysis. Despite the fact that this task appears very obvious, the result is not always considered as straight forward. Actually, a massive work has to be performed to find out the optimum plan that needs to be followed. For this purpose, the common practice is to build a dynamic reservoir model, which may handle large amount of reliable data used as a tool to predict the production forecast for different scenarios and, consequently, choose the best one that will honor the contractual, technical and commercial constraints.

This thesis covers, in the first place, the development plan of a field in south Tunisia by simulating a dynamic reservoir model using ECLIPSE 300 to provide different possible scenarios prior to production. However, the sensitivity study of this work has shown that the most productive case is the one of higher permeability. In the second place, it analyzes the behaviour of the reservoir during the production phase by conducting well testing analyses on Saphir (KAPPA) in order to identify the causes of production drop and hence find solutions to reinstate the relatively high production estimated during the exploration phase. In this case, the results showed that the increase of skin factor is the major reason behind the reduced permeability and thus lower productivity.

Zusammenfassung

Die Definition einer kommerziell und technisch realisierbaren Entwicklungsstrategie ist eine der Hauptaufgaben der Reservoir-Engineering-Analyse. Obwohl diese Aufgabe sehr offensichtlich erscheint, wird das Ergebnis nicht immer als direkt betrachtet. Tatsächlich muss viel Arbeit geleistet werden, um den optimalen Plan zu erstellen und diesen zu verwirklichen. Zu diesem Zweck ist es üblich, ein dynamisches Reservoir-Modell aufzubauen, das eine große Menge zuverlässiger Daten verarbeiten kann, mit denen die Produktionsprognose für verschiedene Szenarien vorhergesagt werden kann, und somit das beste auszuwählen, das den vertraglichen, technischen und kommerziellen Beschränkungen und Anforderungen entspricht.

Diese Dissertation behandelt in erster Linie den Entwicklungsplan eines Feldes in Südtunesien, indem ein dynamisches Reservoir-Modell mit ECLIPSE 300 simuliert wurde, um verschiedene mögliche Szenarien vor der Produktion bereitzustellen. Die Sensitivitätsstudie dieser Arbeit hat jedoch gezeigt, dass das produktivste Szenario in diesem Fall, das mit der höchsten Permeabilität ist. Zweitens analysiert es das Verhalten des Reservoirs während der Produktionsphase, indem es Saphir-Tests (KAPPA) durchführt, um die Ursachen für den Produktionsabfall zu ermitteln und somit Lösungen zu finden, die relativ hohe geschätzte Produktion während der Explorationsphase wiederherzustellen. In diesem Fall zeigten die Ergebnisse, dass der Anstieg des Skin Factor der Hauptgrund für die verringerte Permeabilität und damit die Produktivität ist.

Table of Contents

Declaration.....	iii
Erklärung	iii
Acknowledgements.....	iv
Abstract.....	v
Zusammenfassung	vi
Chapter 1.....	xiii
Introduction.....	15
Chapter 2.....	17
State of the Art.....	17
2.1 Basic well testing theory.....	17
2.2 Reservoir simulation	30
Chapter 3.....	35
Case study	35
3.1 Well testing interpretation.....	37
3.2 Ghrib field reservoir simulation model.....	47
Chapter 4.....	73
Results and Discussion	73
Chapter 5.....	75
Conclusion	75
Chapter 6.....	77
References.....	77
Appendix A.....	A-1
6.1 Ecrin Saphire tutorial.....	A-1
6.2 Completion profiles	A-7

List of Figures

Figure 2.1- Well testing Process: Interpretation of signal response into reservoir properties (slotte, 2017).....	17
Figure 2.2- Drawdown test: Pressure (red line) and flow rate (blue line) versus time (ferrero, 2001).....	21
Figure 2.3- Schematic transient drawdown analysis plot (Matthews, 1967).....	22
Figure 2.4- log-log pressure drawdown plot (Chaudhry, 2004).....	22
Figure 2.5- Pressure buildup test: Pressure (red line) and flow rate (blue line) versus time (ferrero, 2001).....	23
Figure 2.6- Horner plot (jelmert, 2000).....	23
Figure 2.7- Wellbore storage dominated flow period (G.Bourdarot, 2010).....	25
Figure 2.8- Positive skin (slotte, 2017).....	26
Figure 2.9- Negative skin (slotte, 2017).....	26
Figure 2.10- Constant boundary (left) and closed boundary (right) (Pesendorfer, 2015).....	28
Figure 2.11- Upscaling process (chen, 2007).....	31
Figure 3.1- Zaafrane permit location map.....	35
Figure 3.2- History plot of well Cat-1 (pressure [psi], liquid rate [STB/day], Time [hr]).....	38
Figure 3.3 - Log-Log plot of Bourdet derivative and extracted pressure buildup versus time of well Cat-1.....	38
Figure 3.4- Semi-log plot: P [psi] versus Superposition time.....	39
Figure 3.5- History plot of well Cat-1 (pressure [psi], liquid rate [STB/day], Time [hr]).....	40
Figure 3.6- Log-Log plot of Bourdet derivative and extracted pressure buildup versus time of well Cat-1.....	41
Figure 3.7- History plot of well DGH-1 (pressure [psi], liquid rate [STB/day], Time [hr]).....	43
Figure 3.8- Log-Log plot of Bourdet derivative and extracted pressure buildup versus time of well DGH-1.....	43
Figure 3.9- Semi-log plot: P [psi] versus Superposition time.....	44
Figure 3.10- History plot of well DGH-1 (pressure [psi], liquid rate [STB/day], Time [hr]).....	45
Figure 3.11- Log-Log plot of Bourdet derivative and extracted pressure buildup versus time of DGH-1.....	46
3.12- Structural map of the top Hamra.....	48
Figure 3.13- Fault network and grid.....	48
Figure 3.14- Cross section passing thorough CAT-1 and DGH-1 wells illustrating the 6 main reservoir zones used in the Petrel model.....	49
Figure 3.15- CAT-1 fluid properties.....	51
Figure 3.16- DGH-1 fluid properties.....	51
Figure 3.17- Relative permeabilities: oil-water, gas-oil.....	52
Figure 3.18- PVT properties regions and main fault.....	53
Figure 3.19- Permeability distribution in the X-direction for both wells.....	54
Figure 3.20- Permeability distribution in the Z-direction for both wells.....	54
Figure 3.21- Transmissibility for both wells.....	55
Figure 3.22- Porosity distribution for both wells.....	55
Figure 3.23- Water saturation distribution for CAT-1.....	56
Figure 3.24- Water saturation distribution for DGH-1.....	56
Figure 3.25- Net to gross ratio.....	57
Figure 3.26- History marching CAT-1.....	57
Figure 3.27- History matching DGH-1.....	58
Figure 3.28- Base case Forecast CAT-1.....	59
Figure 3.29- Base case forecast DGH-1.....	59
Figure 3.30- Oil production reference case for both wells.....	60
Figure 3.31- Gas production reference case for both wells.....	60
Figure 3.32- Oil production for skin=3 for both wells.....	61

Figure 3.33- Gas production for skin=3 for both wells.....	61
Figure 3.34- Oil production for skin=10 for both wells.....	62
Figure 3.35- Gas production for skin=10 for both wells.....	62
Figure 3.36- Oil production for skin=10 for both wells.....	63
Figure 3.37- Gas production for skin=10 for both wells.....	63
Figure 3.38- Permx_EL atchane distribution.....	64
Figure 3.39- Oil production for Permx_ELAtchane=0.5.....	64
Figure 3.40- Gas production rate for Permx=0.5.....	65
Figure 3.41- Oil production rate for Permx=0.5 and skin=0.....	65
Figure 3.42- Gas production rate for Permx=0.5 and skin=0.....	66
Figure 3.43- Permx El Hamra increased by a factor of four.....	66
Figure 3.44- Permx ElHamra oil production rate.....	67
Figure 3.45- Permx E lHamra gas production rate.....	67
Figure 3.46- Permx El Hamra_4_skin_0 oil production rate.....	68
Figure 3.47- Permx El Hamra_4_skin_0 gas production rate.....	68
Figure 3.48- Oil water contact at 3740.....	69
Figure 3.49- OWC_3740 oil production rate.....	69
Figure 3.50- OWC_3740 gas production rate.....	70
Figure 3.51- The injector CAT-1GI location.....	71
Figure 3.52- Oil production, Gas injection rate for both wells.....	71
Figure 3.53- GAs flow rate, Gas injection for both wells.....	72
Figure 6.1- Initialization dialog 1/2.....	A-1
Figure 6.2- Initialization dialog 2/2.....	A-2
Figure 6.3- Define data source.....	A-2
Figure 6.4- Define data format.....	A-3
Figure 6.5- Flow rates loading.....	A-3
Figure 6.6- History plot.....	A-4
Figure 6.7- Build-up selection.....	A-4
Figure 6.8- Bourdet and delta P plot.....	A-5
Figure 6.9- Model parameters.....	A-5
Figure 6.10- Matched model.....	A-6
6.11 History matching step.....	A-8
6.12- Define simulation case 1/4.....	A-9
6.13- Define simulation case 2/4.....	A-9
6.14- Define simulation case 3/4.....	A-10
6.15- Define simulation case 4/4.....	A-10
6.16- Development strategy.....	A-11
6.17- Define simulation case (forecast) 1/4.....	A-12
6.18- Define simulation case (forecast) 2/4.....	A-12
6.19- DEfine simulation case (forecast) 3/4.....	A-13
6.20- Define simulation case (forecast) 4/4.....	A-13

List of Tables

Table 2.1- Time of measurement versus type of measurement	18
Table 3.1- Reservoir properties of well Cat-1.....	37
Table 3.2- Model of well Cat-1 properties.....	39
Table 3.3- Well test Cat-1-2015 output	40
Table 3.4- Model of well Cat-1 properties.....	41
Table 3.5- well test Cat-1 output.....	42
Table 3.6- Reservoir properties of well DGH-1	42
Table 3.7- Model of DGH-1 properties	44
Table 3.8- Well test DGH-1 output.....	44
Table 3.9- Model properties of well DGH-1.....	46
Table 3.10- Well test DGH-1 output.....	46
Table 3.11- Cumulative production of oil and gas for all cases (both wells)	72

Nomenclature

B	Formation volume factor	rb/stb]
c	Compressibility	[Psi ⁻¹]
c_t	Total compressibility	[Psi ⁻¹]
c_ϕ	Formation compressibility	[Psi ⁻¹]
C	Wellbore storage	[bbl/psi]
h	Thickness	[ft]
m	Mass	[kg]
p_i	Initial reservoir pressure	[psi]
p_{wf}	Bottom-hole flowing pressure	[psi]
p_{ws}	Pressure during shut-in	[psi]
Δp	Pressure drop	[psi]
q	Flow rate	[bbl/d]
R_s	Dissolved gas oil ratio	[scf/stb]
r	Radius	[ft]
r_s	Skin radius	[ft]
r_w	Wellbore radius	[ft]
$r_{w,eff}$	Wellbore effective radius	[ft]
S	Skin	
T	Time	[hr]
μ	Viscosity	[cp]
V	Volume	[bbl]
K	Permeability	[md]
ρ	Density	[kg/m ³]
ϕ	Porosity	[%]

Abbreviations

BHP	Bottom Hole Pressure
DST	Drill Stem Test
GOR	Gas Oil Ratio
IARF	Infinite Acting Radial Flow
MTP	Middle time Period
THP	Tubing Head Pressure
OIIP	Oil Originally In Place
OWC	Oil Water Contact
PLT	Production Logging Tool
PTT	Pressure Transient Test
PVT	Pressure Volume Temperature
WAG	Water Alternating Gas
WBS	Wellbore Storage

Chapter 1

Introduction

The term "Reservoir management" refers to a consisting operational strategies or plans based on analysis of production, reservoir and geological data, designed to optimize the exploitation of a reservoir, in order to achieve a maximum efficient and economic recovery. The secret of a successful field development is collecting the maximum possible data. However, one of the methods where engineers place a high degree of confidence to characterize and understand reservoir properties is well testing. Actually, interpreting the transient pressure response due to a change in flow rate is a powerful technique to have a good estimation of properties such as permeability, skin, boundaries and identification of faults and fractures as well. Any newly drilled well has to be tested in order to forecast its future performance and potential. However, it is different from a field to another; some fields need to be intensively monitored because of their very complex geology or their ongoing enhanced recovery operation. Moreover, considered as 'reality checks', well tests are able to provide vital information about the reservoir under dynamic condition, if they were designed and analyzed carefully. Chapter one in this thesis, will explain what is the purpose of well testing, explain its different methods and show how engineers may interpret them to get a better understanding of the reservoir.

The major concern in reservoir management is uncertainty that is why engineer and geoscientists use numerical models of the reservoir to simulate and acquire, as much as possible, an accurate description of a subsurface hydrocarbon reservoir.

Since 1950, reservoir simulation has been invented, which is an art of combining computer programming, physics, reservoir engineering and mathematics. Thanks to it, engineers have become able to make a more detailed study of the reservoir by dividing it into a various blocks and applying fundamental flow in porous media equation for each in order to maximize the production under different operating strategies. The case study elaborated in this thesis, shows

how vital is the simulation stage during the life cycle of a field and explains how to choose the optimum way of development based on reservoir simulation results.

Chapter 2

State of the Art

2.1 Basic well testing theory

Well testing, known also as pressure transient test, is a fundamental operation wherein pressures and flow rates are manipulated and monitored in one or many wells so that an information about sub surface reservoir is obtained. That is why during well tests, in spite of the name, the reservoir is actually tested not the well production. However, well testing is not limited to petroleum engineering disciplines only but it includes also pollution control, geology, waste disposal and ground water hydrology (slotte, 2017) . Its process, shown in the figure 2-1 below, consists briefly in sending a signal from the well into the reservoir through changing well pressure or production rate and once we receive the response engineers is capable then to estimate reservoir properties.

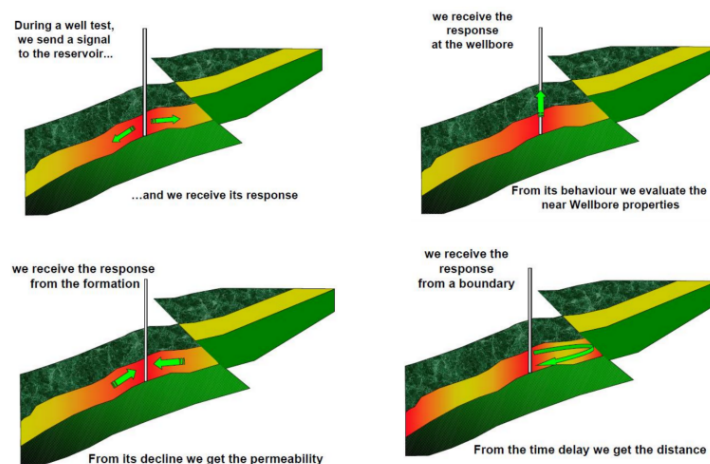


Figure 2.1- Well testing Process: Interpretation of signal response into reservoir properties (slotte, 2017).

The properties obtained may be classified under different classes (shown in table 2.1) which are organized according to time due to the transient nature of pressure front traveling throughout the reservoir. (slotte, 2017)

Table 2.1- Time of measurement versus type of measurement

Early time	Middle time	Late time
Near wellbore	Reservoir	Reservoir boundaries
Skin	Permeability	Reservoir volumes
Wellbore storage	Heterogeneity	Faults
Fractures	Dual porosity	Boundaries
	Dual permeability	

The main purpose of well testing is to provide sufficient data in order to model and describe the reservoir so that an estimation of the reserves, a forecast of the future performance and optimization of the production are possible. Besides, well testing gives also information about the near wellbore reservoir volume which will be, later, used to know whether a well stimulation is required or not. One of the most important advantages of these well tests is its capability to provide a large area of investigation, which can reach 50-500 meters unlike cores and logs that provide respectively an estimated investigation of 10 cm to 50 cm (kuiper, 2009).

2.1.1 Diffusivity equation

The diffusivity equation is considered as a fundamental equation in interpreting well tests analysis. It, actually, correlates the flow rate to the pressure variations in spatial and temporal domain within the field. This can be established by means of parameters of the porous media, which is crossed, by the fluid and the fluid's characteristics. Several assumptions and approximations are considered when deriving the equation such as the fact that the flow is isothermal and single phase, fluid viscosity and compressibility are pressure independent, permeability is isotropic, the well is completed across the full formation thickness and the fluid compressibility is low (slotte, 2017).

The derivation of the diffusivity equation starts based on the continuity equation that consists in mass conservation in a volume element: " Change in mass= mass **in** - mass **out** ".

$$-\nabla \cdot (\rho q) = \frac{\partial}{\partial t} (\phi \rho) \quad (2.1)$$

Where φ is the porosity, ρ is the fluid density and q is the volumetric fluid flux. However, the pore pressure is related to the volumetric flux via Darcy's law.

$$q = \frac{-k}{\mu} \nabla p \quad (2.2)$$

We assume a pressure independent viscosity μ and a constant permeability k , and then if we insert equation (2.2) into equation (2.1) we will get:

$$\frac{k}{\mu} \nabla \cdot (\rho \nabla p) = \frac{\partial}{\partial t} (\varphi \rho) \quad (2.3)$$

We can expand the derivatives of the product on both sides and then we get:

$$\frac{k}{\mu} (\nabla \rho \cdot \nabla p + \rho \nabla^2 p) = \rho \frac{\partial}{\partial t} \varphi + \varphi \frac{\partial}{\partial t} \rho \quad (2.4)$$

The left side of the previous equation (2.4) is firstly investigated; compressibility c measures the relative volume change as a response to a pressure change:

$$c = -\frac{1}{V} \times \frac{\partial V}{\partial p} \quad (2.5)$$

The compressibility can be used to get derivatives of pressure by converting derivatives of density using the density formula of a liquid which is $\rho = m/V_1$ that is the fraction of mass divided by the volume. Therefore, we can derive the liquid compressibility as follows:

$$c_l = -\frac{1}{V_1} \frac{\partial V_1}{\partial p} = -\frac{\rho}{m} \frac{\partial m / \rho}{\partial \rho} \frac{\partial \rho}{\partial p} = -\rho \frac{-1}{\rho^2} \frac{\partial \rho}{\partial p} = \frac{1}{\rho} \frac{\partial \rho}{\partial p} \quad (2.6)$$

Thus, we see that, on the left hand side, the first term is:

$$\nabla \rho \cdot \nabla p = \frac{\partial \rho}{\partial p} \nabla p \cdot \nabla p = \rho c_l |\nabla p|^2 \quad (2.7)$$

This term can be ignored in low compressibility limit since it is proportional to the compressibility, so the left part of the equation (2.4) is simply:

$$\rho \frac{k}{\mu} \nabla^2 p \quad (2.8)$$

By applying the chain rule, we can express the right part of equation (2.4) in terms of time derivatives of pressure:

$$\rho \frac{\partial}{\partial t} \varphi + \varphi \frac{\partial}{\partial t} \rho = \rho \frac{\partial \varphi}{\partial p} \frac{\partial}{\partial t} p + \varphi \frac{\partial \rho}{\partial p} \frac{\partial}{\partial t} p = \rho \varphi \left(\frac{1}{\varphi} \frac{\partial \varphi}{\partial p} + \frac{1}{\rho} \frac{\partial \rho}{\partial p} \right) \frac{\partial}{\partial t} p \quad (2.9)$$

In addition, total compressibility is defined as:

$$c_t = c_l + c_\varphi \quad (2.10)$$

With formation compressibility equals to

$$c_\varphi = \frac{1}{\varphi} \frac{\partial \varphi}{\partial p} \quad (2.11)$$

Then equation (2.9) is simply

$$\rho \frac{\partial}{\partial t} \varphi + \varphi \frac{\partial}{\partial t} \rho = \rho \varphi c_t \frac{\partial}{\partial t} p \quad (2.12)$$

Equating left hand side equation (2.8) and right hand side equation (2.12) and dividing by $\rho \varphi c$ we get the diffusivity equation, which is:

$$\frac{k}{\mu \varphi c_t} \nabla^2 p = \frac{\partial}{\partial t} p \quad (2.13)$$

2.1.2 Types of well test

Several types of test are presented and each one is dedicated to a specific stage. During appraisal stage and exploration, Wire line formation test and Drillstem tests (DSTs) are usually run. While during primary, secondary and enhanced recovery stages, the conventional transient well tests are used such as buildup test and drawdown test. Falloff, injectivity and interference tests are used only in secondary and enhanced recovery. Moreover, there are tests that are executed throughout the life of the reservoir like for instance vertical and multilayer permeability tests. However, the focus in this thesis will be on buildup test since the well testing achieved in next chapter will be executed during production phase for a well that have been ideally producing at constant rate (Asser, 2015).

2.1.2.1 Drawdown test

The drawdown test is the measurement of the surface or downhole pressure and flow rate as a function of time in the wellbore. In fact, it consists of analysing pressure data taken after a well is switched to production either after very long shut-in (till pressure reaches static level) period or initially like shown in figure 2-2 (M.onur, 2010) .

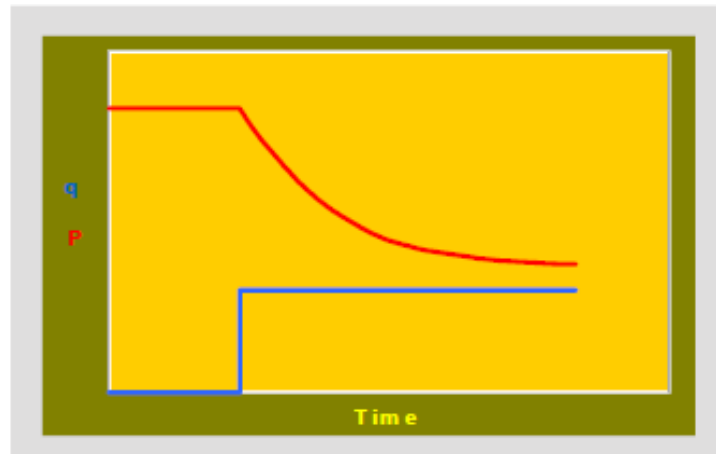


Figure 2.2- Drawdown test: Pressure (red line) and flow rate (blue line) versus time (ferrero, 2001)

Since the test is executed after long shut-in or for new wells there is no production lost, so economically speaking this test might be the most suitable. However, the main disadvantages of this method are maintaining constant production rate and introducing scatter in measured flowing bottom hole pressure.

In an infinite reservoir while flow rate is constant, the simplification of pressure behavior can be given by:

$$p_{wf} = p_i - 162.6 \frac{q\mu B}{kh} \left[\log \frac{kt}{\Phi\mu c_r^2} - 3.23 + 0.87s \right] \quad (2.14)$$

Figure 2-3 shows a schematic transient drawdown analysis plot, which is log time t versus semi log plot bottomhole pressure p_{wf} that has a linear shape with slope m . In fact, the product kh can be estimated from the equation below:

$$kh = 162.6 \frac{q\mu B}{m} \quad (2.15)$$

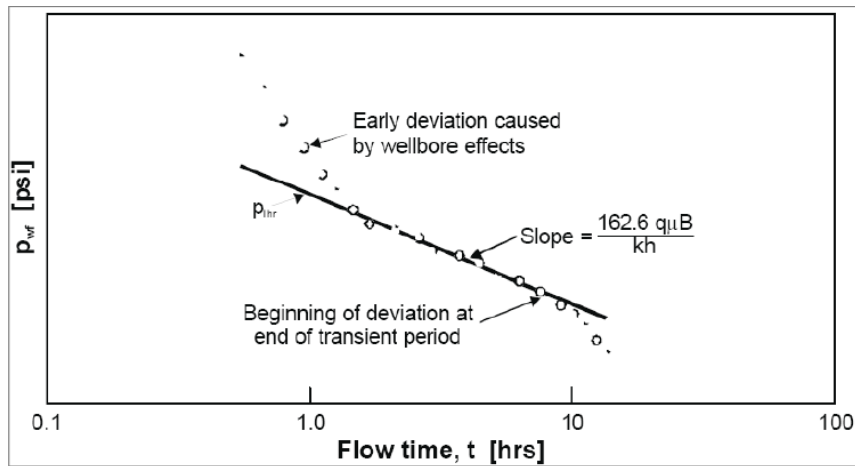


Figure 2.3- Schematic transient drawdown analysis plot (Matthews, 1967)

Once the slope is calculated, skin factor can be derived from the intercept at time equals to one (log t equals to zero) by rearranging equation 14:

$$s = 1.51 \left(\frac{p_i - p_{1hr}}{m} - \log \frac{k}{\phi \mu c r^2} + 3.23 \right) \quad (2.16)$$

The nonlinear part of the plot shown in figure 2-3 can be analyzed using a plot of $\log(p_i - p_{wf})$ versus $\log t$ to calculate wellbore storage coefficient C (figure 2-4) given by:

$$C = \frac{qB \Delta t}{24 \Delta p} \quad (2.17)$$

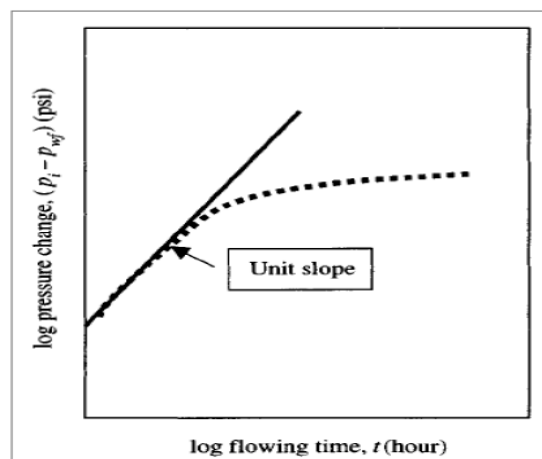


Figure 2.4- log-log pressure drawdown plot (Chaudhry, 2004)

2.1.2.2 Buildup test

During buildup test, the well is first produced at constant pressure and once it is stabilized the well is shut in as shown in figure 2-5 below. In fact, this test is the most preferable since it is

much more easier to get high quality data from it than from drawdown test because , obviously, maintaining zero rate is trivial when compared to maintaining a fixed flow rate (drawdown test). Besides, wellbore storage effect is reduced by using a downhole valve. On the other hand, from an economic perspective, this test has also a disadvantage since the well will not generate income when it is closed, that is why the shut in period has to be as short as possible.

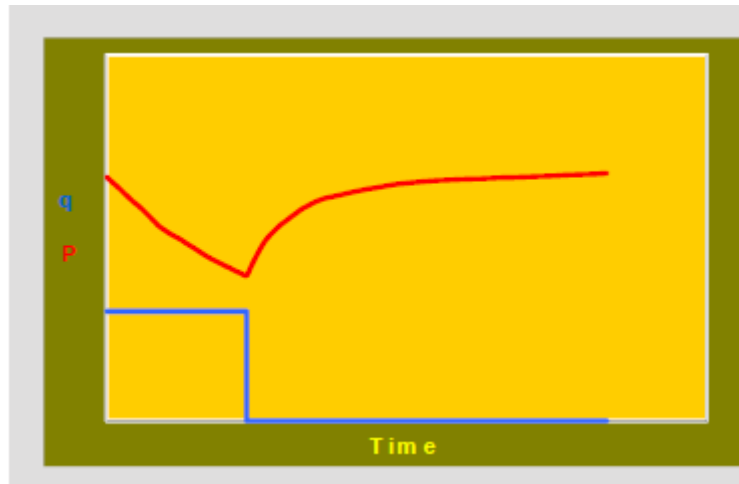


Figure 2.5- Pressure buildup test: Pressure (red line) and flow rate (blue line) versus time (ferrero, 2001)

Horner method is the common method to analyze pressure response within a buildup test, which introduces Horner time that is the superposition in time for radial, single, constant flow rate followed by a shut in (build up). This method shows a linear relationship between shut in pressure p_{ws} and Horner time $\frac{t_p + \Delta t}{\Delta t}$ presented in figure 2-6 during middle transient region.

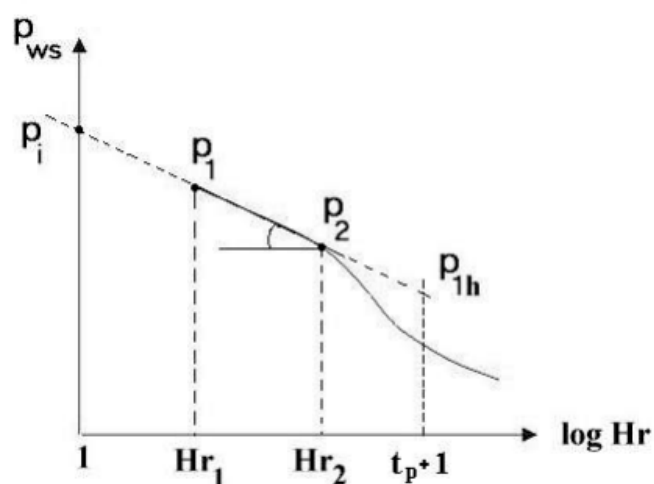


Figure 2.6- Horner plot (jelmert, 2000)

However, the slope of this straight-line m is used to estimate permeability based on the formula below:

$$kh = 162.6 \frac{q\mu B}{m} \quad (2.18)$$

This is itself derived from equation that describes the pressure response in a build up period assuming infinite acting reservoir, slightly compressible, homogenous and single-phase fluid flow.

$$p_{ws} = p_i - 162.6 \frac{q\mu B}{kh} \log \frac{t_p + \Delta t}{\Delta t} \quad (2.19)$$

The non-linear part of the plot represents the wellbore storage and skin effect that explains the early time deviation, while the late time region shows the presence of boundaries or the interference of wells nearby wells. The duration of after flow effect in a build up test depends mostly on the configuration and size of the wellbore .The simplified equation for skin estimation is as follow:

$$s = 1.51 \left[\frac{p_{1hr} - p_{wf(\Delta t=0)}}{m} - \log \left(\frac{k}{\phi\mu cr_w^2} \right) + 3.23 \right] \quad (2.20)$$

2.1.3 Relevant reservoir properties

Typical pressure transient test (PTT) is normally divided into three periods; the first period represents early time wherein wellbore storage and skin factor can be estimated. The second period is middle time (MTP) during which the direct effect of reservoir heterogeneities and well geometries vanished, wellbore storage become negligible and the flow may reach a state defined as infinite acting radial flow (IARF). Actually, IARF is considered as the main flow regime of interest in pressure transient test analysis. Its response on selected semi log plot will show linearity from which the interpreter will be able to estimate flow capacity (kh). The last period is known as late time where boundaries can be defined.

2.1.3.1 Wellbore storage

When the well is shut in to make transient tests, the production at the surface is stopped but the formation keeps producing for a while until the completely wellbore is full of fluid, which will be then stored in it. This phenomenon is called wellbore storage or also called after flow, wellbore loading or unloading, after injection and after production. It is necessary that wellbore storage is taken into consideration while analysing transient test otherwise the pressure will be influenced and a wrong estimation of reservoir properties will be done. The wellbore storage dominated flow period, shown in figure 2-7 is explained by the compressibility of the fluid within the wellbore. Actually, the constant or variable flow rate applied at the surface will not be able to propagate to the sand face instantaneously because of the compressibility of the fluid.

Consequently, the sand face rate starts to increase gradually or decreases in case of buildup test until it becomes equal to a constant rate or zero (M.onur, 2010).

A coefficient called C is used to quantify wellbore storage effect. C is defined as the ratio of the volume of fluid produced from the well alone, V, to unit pressure drop:

$$c = \frac{V}{\Delta p} \text{ m}^3 \text{ Pa}^{-1} \tag{2.21}$$

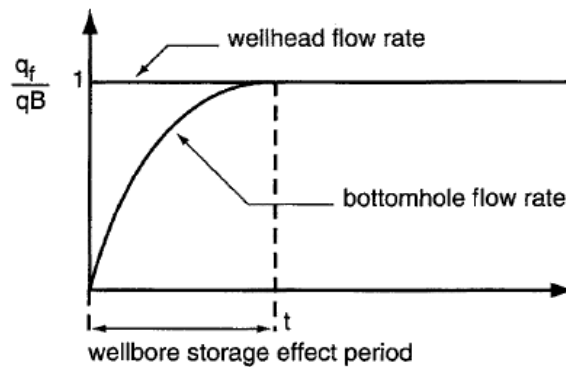


Figure 2.7- Wellbore storage dominated flow period (G.Bourdarot, 2010)

2.1.3.2 Skin Factor

Well completion or drilling activities often lead to a small zone of altered permeability near the well, which is called 'skin'. Actually, this zone has a significant impact on the performance of the well as it defines the well conditions and the degree of connectivity between the well and the reservoir. The higher the skin value the higher the damage. For a positive skin, a flow restriction exists between the reservoir and the well, with an increase in pressure drop this could be due to some plugged perforations or insufficient numbers, partial penetration or mud invasion. Figure 2-8 shows Δp_s which is the difference between the actual well flowing pressure and the one that would be measured in case the well was undamaged. To reduce this skin effect, different treatments can be used such as making new perforations, hydraulic fracturing and acidification (skin factor).

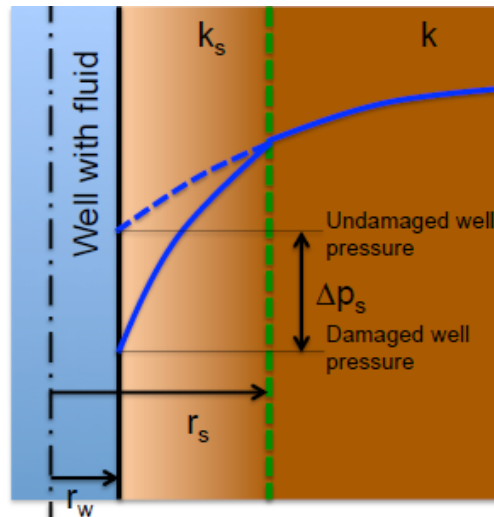


Figure 2.8- Positive skin (slotte, 2017)

In case of negative skin, the interface between the wellbore and the reservoir is increased and thus a reduction in pressure drop occurred shown in figure 2-9. Small negative skin values are explained by the presence of fissured or natural fracture or acidification while large negative skin values are explained by hydraulic fracture. Generally, a skin value equals to -3.5 to -4 is considered as excellent (ferrero, 2001)

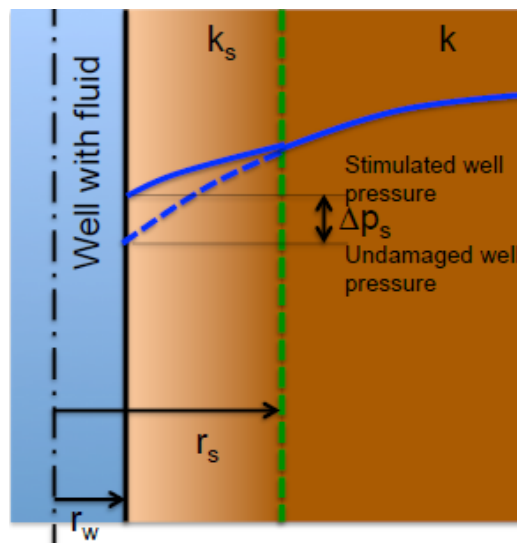


Figure 2.9- Negative skin (slotte, 2017)

The magnitude of the skin effect can be quantified by the dimensionless so-called skin factor, which can be expressed as follows:

$$\frac{2\pi kh}{qB\mu} \nabla p_s \quad (2.22)$$

Assuming that skin effect is caused due to a reduced permeability K_s and damage zone of radius r_s the skin effect can be expressed also by:

$$s = \left(\frac{K}{K_s} - 1 \right) \ln \left(\frac{r_s}{r_w} \right) \quad (2.23)$$

Alternatively, in terms of effective wellbore radius:

$$r_{w,eff} = r_w e^{-s} \quad (2.24)$$

2.1.3.3 Permeability

Permeability describes the property of rock that indicates the ability of one fluid to flow through it. Actually, it is considered as the most important parameter that may be retrieved during well testing as it plays a major role in controlling reservoir performance. However, there are several methods to measure permeability, as for example logs, cores and wireline formation testing, but the main source for effective permeability is production tests and well tests. The value of permeability is essential to estimate well performance, different well stimulation processes and recovery potential (secondary and tertiary).

2.1.3.4 Boundaries

The first thing to do when discovering a reservoir is to estimate the amount of oil recoverable from it. Therefore, the size of the reservoir is very important, that is why engineers aim to locate and define the type of boundaries. In fact, the effects of boundaries appear during late time period within a PTT that is why the more long the test is, the more the engineers are able to understand the nature of the boundaries. In other words, this encounter is inevitable during long-term production data and deliberate or accidental in limited testing (Oliver houzé, 2008). There are two common types of boundaries shown in figure 2-10 ; the first one is closed or no-flow boundaries which means that there is no flow is possible through it like for example faults, intersection of wells and juxtaposition of low permeability rocks along the fault. This behavior can be described by a state known as pseudo-steady state during late time region in PTT. The second type is open boundaries, which means that a constant pressure exists which is supported either by a fluid injection or an aquifer (Pesendorfer, 2015).

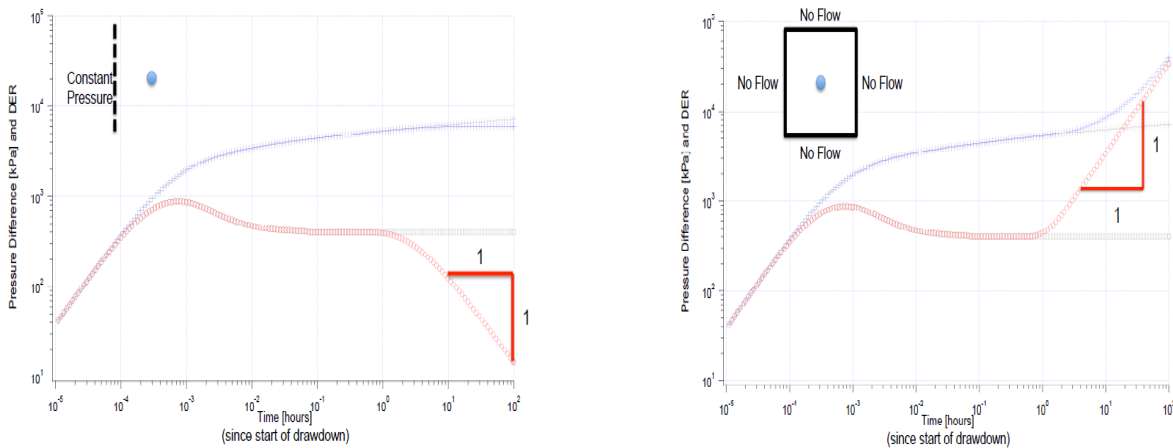


Figure 2.10- Constant boundary (left) and closed boundary (right) (Pesendorfer, 2015)

2.1.4 Typical flow regimes

Flow regime is considered as a period during which pressure shows specific behavior with respect to the elapsed time. This pressure change behavior has three different known types; the first one is steady state during which the pressure does not change with time so it is constant at every location of the reservoir because of strong water drive or a powerful gas cap (rossito, 2003) . Mathematically, it can be expressed as follows:

$$\frac{\partial p}{\partial t} = 0 \tag{2.25}$$

The second regime is **pseudo steady state** where the pressure change is declining linearly as a function of time at different locations of the reservoir and thus considered as constant. This type of flow is observed during pure wellbore storage or in closed reservoir where all boundaries are reached:

$$\frac{\partial p}{\partial t} = cst \tag{2.26}$$

The third flow regime is **transient state** where pressure changes are governed by the reservoir characteristics and the well geometry so the rate of change is not constant nor zero at any location of the reservoir. it can be expressed as follows :

$$\frac{\partial p}{\partial t} = f(x, y, z, t) \tag{2.27}$$

A complete reservoir model is determined usually by a sequence of flow regimes, each one shows a characteristic pressure behavior. Besides, the time limits and the chronology of this several regimes help later to realize the interpretation model which is basically made of three

legs; **early time** which is characterized by well response, **middle time** characterized by reservoir response and **late time** characterized by boundaries response (Rossito, 2003).

2.1.5 Production logging tool PLT

Production logging provides vital information about well performance by running different well logging techniques on completed, injection or production wells. In essence, it is the measurements of flow dynamic behavior and fluid parameters on a zone by zone basis to collect the most detailed knowledge possible within and near the wellbore so that engineers could identify the major problems and take remedial action prior to production interruption. In addition, PLT is also considered as the key information to evaluate completion efficiency and clean up. Production logging (PL) is very important since it surveys the integrity of well completion. For example, it shows if there is a flow behind the casing or not. Besides, it helps in evaluating the drastic and sudden reduction of production rate or an increase in GOR or water cut. When PL is executed periodically, it can determine also problems related whether to water/gas coning or fingering. One other efficient application of PL is achieving a better understanding of the injection process within injection wells to prevent flooding of undesired layers that may lead to serious problem like casing annulus cross flow.

Typical production logging tool is equipped with different sensors, each one of them contribute to a specific measurements:

- Pressure and temperature sensor: which is used for PVT, ideally helps to determine pressure drawdown and considered as a good flow indicator.
- Gamma Ray (GR): it is essential to detect radioactive scale and for depth correlation within the well.
- Gradio manometer: used when the well deviation is less than 60° to measure accurately water holdup and fluid density.
- Caliper: important to centralize the tool and to correct inner diameter (ID).
- Spinner: it is considered as the most important part of a production logging tool string, which is a small propeller that will rotate because of the relative movement between the fluid and the PLT. This means, it is directly proportional to fluid velocity.

2.1.6 Software description: Saphir NL

Saphir is a module of pressure transient included in Ecrin, which is Kappa's integrated software platform (Kappaeng). Actually, it offers a completed built-in analytical catalog that combines reservoir, well, and boundary models. It also, allows user to load unlimited number of rates, pressure and other different data in almost any format even Excel or ASCII (Kappaeng). The

diagnostic of the loaded data leads to a choice of model that will be later matched by changing its parameters. However, once the best possible match is achieved and based on its interactive analysis tools, users may interpret the results obtained from well testing and thus getting accurate information about reservoir properties and geometries within the radius of investigation from the Bourdet derivative on log log plot. A simple example of well testing analysis on Ecrin Saphir is explained gradually in appendix-A (6.1).

2.2 Reservoir simulation

Simulation is considered as a fundamental part of a certain reservoir study. Literally, the term "reservoir simulation" means the fact of building a model that represents the actual reservoir. In other words, it is like assuming the appearance without reality. However, this model will not make the future performance prediction easier but also will help to save money and time since the model can be produced and run several times over a short period. It will, also help in finding new ways to maximize the recovery of some of the hydrocarbon under certain operating conditions.

Reservoir simulation consists of four essential linked stages; the first one is a physical model that involves all the necessary processes to describe the essential characteristics of the elemental phenomena. The second stage consists in analyzing the existence, uniqueness, stability and regularity by defining a coupled system of nonlinear partial differential that are time-dependent. The third stage is known as numerical model where the basic features of the mathematical and physical models are analyzed. The last stage is a computer algorithms during which, the systems of nonlinear and linear algebraic equations gotten from the numerical discretization are solved efficiently. Sometimes it requires a lot of iteration to adjust the physical, mathematical and numerical models and computer algorithms in order to achieve a successful reservoir performance prediction (chen, 2007).

In petroleum engineering, the most known reservoir simulator types are the black oil simulator and the compositional simulator. However, the choice of the appropriate one depends on the reservoir itself and the available data. The main difference between compositional and black oil simulation is the data used within fluid properties section. In fact, within black oil simulation, the PVT table that involves solution gas ratio and formation volume factor determines the fluid property section. While for compositional simulator, in addition to what is included within black oil model, the PVT table involves also gas and oil mole fraction as single values versus pressure derived from the equation of state (EOS). However, this Equation of state gives a relationship between pressure, temperature and volume that describes in a very accurate way the volumetric and phase behavior of mixtures and pure compounds. Besides,

EOS provides essential information concerning the composition of equilibrium oil and gas, which is critical in the planning of some recovery methods that aim to enhance the recovery of more valuable compounds.

2.2.1 Upscaling

Upscaling is the process of averaging from one scale to another larger one. In other words, it is the approximation of high-resolution geologic description to a lower resolution flow simulation. In fact, it is considered as one of the most challenging step in reservoir heterogeneity description and modeling. It may be, generally, divided into two stages. The first one is up scaling from laboratory measurement (a length of a few centimeters) to geophysical cells of several meters. While, the second stage is upscaling from geological fine grid to coarser fluid flow simulation grid (figure 2.12) and this refers to upscaling during simulation process. Normally, the geological models may include 10^7 - 10^8 cells for a typical reservoir whereas dynamic models may have 10^5 - 10^6 grid blocks. A grid describes a spatial domain by using grid cells that contain a grid point and several cell facies.

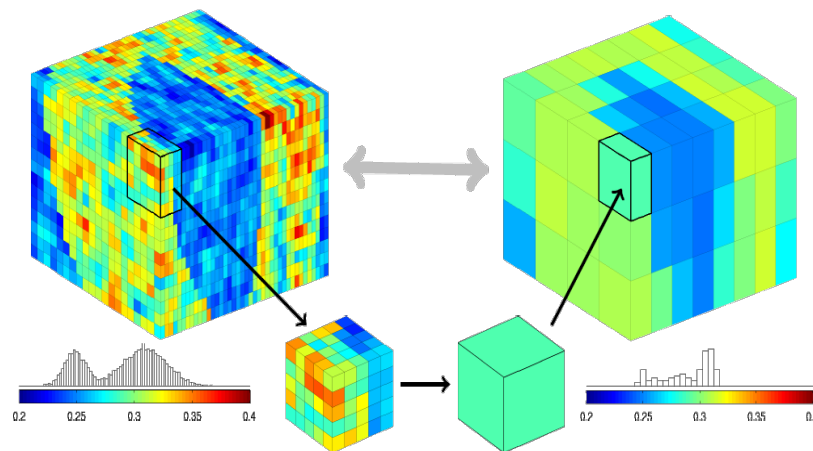


Figure 2.11- Upscaling process (chen, 2007)

It should be mentioned that upscaling is the major source of uncertainty of simulation output. So, we need to minimize as much as possible the amount of upscaling that needs to be achieved because somehow, it will tend to homogenize the reservoir since small scale heterogeneities will be represented as effective or completely disappear. Upscaling methods may be classified into two common types; single phase upscaling (flow in one direction) that includes analytical methods such as arithmetic , geometric ,harmonic average, power average, directional

dependent average besides numerical methods which operate based on Darcy law and mass conservation of each gridblock such as diagonal tensor and full tensor .

2.2.2 History matching

As known, the process of upscaling a static geological model carry a big range of uncertainty since all the field data are considered as noisy and sparse. That is why, the prediction of the production profile cannot be exactly done. Actually, a History matching (HM) consists in incorporating a dynamic model, which is a direct measure of reservoir behaviour toward the recovery process applied, in the creation of reservoir models and thus helps to quantify uncertainties and errors in prediction.

The main purpose of history matching is providing an output model close, as much as possible, to the historical production and this could be done by adjusting the reservoir simulation model parameters.

Moreover, the history of data used during matching may be of various types such as; observed WOR and GOR, observed average pressures or observed flowing well pressure. Whereas, the less frequent matching data are pressure during drawdown or build up and breakthrough time. History matching is considered as a time consuming process and normally occupies a large portion of the total cost of a study. It is usually done through two different ways; manually by adjusting data by a trial and error procedure or automatically by using an inverse simulation wherein equation are solved based on the values of selected reservoir parameters in a way that the difference between the computed and observed results are minimized. The basic rule in manual history matching is to change the parameters that have the largest uncertainty and thus the largest impact on the final solution. However, the sensitivity of the result over some parameters is sometimes achieved during the history matching process itself. Each case has its own way of procedure for example the match of a pressure drawdown is mostly affected by the skin and by the horizontal permeability. Besides, the average pressure is affected by fluid volumes in place, size of the aquifer and the degree of the communication between the reservoir and the aquifer. Fluid contacts depth and the thickness of the transition zone have a large impact on WOR and GOR match. Finally yet importantly, matching the breakthrough time is usually affected by truncation errors (numerical dispersion) that are why it is considered as one of the most difficult tasks as they require finer grid.

The prediction stage consists in predicting the future performance of the reservoir under different recovery process and it starts after matching the historical reservoir performance successfully. In other words, the engineers perform a study of several development scenarios and choose the optimum operating strategy that will likely provide the most desirable performance. This will allow also the engineers to test different ideas and show their potential

benefits on a field. However, prediction process may be done by using black oil, compositional or thermal simulators. This stage requires a selection of a prediction cases, good use of history matching, preparation of input data, review and evaluation of the predicted results (chen, 2007).

The prediction process starts with preparing a base case prediction. This case assumes a forecast with the already existing operating conditions. For instance, for a new developed wells which are undergoing primary depletion the base case needs to be primary depletion case by whereas when the field was waterflooded the base case should be a waterflood and alternatives may be water alternating gas WAG or gas injection.

The base case prediction provides also a basis to compare changes resulted from changing the strategies or changing in the existing operating conditions. Besides, engineers should perform a sensitivity analysis as well as well to get an insight into uncertainty associated with the model predictions.

2.2.3 Eclipse simulator

Eclipse is an oil and gas reservoir simulator, which is owned, maintained and developed by GeoQuest, which is a division of Schlumberger. Actually, there are two versions of Eclipse; one is Eclipse 100 that is used in black oil simulation and Eclipse 300, which is used for thermal and compositional simulation. By dint of its advanced different tools, Eclipse is able to provide extensive well control and support field operations planning in an efficient way. Eclipse is considered as a batch program that contains a data file with a complete description of the model. The model consists itself of a full reservoir description such as rock and fluid property description, surface facilities, wells flow rates and initial conditions. The input file consists in a normal text containing different collections of comments and keywords that have a specific syntax. This data file is split into sections by a few specific keywords as well. The process of reading of those sections is done one by one, of course, after checking the consistency of each. The first task achieved by Eclipse is to allocate memory for the completely input data. Once the simulation grid is processed, Eclipse calculates for each cell the pore volume, transmissibility in three dimensions and cell centre depth then creates connections to other cells where the fluid could flow. Next, the fluid and rock properties are specified. On the other hand, the term rock properties determine a set of input tables that describes relative permeability and capillary pressures versus saturations. This will, effectively, determine critical, maximal and irreducible saturation and thus defining transition zone and condition of flow. Then, after defining the OWC or/and GOC depths the initial conditions are defined as well. Finally, Eclipse uses all the information mentioned above besides information from previous stages to calculate hydrostatic pressure gradients in each zone of the reservoir and thus allocate the initial saturation of each phase in every grid cell before production and injection (Kirmaci, 2014).

This is known as initialization. Once the wells are completed and put into productions, Eclipse outputs different information at different time steps, which will be examined later using text editors and post-processors.

Chapter 3

Case study

In 2015, Mazarine Energy, which is a subsurface-driven private oil& gas exploration and production company, drilled two exploration wells; Chouchet el Atrous -1 (CAT-1) and Douar ghrib-1 (DGH-1) in the Ghrib concession that is a part of Zaafrane exploration permit situated in Kebili Governorate in southern onshore Tunisia as shown in figure 11 below.

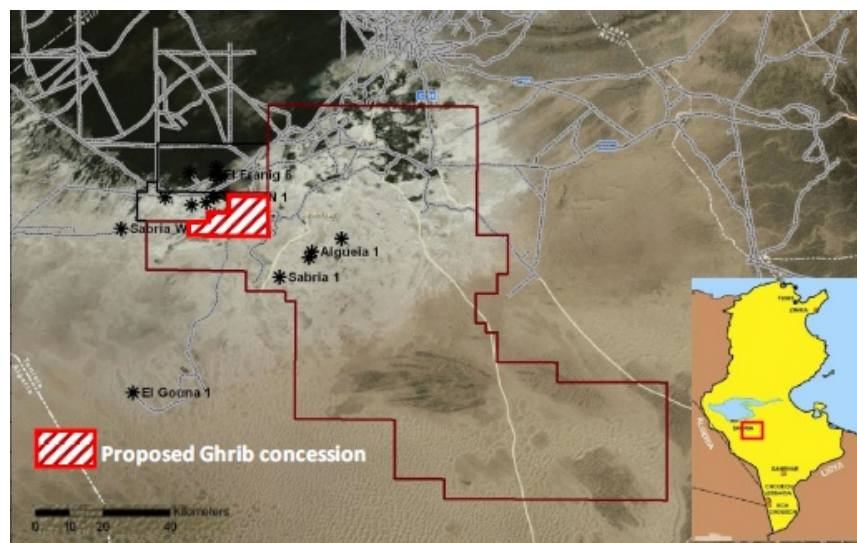


Figure 3.1- Zaafrane permit location map

The two wells have been tested and flowed hydrocarbons from two Ordovician sandstones formations called El Hamra and El Atchane.

The Hamra formation is quartz-rich sandstone that was deposited in marine and marginal marine environment. In the study area, the Hamra consists of an upper sand-rich section of

variable thickness, and of a lower, shalier unit. The variable thickness (0-35m) of the upper portion of the Hamra massive sandstone unit is function of how deep the erosion from the overlying unconformity has cut into the formation. This is a feature that is clearly recognizable in the seismic, and it is definitely supported by cross-well correlation, especially when using wells from the nearby concession. The erosion front generally progressed from N-NE. According to the cutting description, the Hamra sandstone is predominantly made of fine-medium quartz grains; it is moderately to poorly sorted and appears to have poor to fair visible porosity due to quartz cement and, probably, compaction. Accessory components are Kaolinite, pyrite and glauconite. The log signature is one of relatively clean sandstone, with gamma ray amplitude of 20 to 40 API. Down section, the Hamra gradually becomes shalier, the predominant granular component is silt-sized, but the bulk of unit is made by grey claystones. Not being affected by erosion, the thickness of this member is uniform, averaging 30 m. Both gamma ray and the neutron-density log gave a clear shale signature (Ghrib concession POD, 2015).

The EL Atchane formation shows similar lithological and depositional characteristic as the overlying formation (Hamra). It can be broadly subdivided into an upper sand-rich and a lower clay rich section. Compositionally and texturally, it is similar to the previous formation. However, it is described as being better sorted, coarser-grained and less cemented. This, together with a slightly better estimated (visible) porosity makes this reservoir a comparatively better reservoir than the Hamra, which is also confirmed by well performance (e.g. well tests). The average thickness of the sandrich portion of the EL Atchane is approximately 35 m, while the lower clay-dominated member is about 30 m thick (Ghrib concession POD, 2015).

The first well CAT-1 completion was designed to have the option to isolate the Atchane with a plug set in a nipple and has the ability to flow the Hamra alone. This involved setting a dual packer completion. The upper completion is connected to the lower one with an On-Off tool that is modified to prevent it from latching. The purpose for this is to prevent the string from rotating, as there are two control lines in the completion. The On-Off tool only works as a guide so there is no misalignment when running slick line. The production from the Hamra layers will flow through the slotted joints located above the On-Off tool while the production from EL Atchane layers will flow directly through the tubing end. However, for the second well DGH-1, the completion was designed to allow underbalanced perforation and commingled testing of both Hamra and Atchane reservoirs for evaluation and future production. The completion was designed based on the CAT-1 production test capabilities. Both completions are presented in appendix A (6.2) (Ghrib concession POD, 2015).

The CAT-1 well successfully tested oil from Ordovician aged reservoirs-EL Hamra and EL Atchane, which produced at rates in excess of 5400 bbl/day with a GOR of 2810 Scf/bbl from

a 4 ^{1/2} inch DST sting. While the DGH-1 well successfully tested oil from the same formations at a rate of 1000 bbl/ day with a GOR of 1860 scf/bbl on a 3 ^{1/2} inch DST string (Ghrib concession POD, 2015).

3.1 Well testing interpretation

3.1.1 Analysis of well Cat-1-2015

A pressure build-up test was conducted on a vertical well CAT-1 for **44 hours** from **30/04/2015** at **16h** to **02/05/2015** at **12h**. Afterwards, the results of pressure data versus time as well as flow rates were brought as an input to be used on Saphir (Ecrin). In addition, properties such as well radius, thickness of the productive layer and fluid type was also added to the model. However, the following table summarizes all the properties used as an input.

Table 3.1- Reservoir properties of well Cat-1

Reservoir properties (Unit)	
Thickness (ft)	32.8
Well radius (in)	4.25
Oil saturation (%)	100
Formation volume factor (cf/stb)	2.54
porosity	0.1
GOR (scf/bb)	2810
Compressibility (psi ⁻¹)	2.4846 E-5
Temperature (°F)	215.6
Pressure (psi)	8702
Viscosity (cp)	0.182

After loading pressure and flow rates data, the software shows the history plot including both flow rate and pressure as shown in figure 3.2. Pressure build up is the subject of this transient test analysis, and as we can see, there are two build-up periods. However, the interpretation is based on the second one since it is more reliable (longer) and confirmed by the first one.

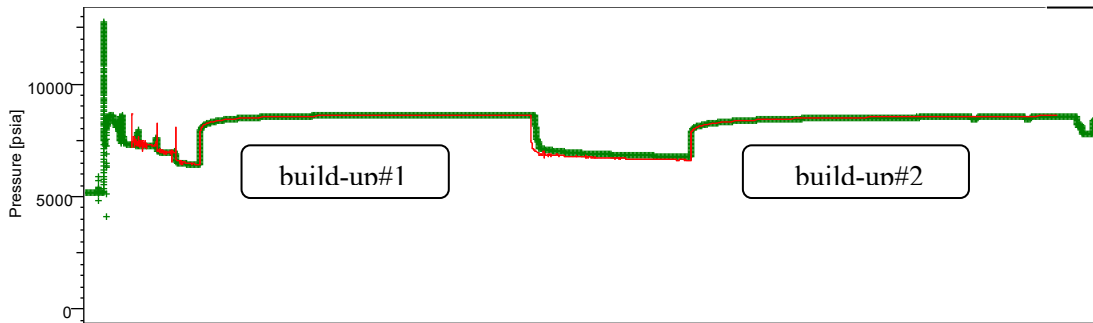


Figure 3.2- History plot of well Cat-1 (pressure [psi], liquid rate [STB/day], Time [hr])

The Bourdet derivative displayed together with the extracted pressure build up on log-log plot exhibit three different regions shown in the figure 3.3 below ;

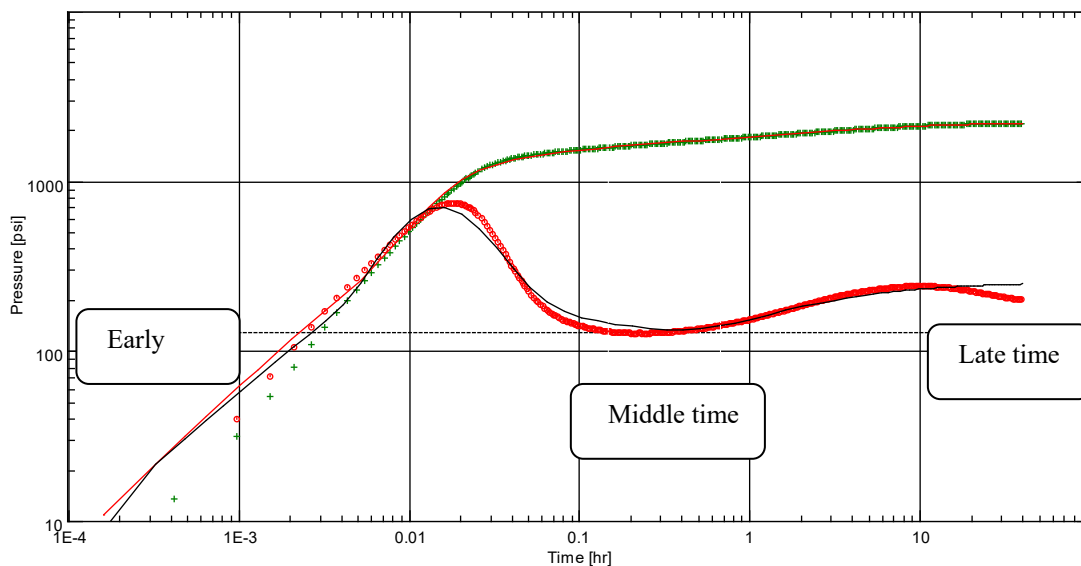


Figure 3.3 - Log-Log plot of Bourdet derivative and extracted pressure buildup versus time of well Cat-

1

From the early time region, we can get information (deduced from the straight line and the following hump) about the wellbore storage (WBS) and skin as explained in the literature part. However, as we can see in the figure, the Bourdet point values in the beginning do not fit perfectly the straight line, so in our case we have a changing WBS. This could be the consequence of phases redistribution. This phenomenon occurs when gas and liquid are flowing simultaneously within tubing during shut-in. In this situation, the gravity effect will cause the gas to rise to the surface and the liquid to fall down and hence a perturbation in pressure gauge.

After the wellbore storage effect has vanished, the middle time region takes place, which describes the radial flow regime where we can get information about kh product. In addition, on a semi log plot it exhibit linearity where we can estimate the mobility from calculating the slope or estimate well productivity from the intercept with Y-axis as sown in figure 3.4 below.

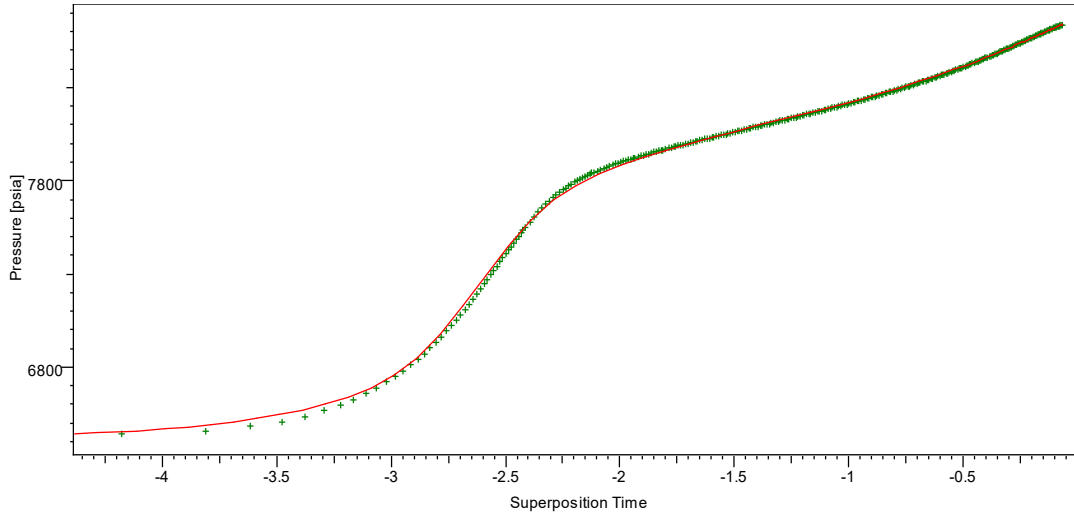


Figure 3.4- Semi-log plot: P [psi] versus Superposition time

During the late time region, the log-log plot shows upward deviation this could be explained by the presence of a sealing fault. In general, the existence of fault is described by the doubling of radial flow slope, however the full doubling rarely occurs since it requires long tests (one and a half log cycles in time after the initial deviation from the first radial flow) which is not the case here. [7]

To run the model with the best possible fit, we consider single fault model even though the slope is less than double because it is the simplest boundary model that provides association between distance and time. The table 3-2 below summarizes the parameters selected for the model.

Table 3.2- Model of well Cat-1 properties

Model properties	
Wellbore model	Changing wellbore storage
Well model	Vertical
Reservoir model	Homogenous
Boundary model	One fault

The transient test with the possible best model has given the following results:

Table 3.3- Well test Cat-1-2015 output

Well testing final results	
Well type	vertical
WBS type	Changing wellbore storage
Reservoir	Homogenous
Boundary	One fault
Initial pressure (psi)	8679.02
Kh product (ft.md)	1300
Permeability (md)	39.7
Distance to boundary (ft)	175
Skin	0.547
Wellbore storage coefficient C (bbl/psi)	0.0027

3.1.1.1 Analysis of CAT-1-2017

In 2017, a new build up test was conducted for **176 hours** from **20/11/2017** to **27/11/2017**. Obviously, the same reservoir properties used in the last transient test is again used as input.

The pressure history plot shows significant fluctuations (as shown in figure 3.5) because of the consecutive close and open of the well in a short period of time which will, as consequence, make the operation of finding the good match more complicated.

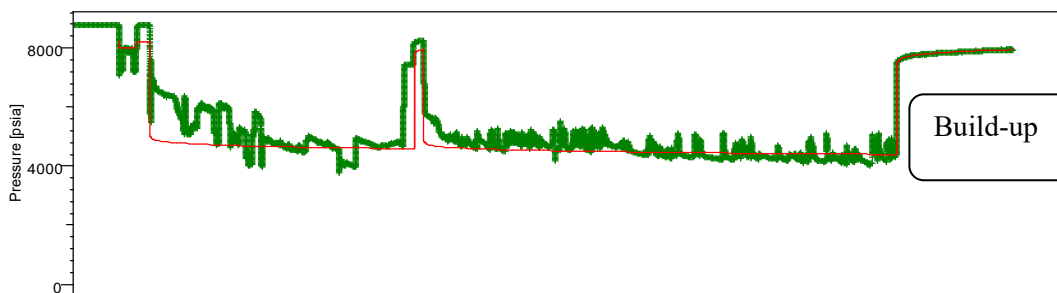


Figure 3.5- History plot of well Cat-1 (pressure [psia], liquid rate [STB/day], Time [hr])

The Bourdet derivative displayed together with the extracted pressure build up on log-log plot exhibit three different regions shown in the figure 3.6:

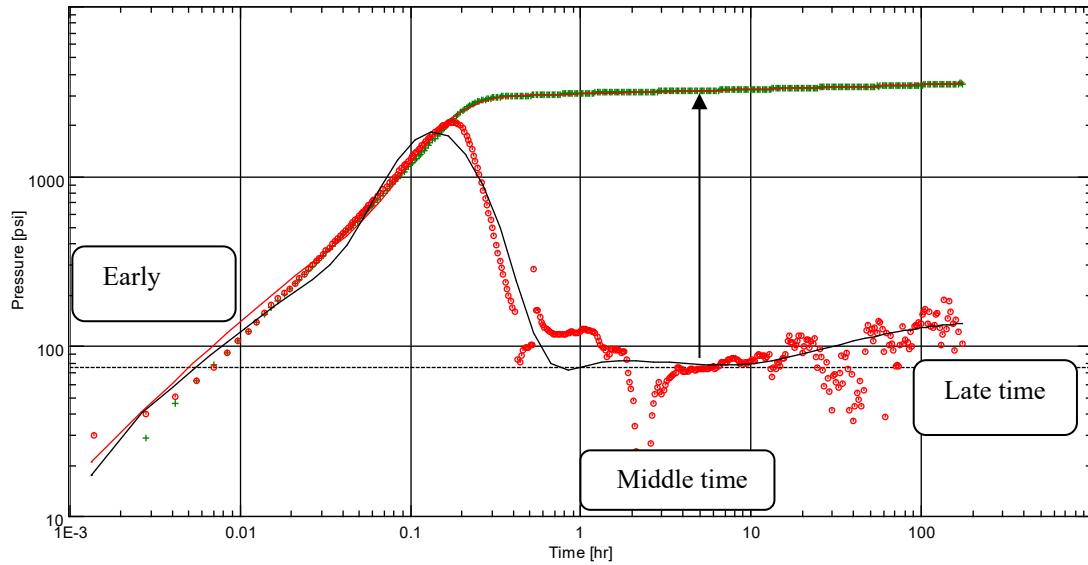


Figure 3.6- Log-Log plot of Bourdet derivative and extracted pressure buildup versus time of well Cat-1

The scattered dots shown in figure 3.6 are explained by the fluctuations mentioned above, however we are still able to identify the three regions.

The early time region exhibit a changing WBS like in the previous test conducted in 2015, but we can observe the gap between the horizontal radial flow of the derivative and the Bourdet (shown by an arrow on the figure 3.6) curve are larger than the one during the previous test which means that the skin has been increased. As we know, the stabilisation of the radial flow in middle time region is proportional to the transmissivity $T=kh/\mu$ so lower transmissivity, which is the case of this test, means lower permeability and thus additional pressure drop. During the late time region, the scattered dots deviated upward and the slope is almost doubled from the radial flow.

The best possible matched model was found based on the following parameters:

Table 3.4- Model of well Cat-1 properties

Model properties	
Wellbore model	Changing wellbore storage
Well model	Vertical
Reservoir model	Homogenous
Boundary model	One fault

The transient test with the possible best model has given the following results:

Table 3.5- well test Cat-1 output

Well testing final results	
Well type	Vertical
WBS type	Changing wellbore storage
Reservoir	Homogenous
Boundary	One fault
Initial pressure (psi)	8220.49
Kh product (ft.md)	917
Permeability (md)	27.1
Distance to boundary (ft)	775
Skin	14
Wellborestorage coefficient C (bbl/psi)	0.00249

3.1.1.2 Analysis of DGH-1-2015

A pressure build-up test was conducted on a vertical well DGH for **19 hours** from **06/09/2015** to **07/09/2015**. Afterwards, the results of pressure data versus time as well as flow rates were brought as an input to be used on Saphir (Ecrin). The following table summarizes all the properties used as input.

Table 3.6- Reservoir properties of well DGH-1

Reservoir properties (unit)	
Thickness (ft)	42
Well radius (in)	3.5
Oil saturation (%)	100
Formation volume factor (cf/stb)	2.54
Porosity	0.1
GOR (scf/bb)	1860
Compressibility (psi ⁻¹)	1.8E-5
Temperature (°F)	215.6
Pressure (psi)	8809
Viscosity (cp)	0.182

After loading pressure and flow rates data, the software shows the history plot containing both flow rate and pressure as shown in figure 3.7. Pressure build up is the subject of this transient test analysis and as we can see there are two build-up periods. However, the interpretation is based on the second one.

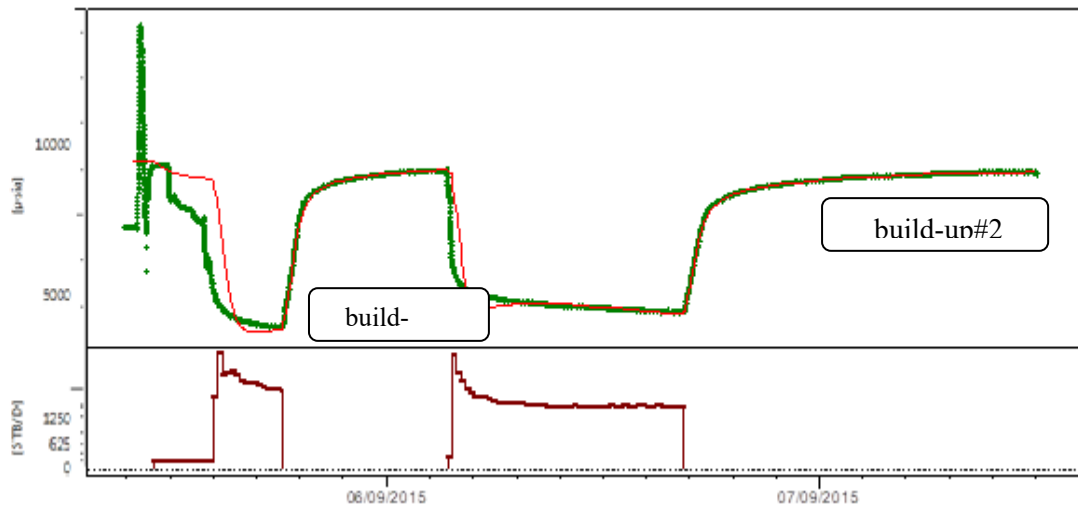


Figure 3.7- History plot of well DGH-1 (pressure [psi], liquid rate [STB/day], Time [hr])

The Bourdet derivative displayed together with the extracted pressure build up on log-log plot exhibit three different regions shown in the figure 3.8:

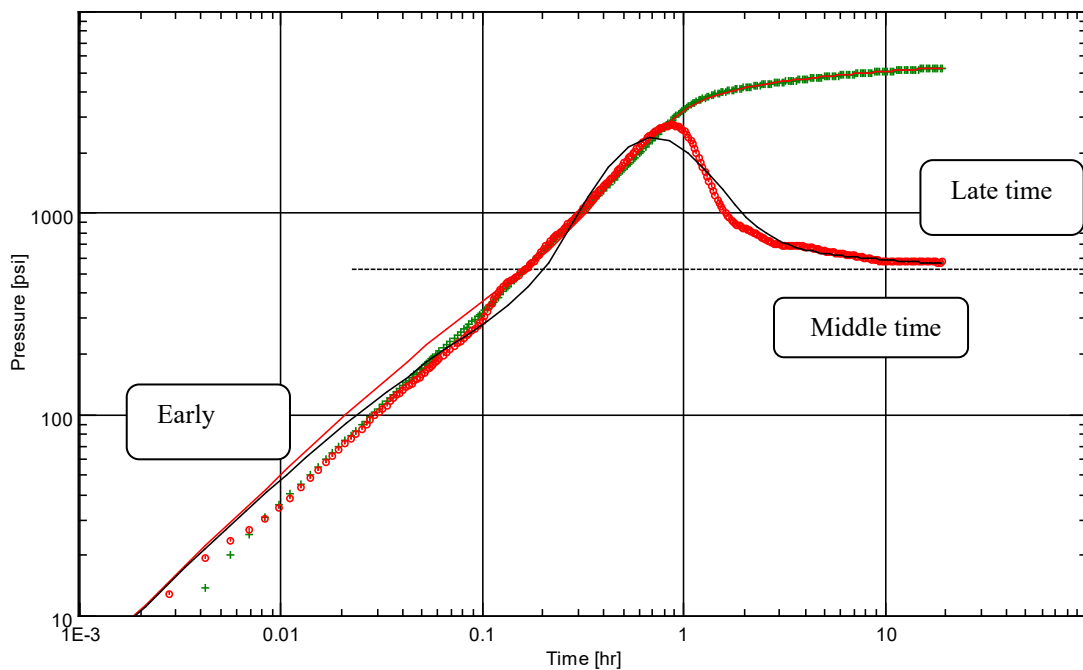


Figure 3.8- Log-Log plot of Bourdet derivative and extracted pressure buildup versus time of well DGH-1

During the early time region, the curve exhibits what we call a decreasing WBS. In other words, this phenomenon is due to the gas compressibility that could dominate firstly when the well is shut in and then later when the oil compressibility takes over. This phenomenon has led to a late stabilization of radial flow within the middle time region.

In late time region, the curve keeps the same level of stabilisation with no deviation upward nor downward so no boundary was detected that's why we consider that we have an infinite reservoir.

In addition, on a semi log plot it exhibit linearity where we can estimate the mobility from calculating the slope or estimate well productivity from the intercept with Y-axis as shown in figure 3.9.

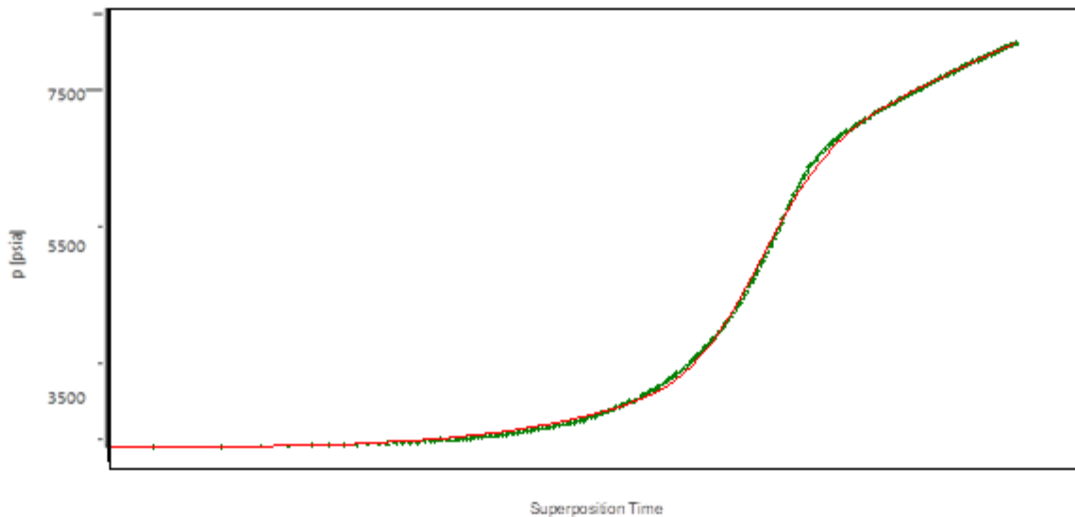


Figure 3.9- Semi-log plot: P [psi] versus Superposition time

The table below summarizes the parameters selected for the model.

Table 3.7- Model of DGH-1 properties

Model properties	
Wellbore model	Changing wellbore storage
Well model	Vertical
Reservoir model	Homogenous
Boundary model	Infinite

The transient test with the possible best model has given the following results:

Table 3.8- Well test DGH-1 output

Well testing final results	
Well type	vertical

WBS type	Changing wellbore storage
Reservoir	Homogenous
Boundary	Infinite
Initial pressure (psi)	8703.82
Kh product (ft.md)	64.6
Permeability (md)	1.54
Skin	-0.768
Wellbore storage coefficient C (bbl/psi)	0.00365

3.1.1.3 Analysis of DGH-1-2017

In 2017, a new build up test was conducted for **26 hours** from **17/12/2017** to **19/12/2017**. Obviously, the same reservoir properties used in the last transient test are again used as input. The pressure and flow rate history (figure 3.10) shows one pressure build-up where the necessary properties were derived:

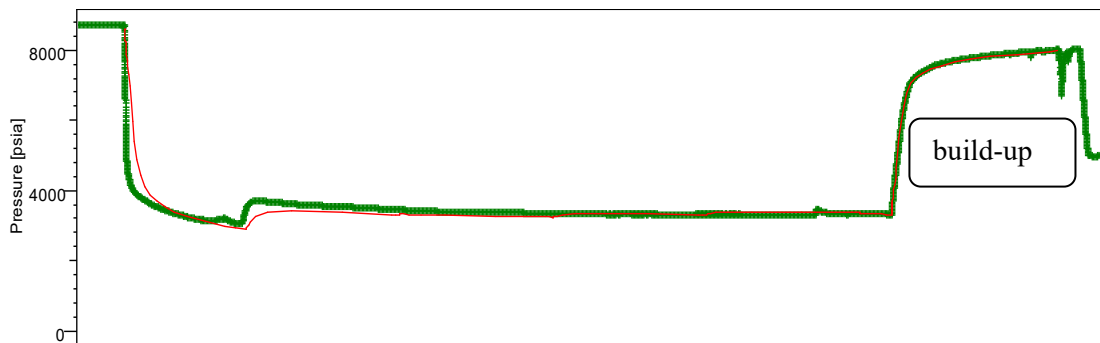


Figure 3.10- History plot of well DGH-1 (pressure [psi], liquid rate [STB/day], Time [hr])

The Bourdet derivative displayed together with the extracted pressure build up on log-log plot exhibit three different regions shown in the figure 3.11:

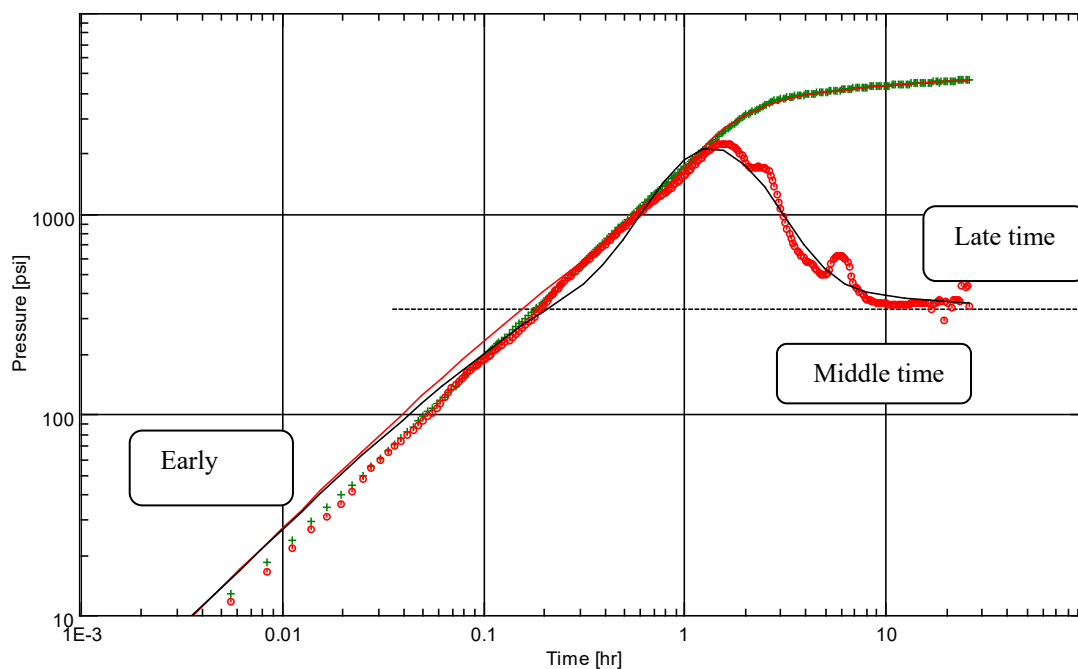


Figure 3.11- Log-Log plot of Bourdet derivative and extracted pressure buildup versus time of DGH-1

The two curves show the same behavior as the previous test conducted two years ago with less consistency due to the consecutive close and open of the well. A decrease in the radial flow stabilisation is observed also, which can be explained by an increase of the skin factor.

We used the same properties for the model to realize the match:

Table 3.9- Model properties of well DGH-1

Model properties	
Wellbore model	Changing wellbore storage
Well model	Vertical
Reservoir model	Homogenous
Boundary model	Infinite

The transient test with the possible best model has given the following results:

Table 3.10- Well test DGH-1 output

Well testing final results	
Well type	Vertical
WBS type	Changing wellbore storage
Reservoir	Homogenous
Boundary	Infinite
Initial pressure (psi)	8613
Kh product (ft.md)	54.6
Permeability (md)	1.09
Skin	1.5
Wellbore storage coefficient C (bbl/psi)	0.00404

3.2 Ghrib field reservoir simulation model

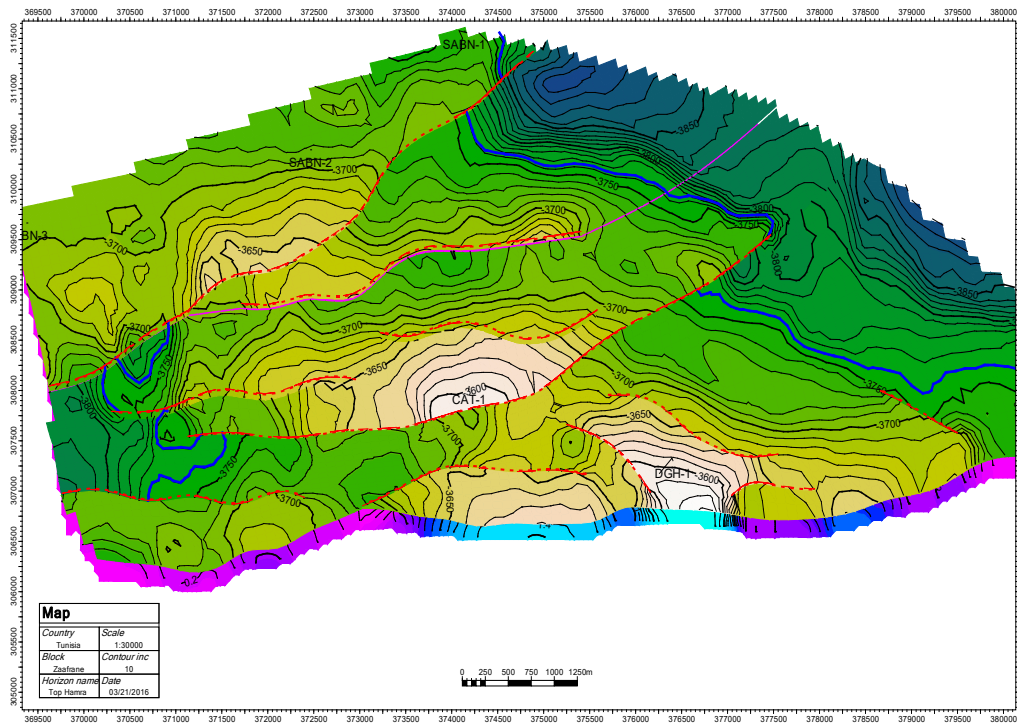
3.2.1 Geological static model

The geologist team has built a static reservoir model over the EL Hamra and EL Atchane reservoirs of the western portion of the license area using PETREL. In fact, the model grid is composed of 111*52*155 blocks with dimensions of 100*100m.

The common structural configuration of the two hydrocarbon accumulations separately drilled by the CAT-1 and DGH-1 wells is a 3-way dip closure bounded to the south by a Minor fault. Faults are also present in the proximity of the wells, but they represent minor structural features. However, these faults do not affect the volumetric calculated in this project (figure 3.12).

The 3D grid (I-, J- and K- grid) was selected in such a way that the j-direction(E-W) aligns with the predominant fault strike direction. This allowed for the making of a structural grid with minimal distortion; the dimension of which were set to 100 by 100 m. Fault pillars have been made vertical to reduce cell distortion and to avoid computational problems with the dynamic simulator.

The project area is heavily faulted (figure 3.13); only 12 faults have been included in the static model out of 23 faults that have been originally interpreted in the seismic. These are only those faults that are important for two accumulations, or those faults that might be relevant to this study (e.g. relevant for aquifer support) .Far away fault or minor faults that would only complicate the structural framework have been excluded from the model.



3.12- Structural map of the top Hamra

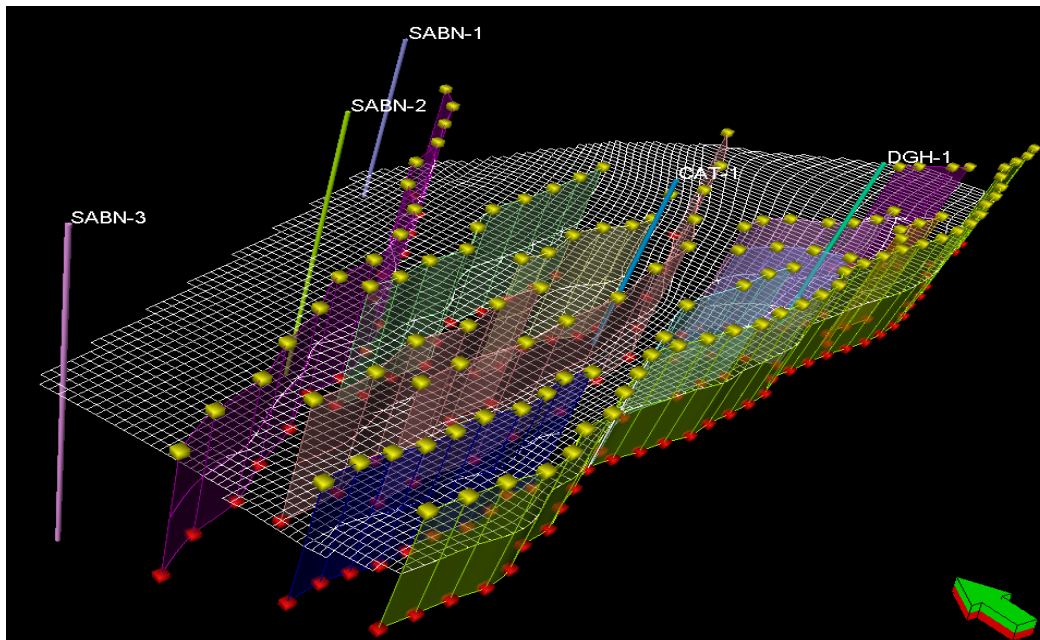


Figure 3.13- Fault network and grid

The zonation strategy utilized in this project follow both lithostratigraphic and petrophysical property drive criteria. The only two clearly identifiable formation tops used as main zonation

are the top EL Hamra and top El Atchane. However, further zonal subdivisions have been produced mainly following petrophysical quality criteria. In this view shown in figure 3.14 below, the top Hamra has been subdivided into two zones, while El Atchane was subdivided into four zones. The main purpose of using layered reservoirs is to provide better control over properties, and ultimately to make more accurate volumetric calculations. Main guidance to assess the number of layers was adequate capture of property and/or lithology each layer should compromise a portion of reservoir with comparatively constant lithological and petrophysical characteristics.

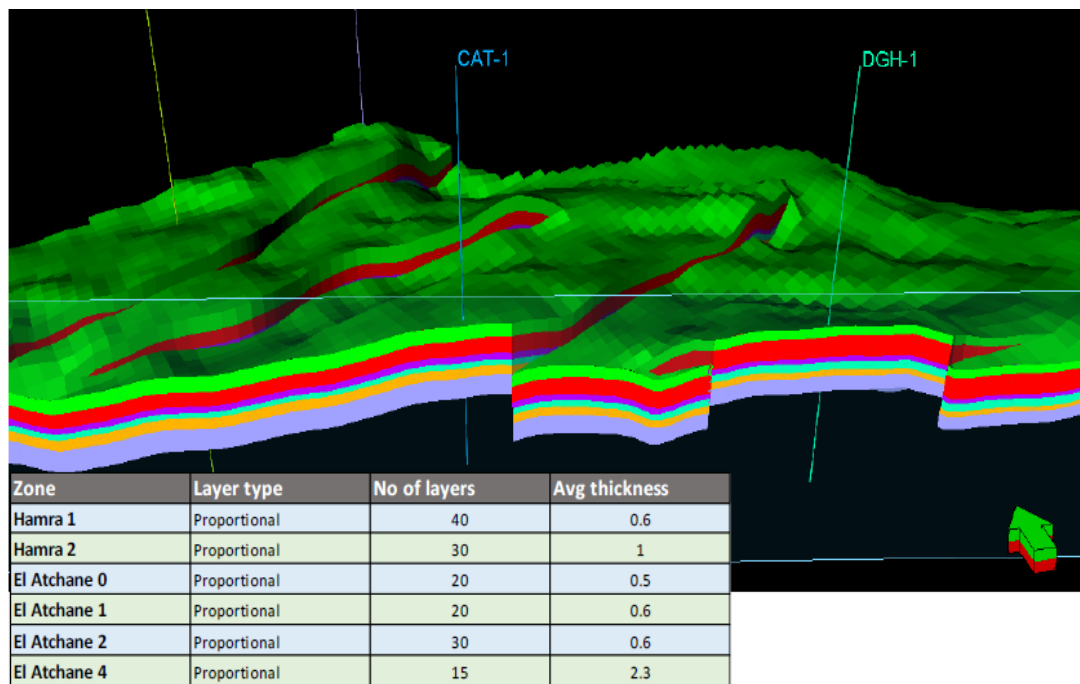


Figure 3.14- Cross section passing thorough CAT-1 and DGH-1 wells illustrating the 6 main reservoir zones used in the Petrel model

Because of a lack of statistics, it was decided to distribute the properties uniformly across each accumulation following the vertical detail as inferred in the wells. The petrel model utilizes the results from the petrophysical study as direct input for the property model. These consists of a net reservoir flag log used to derive net-to-gross, an effective porosity log and a permeability log then all three logs have been scaled up to the layer level.

The scaled up value of each cell-layer for every specific property has been propagated laterally across the relevant segment (or fault block).The result is a layer-cake model with a unique value in each layer and for every property.

For calculating the water saturation, a height above free water level property was made, using regional fluid contact at 3760m as reference.

The water saturation was calculated by means of the property calculator available in petrel, and using a zone-calibrated saturation-height function. Constant formation volume factors have been assigned in each of the CAT-1 and DGH-1 segments.

3.2.1.1 OOIP volumetric calculations

Hydrocarbon volumes have been computed using the volumetric calculation module available in Petrel. This uses the following formula

$$\text{STOOIP} = (\text{Bulk Rock Volume}) * (\text{Net-to-Gross}) * (\text{Porosity}) * (1 - \text{Water saturation}) * \text{FVF}$$

All of the above inputs are integral part of the geological reservoir model implemented Petrel. The results of which are reported in table below:

Table 3.11- STOOIP Volumetric Calculation

Segment / Fault block	STOIP
CAT-1	25.2 MMstb
DGH-1	18.1 MMstb
Total	43.3 MMtsb

3.2.2 Dynamic reservoir model

The objective of the dynamic simulation study is to develop reservoir simulation models of Zaafrane field, match history production of two existing wells, perform sensitivity study for several key parameters of the reservoir, and make production forecast for different development strategies.

3.2.2.1 Fluid parameters

Fluid parameters of the model are based on laboratory test of CAT-1 samples. The fluid is considered volatile oil; however, there is a possibility that the fluid could be a gas condensate in CAT-1 area.

DST results of well DGH-1 showed that fluid from the well DGH-1 is oil with a lower gas-oil ratio than CAT-1 fluid. Therefore, the model contains two separate regions with different reservoir fluid properties shown in figure 3.15.

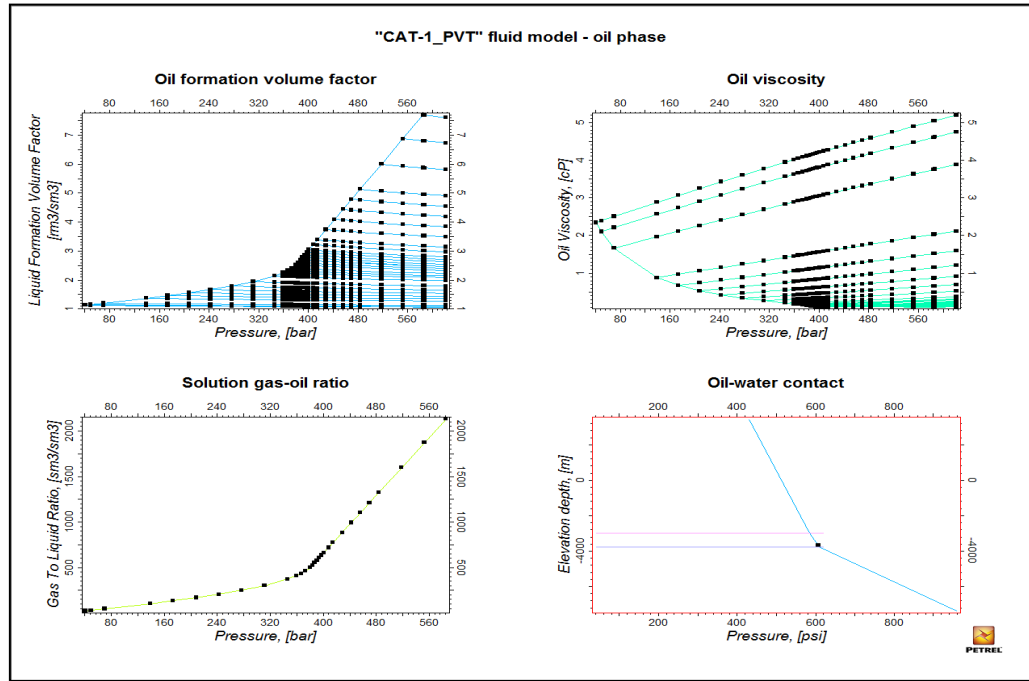


Figure 3.15- CAT-1 fluid properties

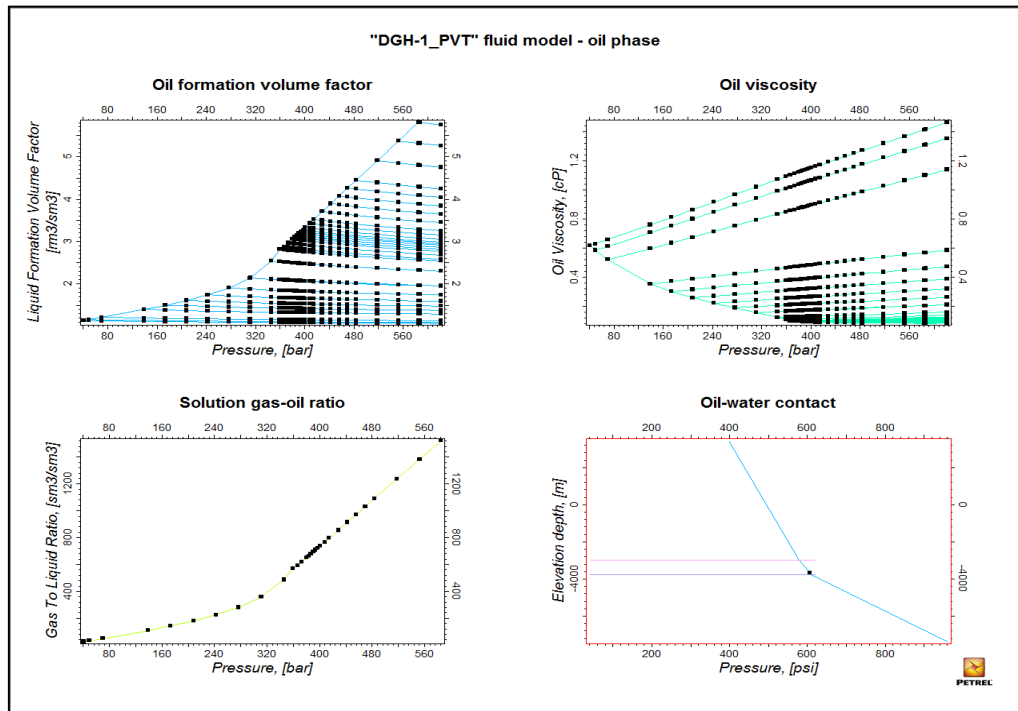


Figure 3.16- DGH-1 fluid properties

CAT-1 fluid properties using in the model are following: oil API gravity 40.86, saturation pressure=5600 psi, $R_s=3.05$ Mscf/stb. DGH-1 fluid properties using in the model are the following: oil API gravity 41.4, saturation pressure=4521 psi, $R_s=2.015$ Mscf/stb.

However, the scale properties using Corey function are shown in the plot 3.16 below of relative permeability of oil-water and gas-oil system systems.

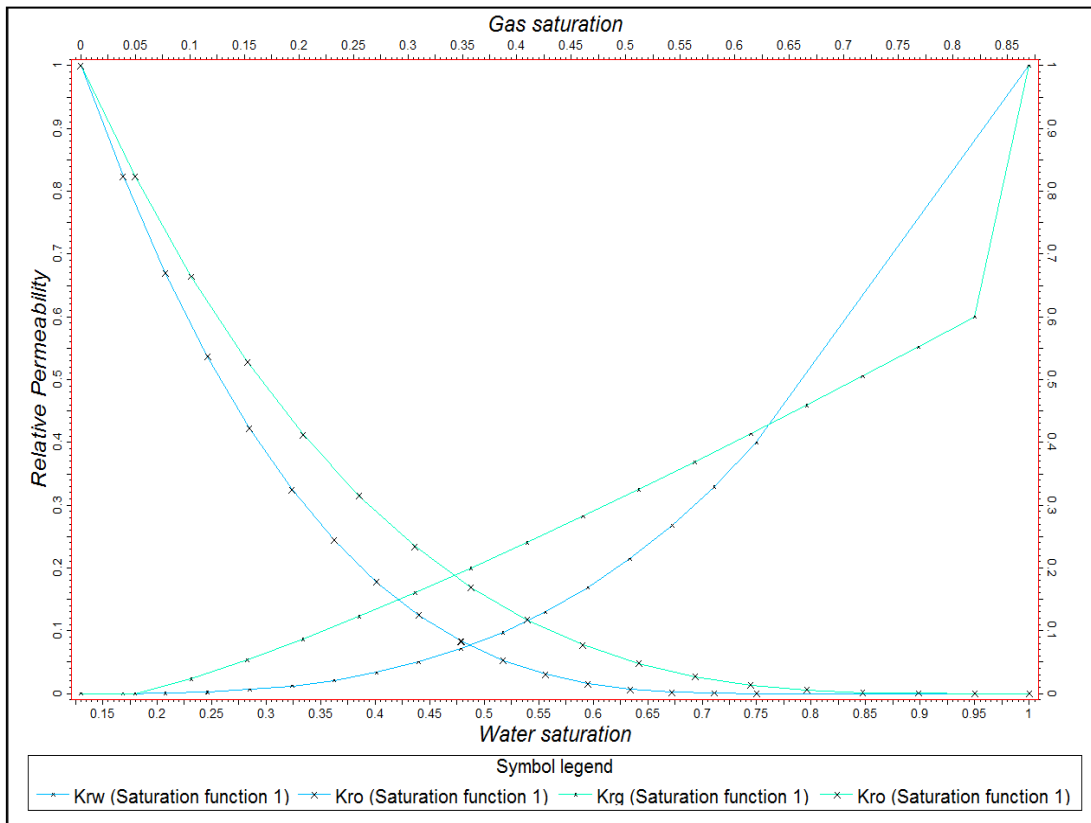


Figure 3.17- Relative permeabilities: oil-water, gas-oil

The dynamic model was upscaled from the static model factor 2. The dynamic model's dimensions are 111*52*77. Upscaling procedure was performed using arithmetic average volume weighted method for key properties of the reservoirs.

In the dynamic model the initial water saturation was taken from the static model upscaled with arithmetic average weighted by effective pore volume method while the initial water saturation in the static model was calculated using Leverett J-function. Mainly, the models consist of two regions with different PVT properties: region 1 with CAT-1 fluid properties and region 2 with DGH-1 fluid properties. Each region is not connected with another and divided by main sealing fault like shown in figure 3.18.

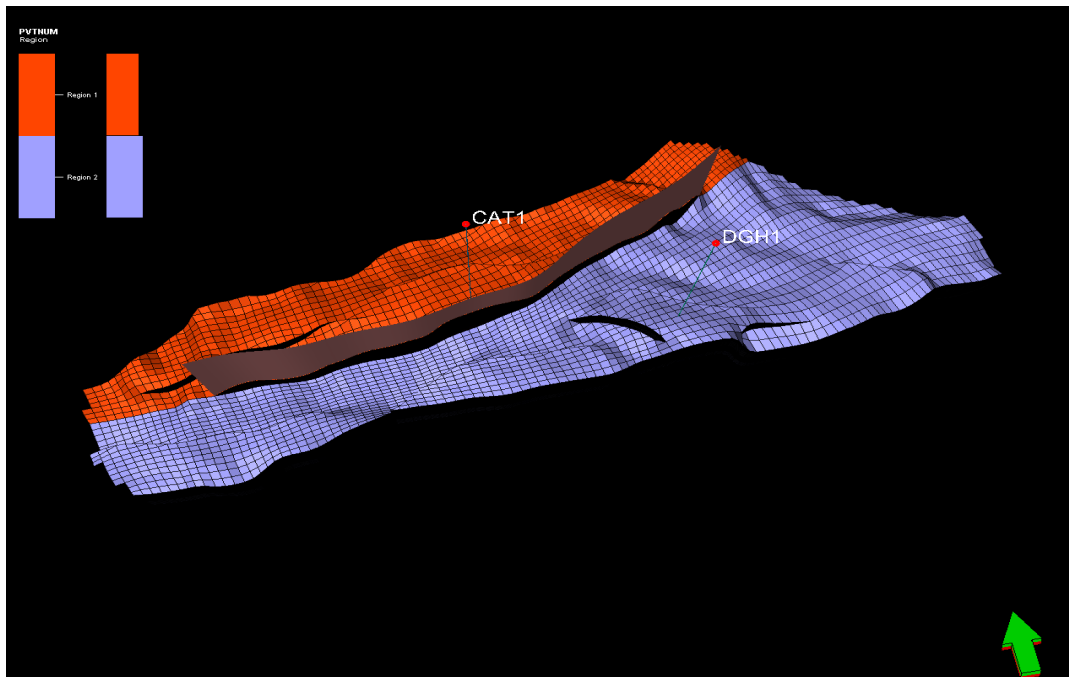


Figure 3.18- PVT properties regions and main fault

3.2.3 History matching

History matching process has been performed with the results of DST of wells CAT-1 and DGH-1. Actually, CAT-1 was tested during the period between 24-04-2015 until 02-05-2015. Maximum liquid rate was 5400 stb/d while DGH-1 was tested during the period from 03-09-2015 to 05-09-2015 has shown maximum liquid rate of 1605 stb/d.

The methodology followed during history matching is shown in Appendix A (6.3). However, the input data used when defining the simulation case for both wells such as water saturation, porosity, permeabilities, net to gross ratio and transmissibility are shown in figures below:

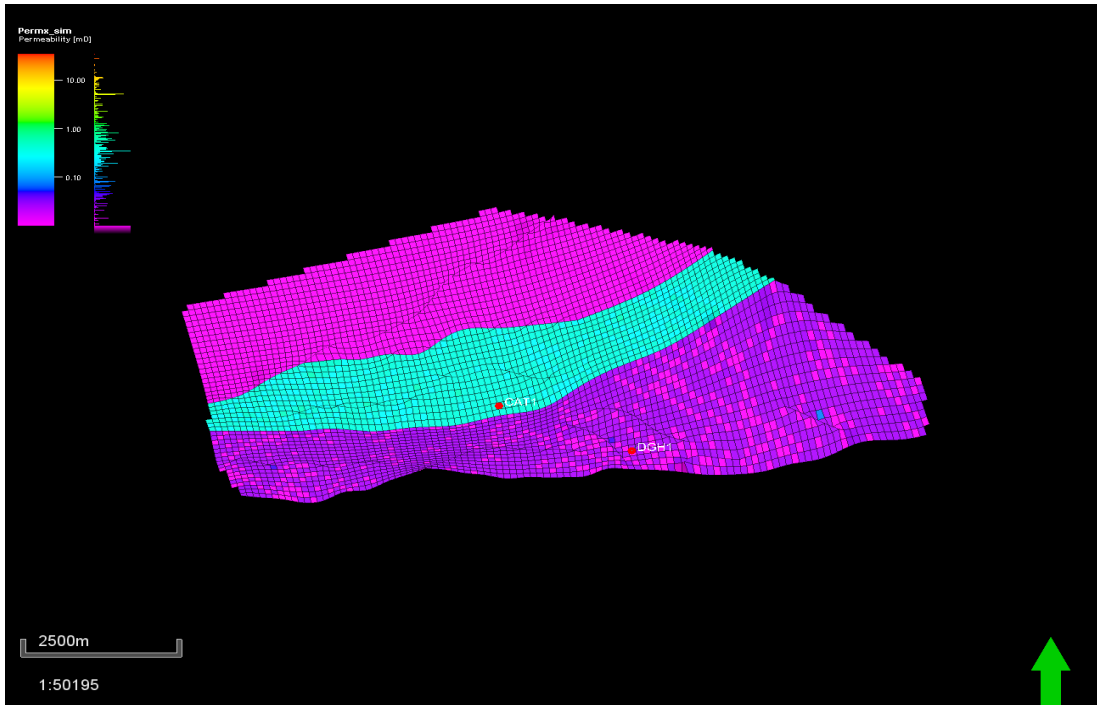


Figure 3.19- Permeability distribution in the X-direction for both wells

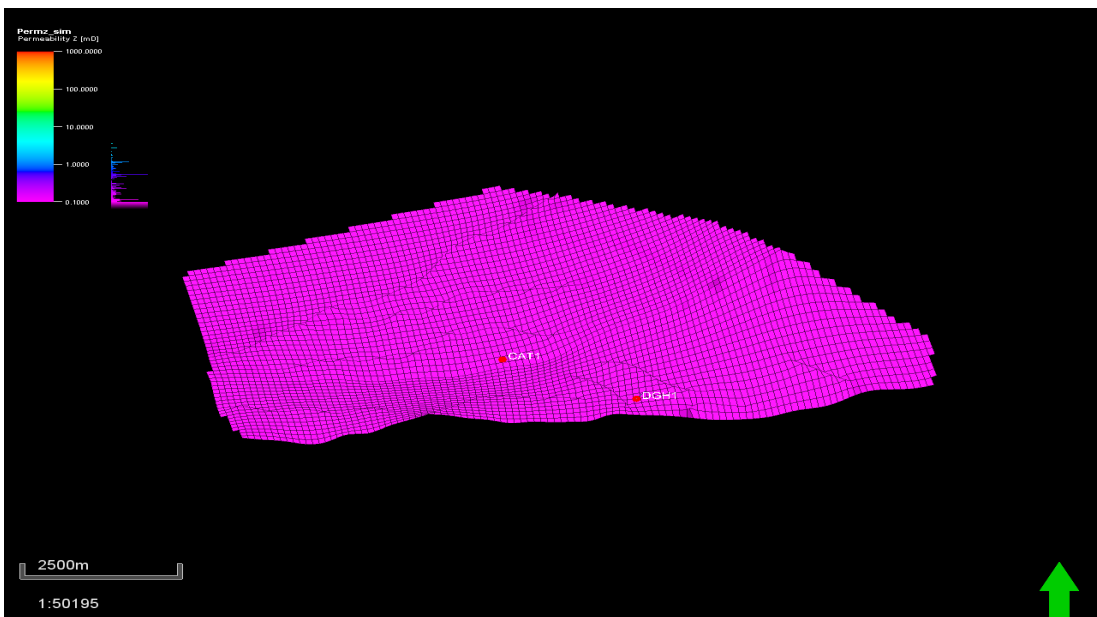


Figure 3.20- Permeability distribution in the Z-direction for both wells

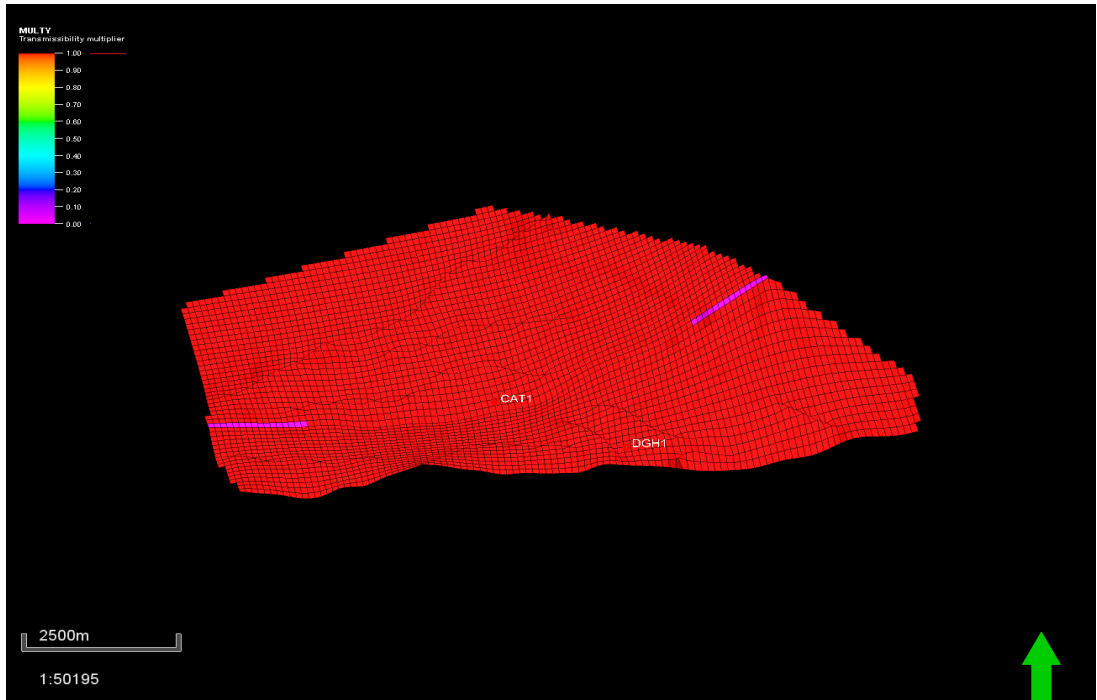


Figure 3.21- Transmissibility for both wells

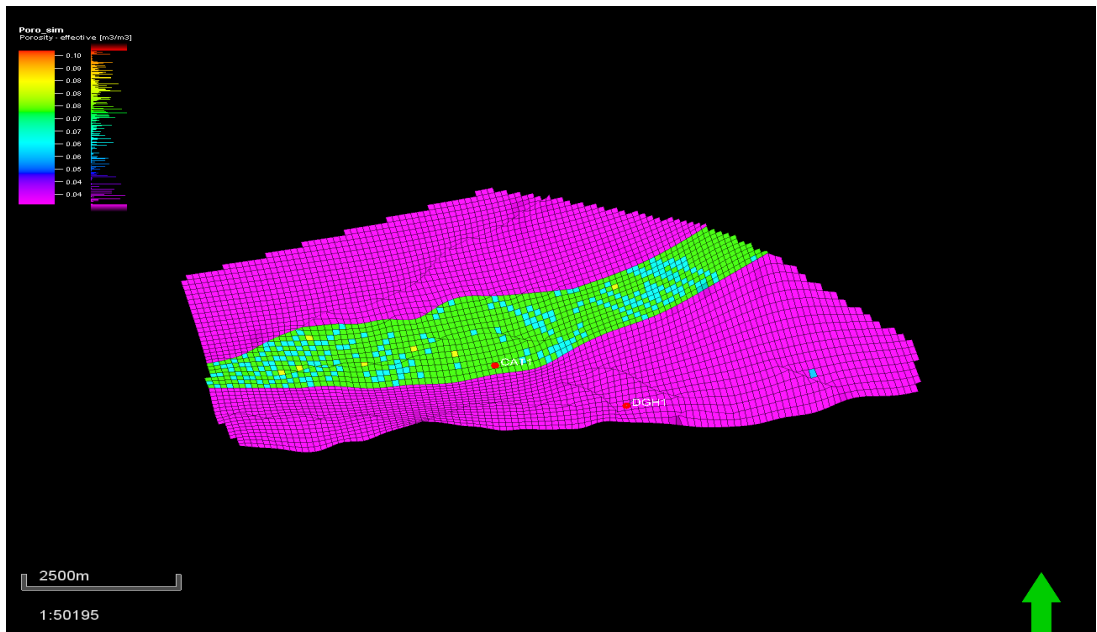


Figure 3.22- Porosity distribution for both wells

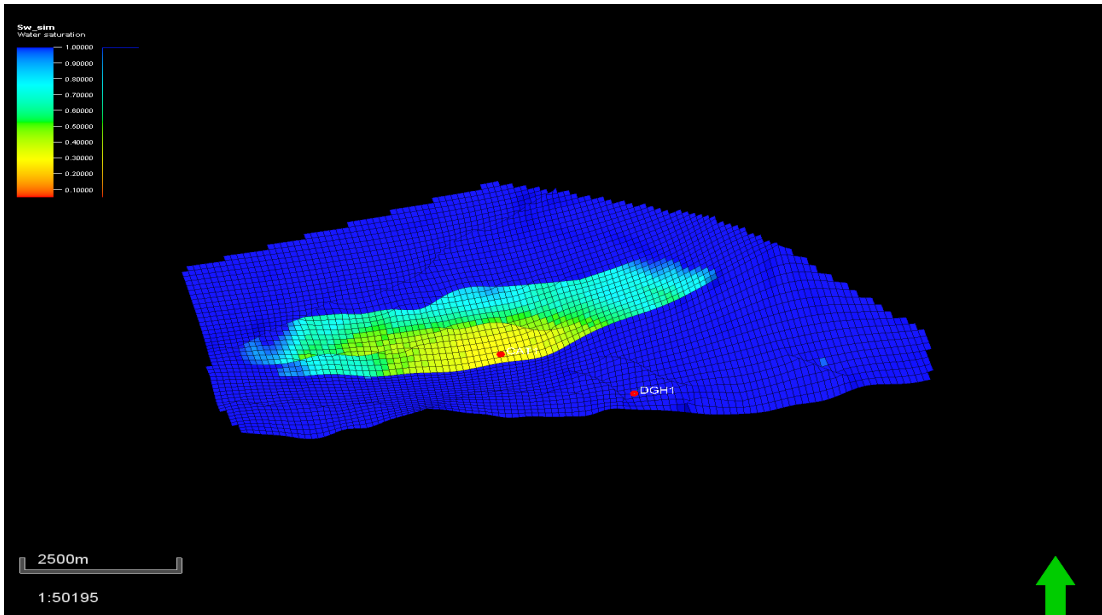


Figure 3.23- Water saturation distribution for CAT-1

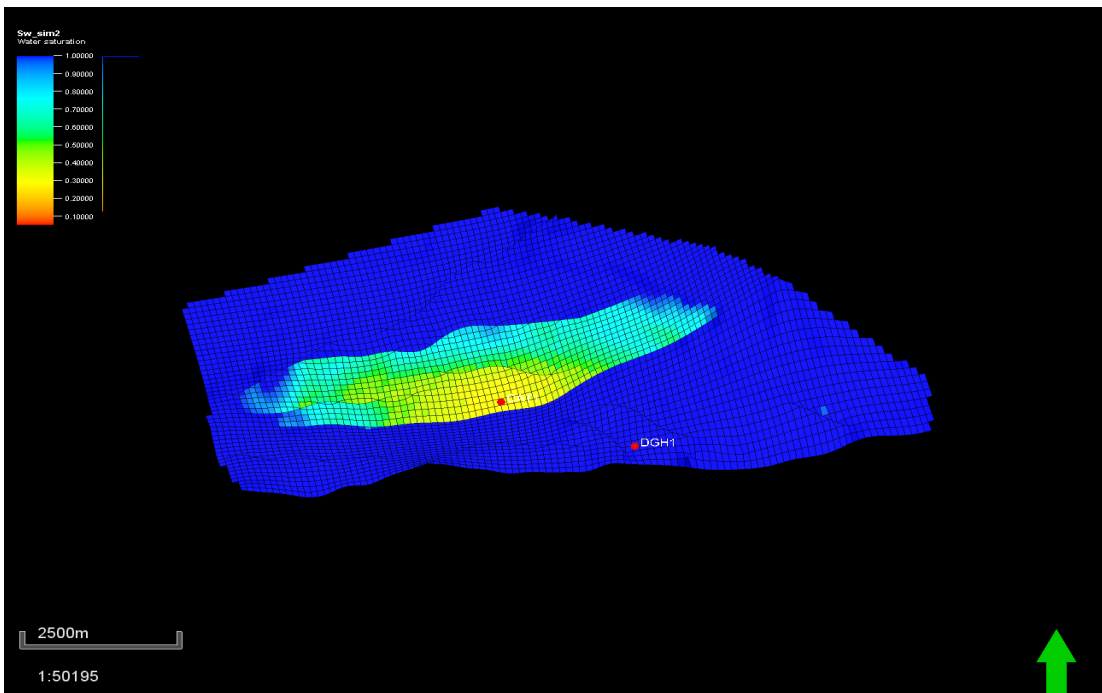


Figure 3.24- Water saturation distribution for DGH-1

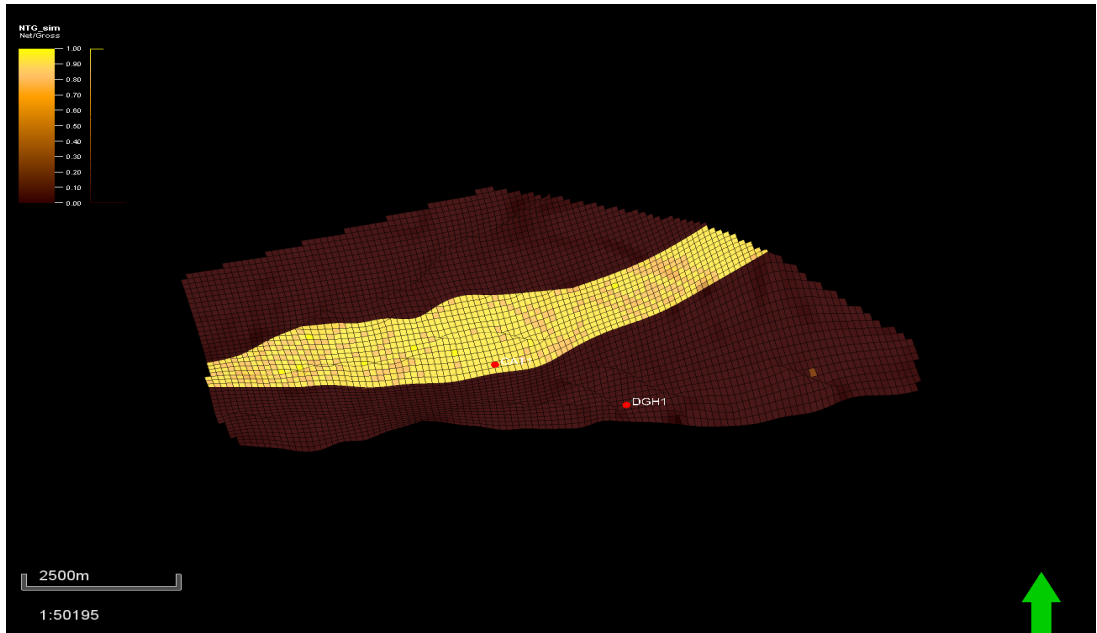


Figure 3.25- Net to gross ratio

After checking and running the simulation case successfully, we visualize the history matching of bottomhole pressure, oil production rate versus time for both wells as shown below:

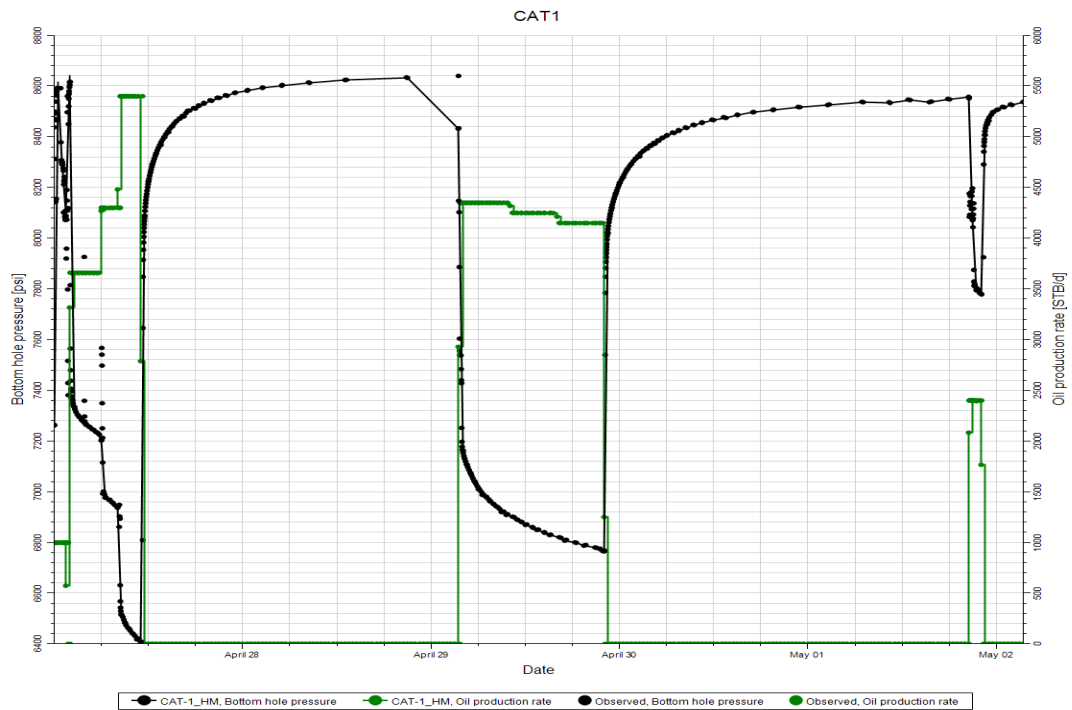


Figure 3.26- History marching CAT-1

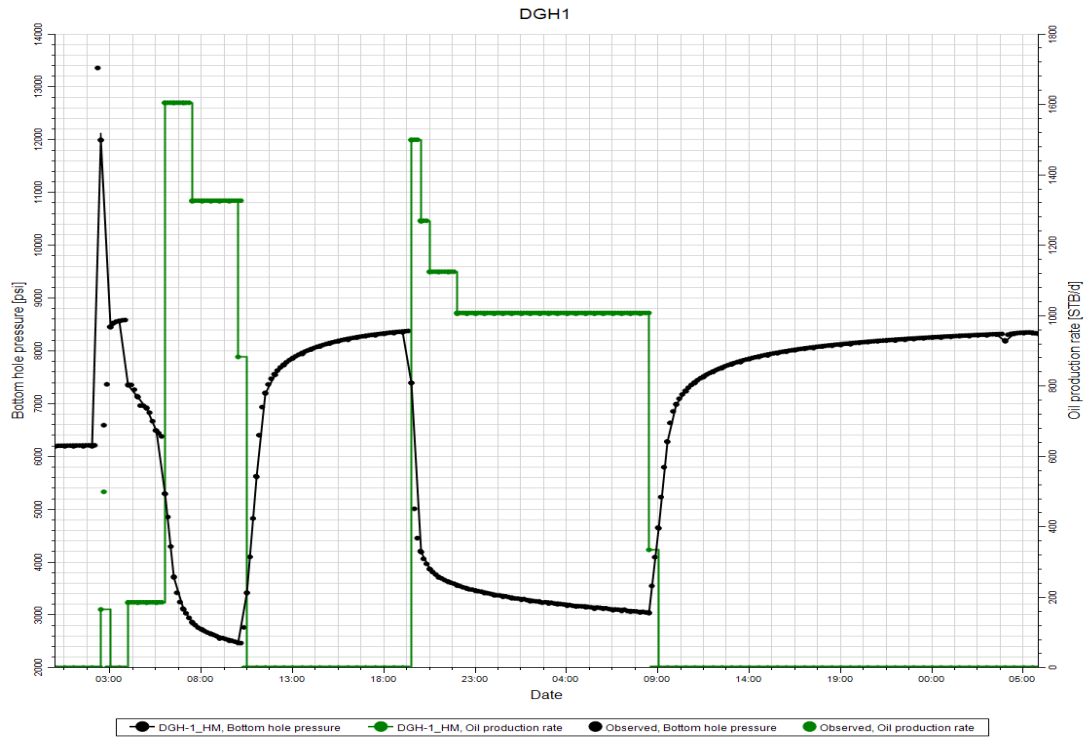


Figure 3.27- History matching DGH-1

3.2.4 Sensitivity analysis

Sensitivity analysis is mainly performed to gain a better knowledge about the influence of certain parameters on the simulated results. In this case study, sensitivity analysis was performed for 8 cases including a base case which is a case with no further action (NFA) including two existing wells CAT-1 and DGH-1. However, four factors were used in the study: skin factor, Permeability of Hamra reservoir, permeability of El Atchane reservoir and oil water contact.

For all cases, minimum THP value is 360 psi and field production is restricted to 4000 stb/day.

3.2.4.1 Base case prediction

We start the production forecast of the base case (no further action) by creating a new prediction strategy starting from 2017-01-01 till 2036-01-01 for both wells with setting new rules that state an oil rate equals to 4000 bbl/d for both wells and a constraint of a tubing head pressure equals to 360 psi (see appendix-D). However, the input used in defining the simulation case are the same used in history matching. Furthermore, the skin in this case is derived from the well tests conducted in 2015 and equals to 0.547 for CAT-1 and -0.768 for DGH-1.

The prediction results for oil, gas and water rates in this case for both wells are shown as follows:

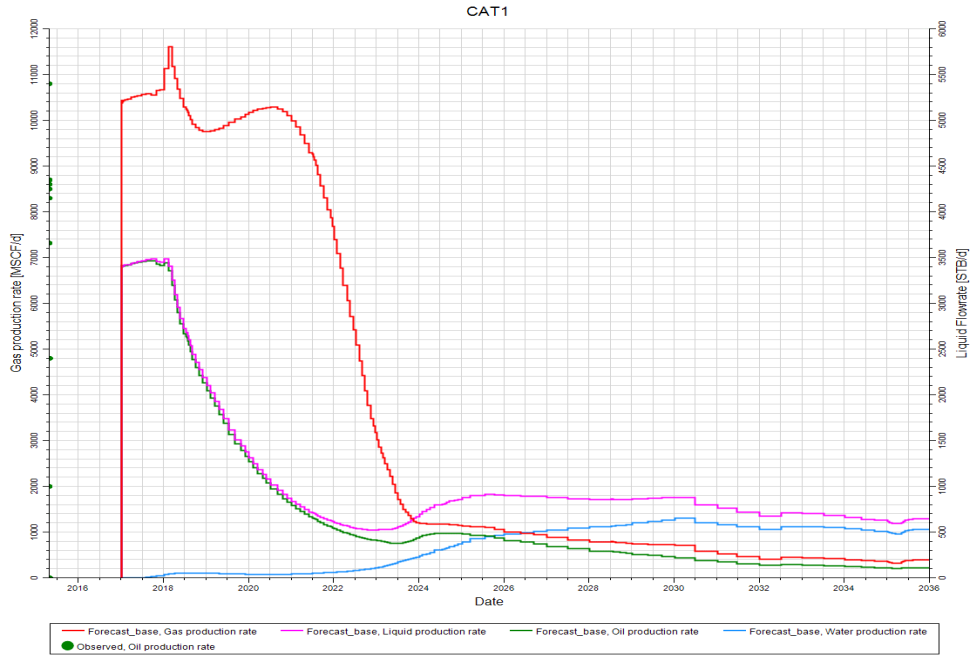


Figure 3.28- Base case Forecast CAT-1

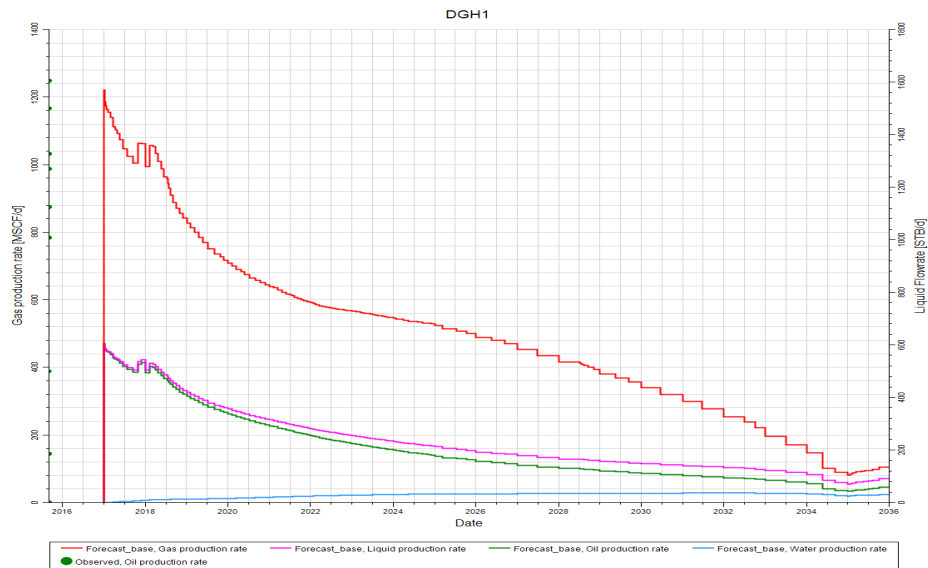


Figure 3.29- Base case forecast DGH-1

3.2.4.2 Case skin 0 (reference case)

In this case, the skin is equal to zero. The results of the reference case in oil and gas production are shown in figures below:

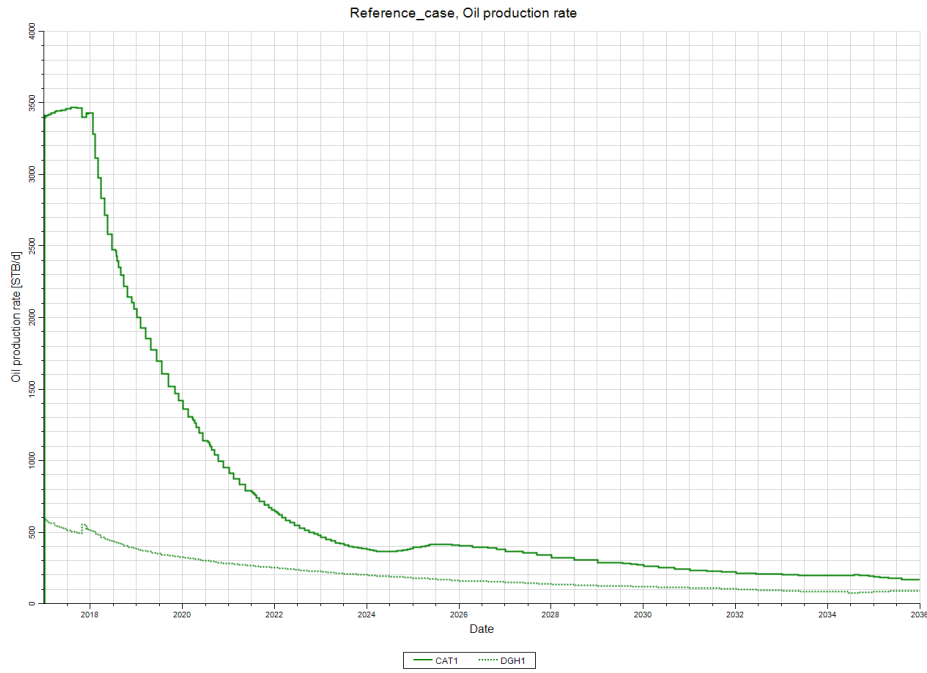


Figure 3.30- Oil production reference case for both wells

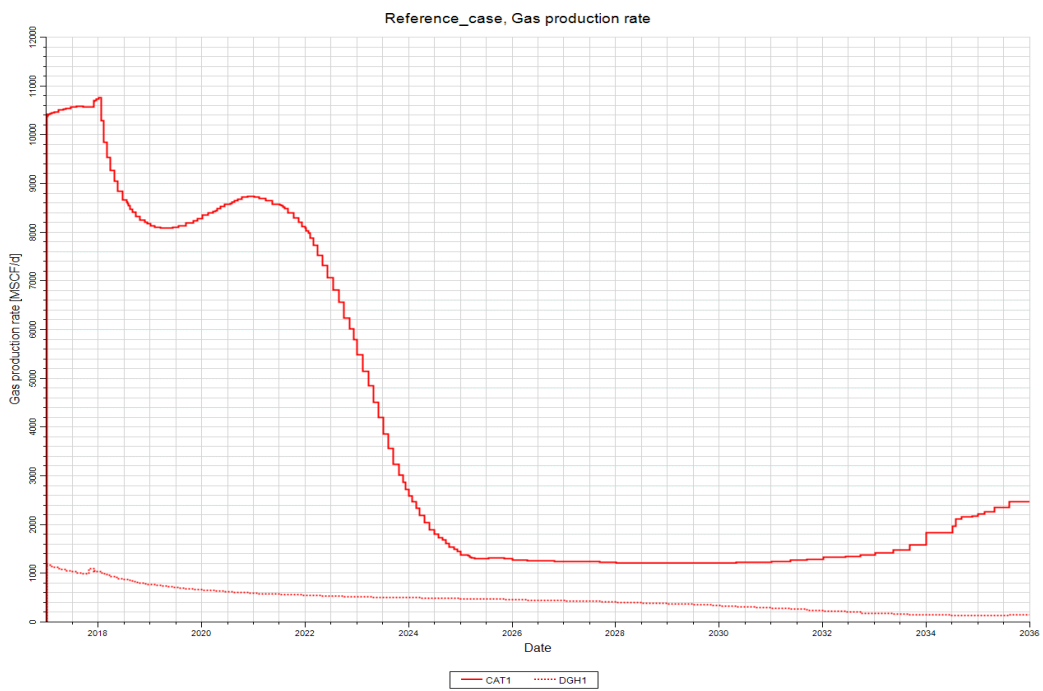


Figure 3.31- Gas production reference case for both wells

3.2.4.3 Case skin 3

In this case, the skin is increased to three so the output results were as follows:

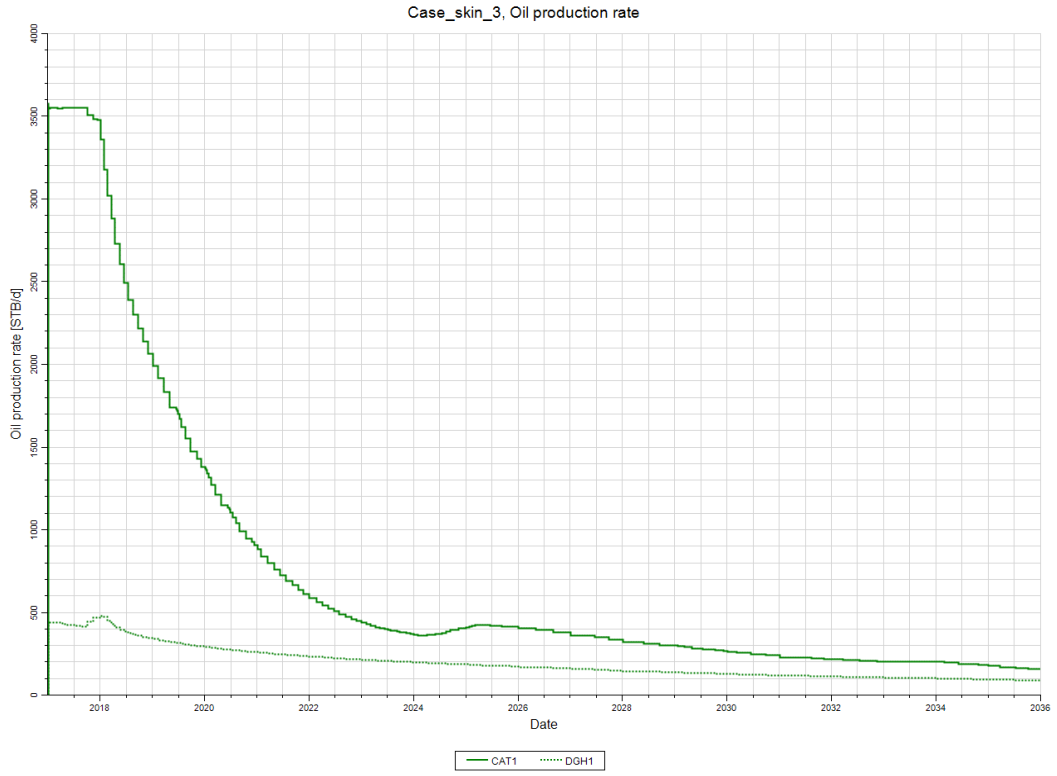


Figure 3.32- Oil production for skin=3 for both wells

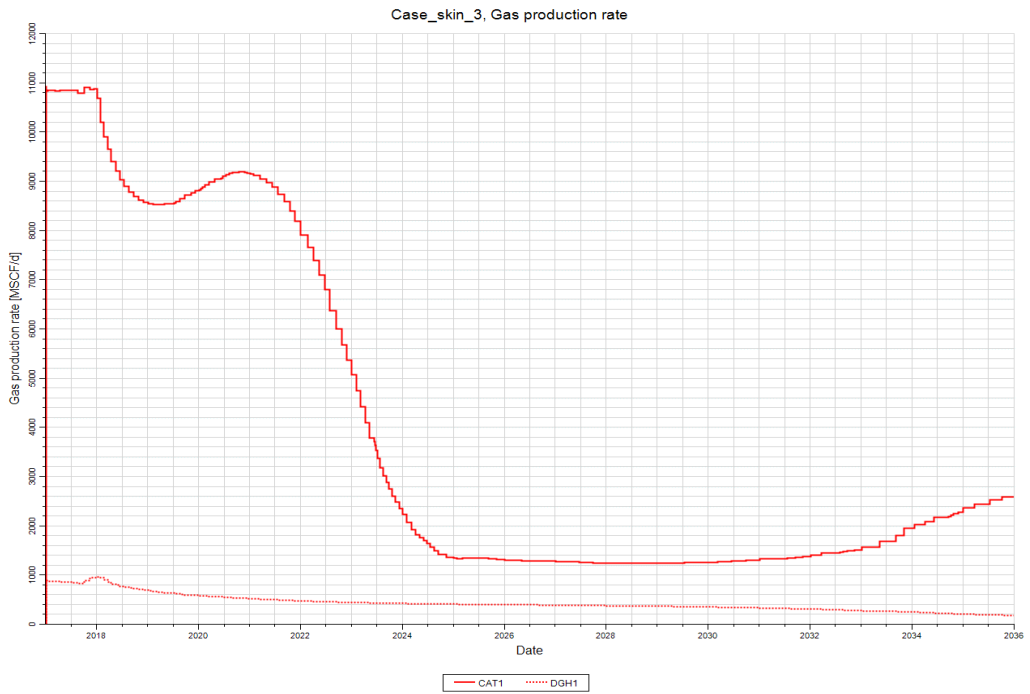


Figure 3.33- Gas production for skin=3 for both wells

3.2.4.4 Case skin 10

In this case the skin is equal to 10 the results are as follows:

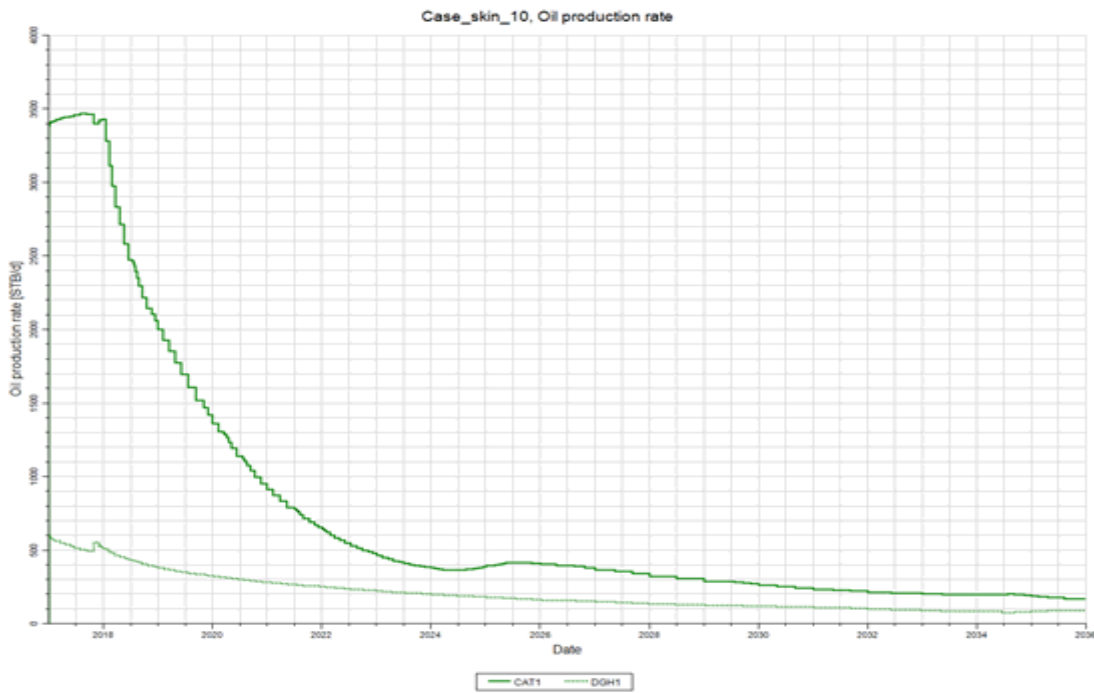


Figure 3.34- Oil production for skin=10 for both wells

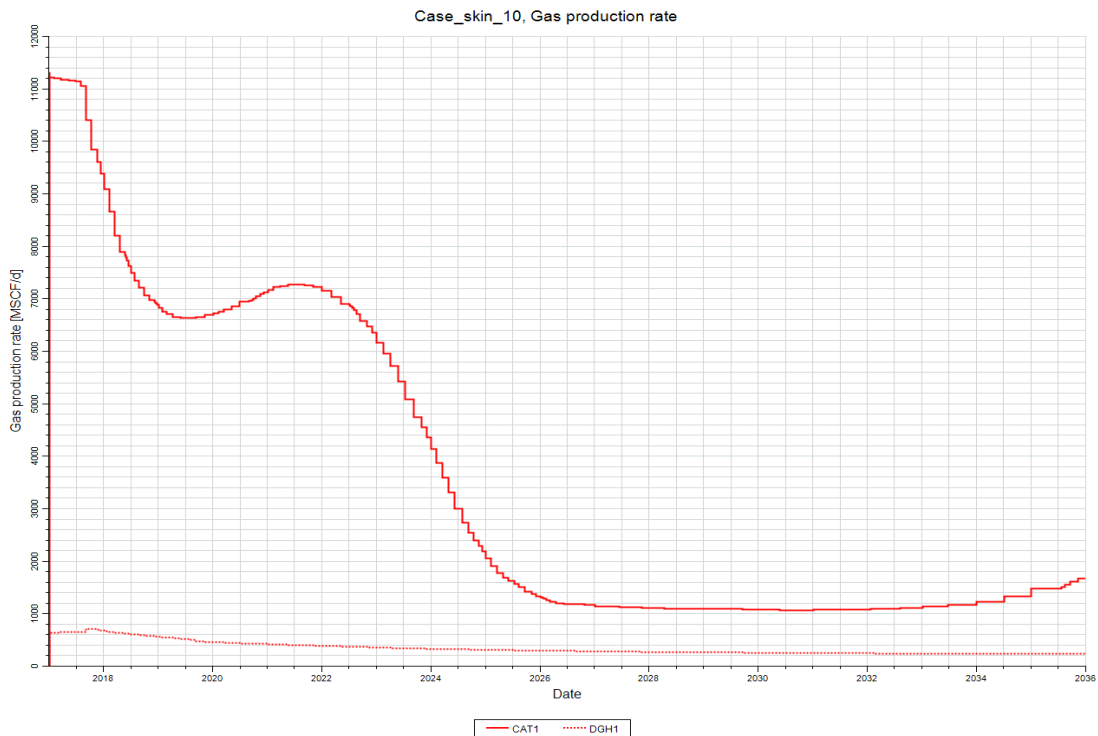


Figure 3.35- Gas production for skin=10 for both wells

3.2.4.5 Case skin 13

In this case, the skin is equal to 13 that is, almost, equal to the skin determined in 2017 by well test analysis:

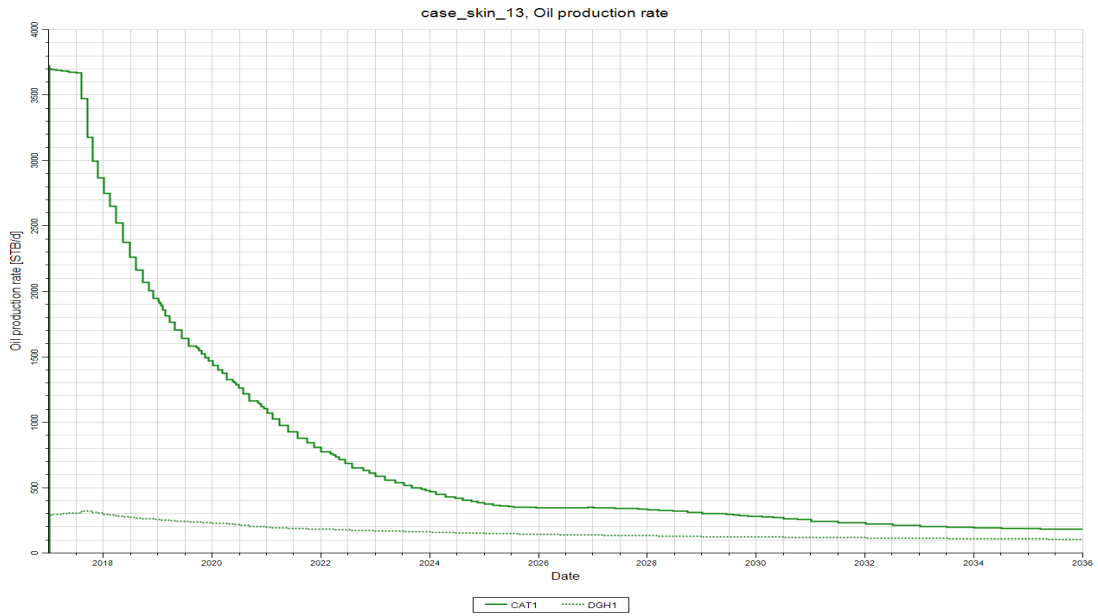


Figure 3.36- Oil production for skin=10 for both wells

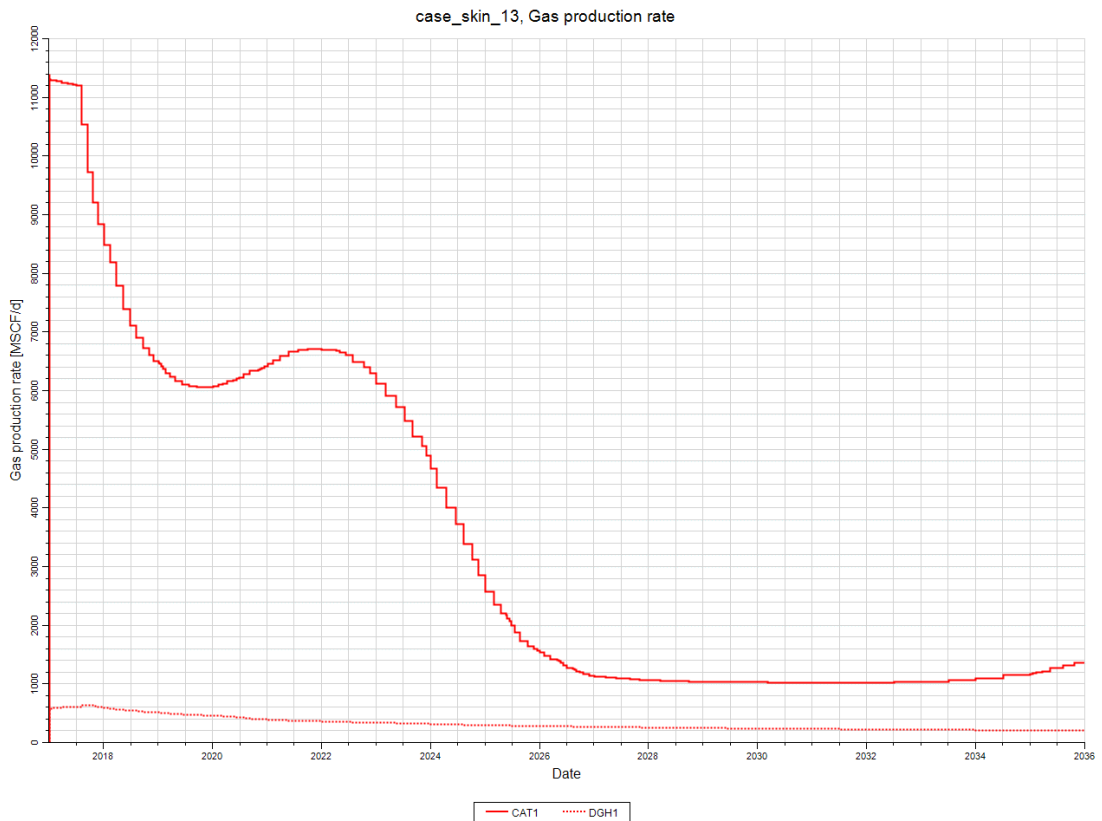


Figure 3.37- Gas production for skin=10 for both wells

3.2.4.6 Permx EL Atchane=0.5

In this scenario, we assume, as shown in figure below, permeability equals to 0.5 mD (reduction by a factor of 3) of EL Atchane formation (1.5 mD) which is considered as tighter than EL Hamra formation. All the other input properties are the same as in the reference case.

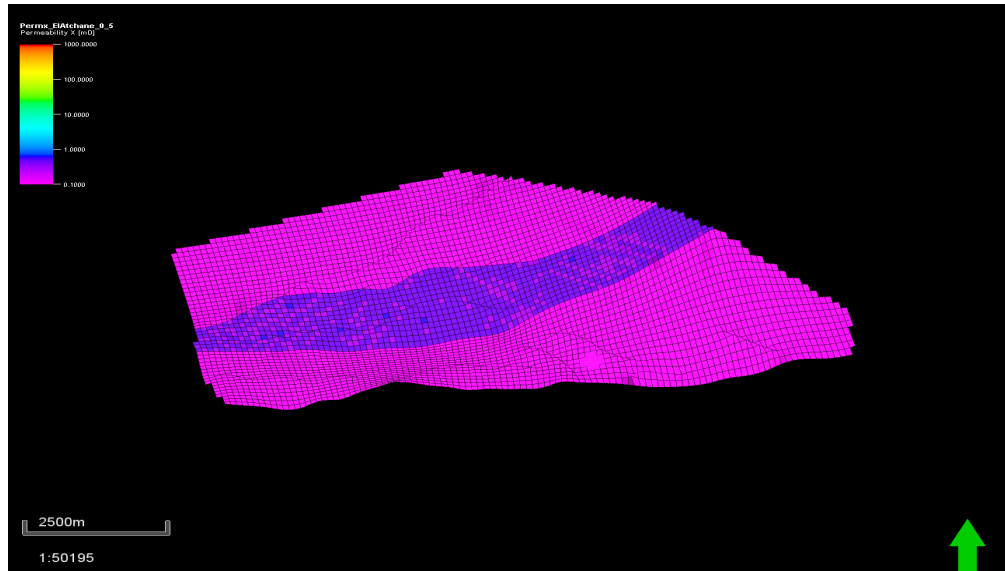


Figure 3.38- Permx EL atchane distribution

The output of oil and gas rate prediction for both wells is shown in figures below:

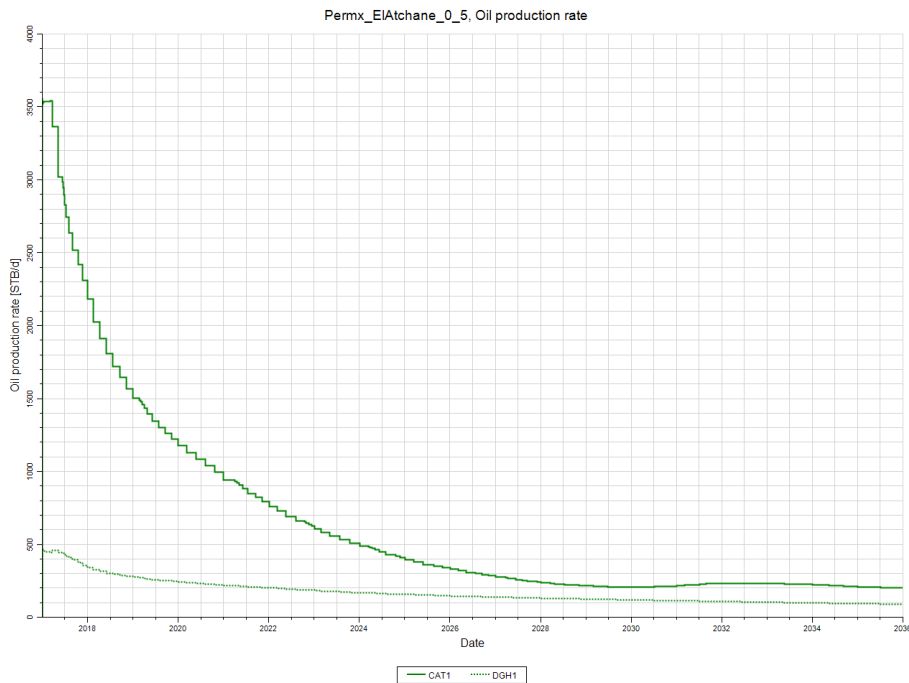


Figure 3.39- Oil production for Permx_ELAtchane=0.5

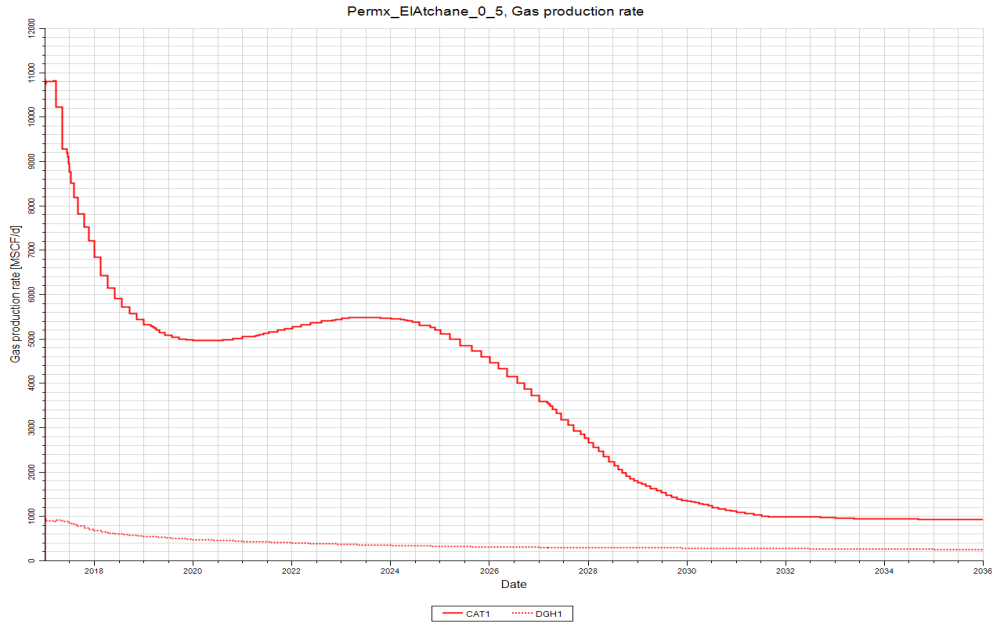


Figure 3.40- Gas production rate for $Perm_x=0.5$

3.2.4.7 Perm_x EL Atchane =0.5 and skin=0

The permeability is kept reduced to 0.5 with a skin equals to zero. All the input properties are the same as in the reference case.

The prediction output of oil and gas rate for both wells are as following:

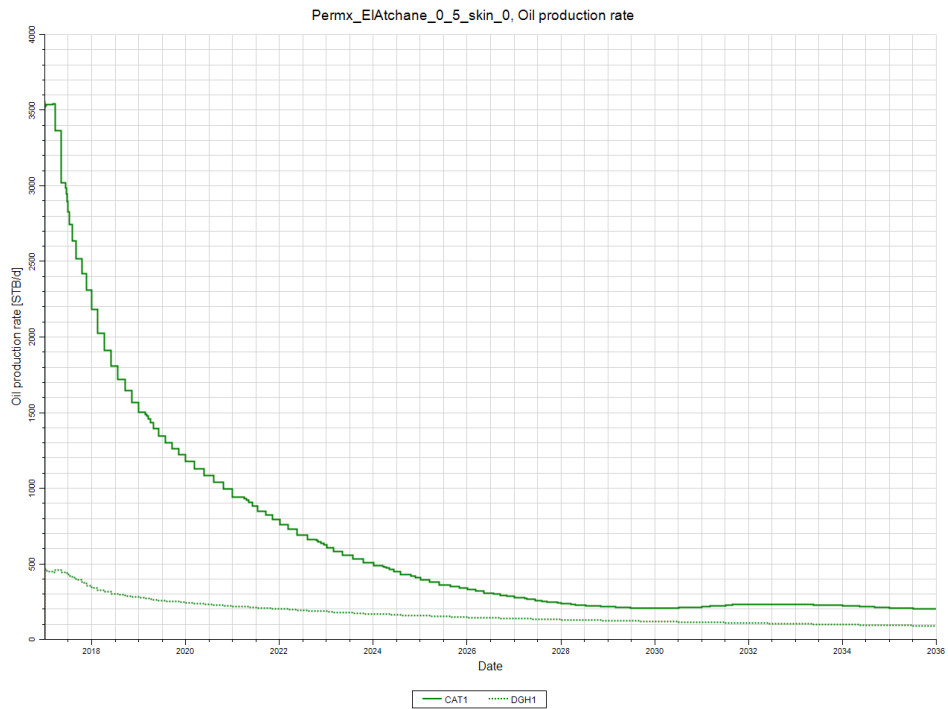


Figure 3.41- Oil production rate for $Perm_x=0.5$ and $skin=0$

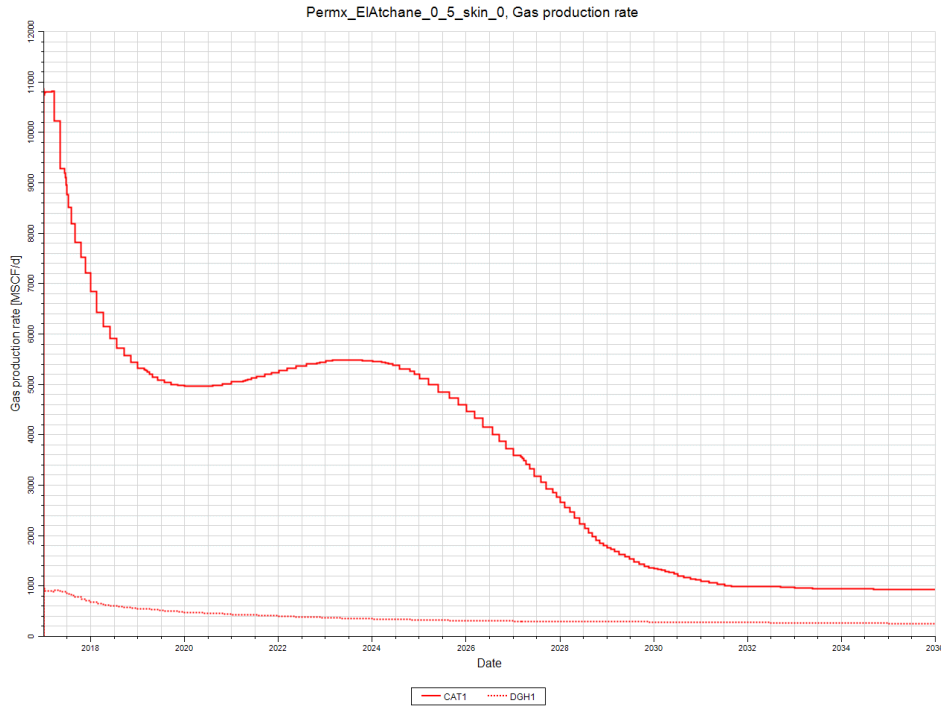


Figure 3.42- Gas production rate for Permx=0.5 and skin=0

3.2.4.8 Permx EL Hamra_4

By means of hydraulic fracturing, the permeability of el Hamra formation may be increased by a factor of four as shown in figure below:

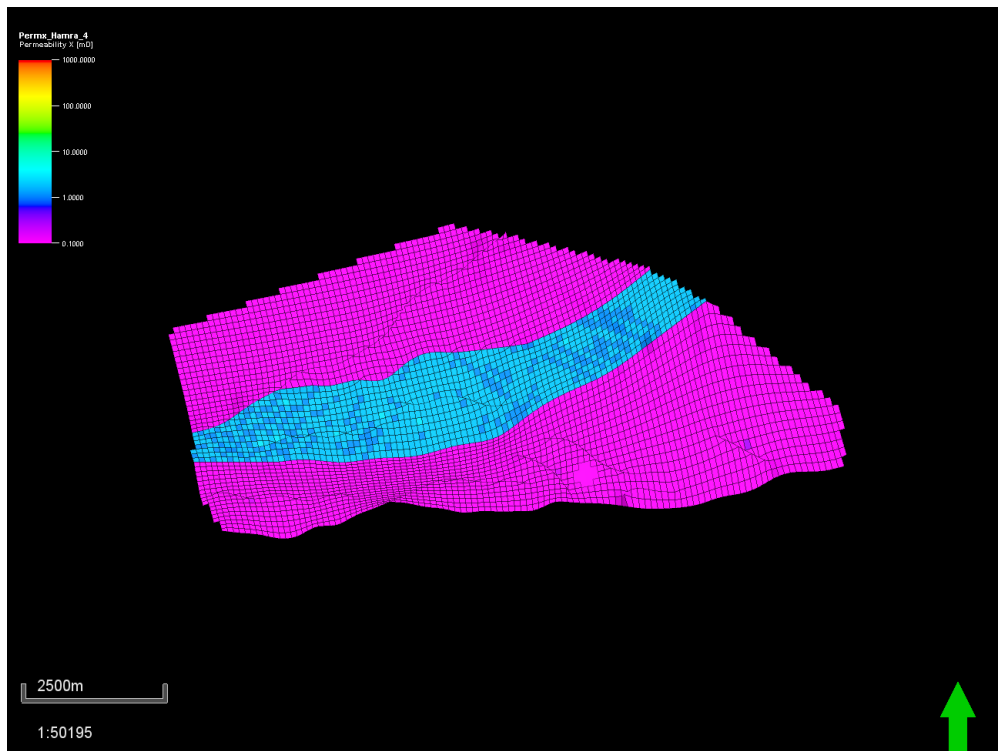


Figure 3.43- Permx El Hamra increased by a factor of four

The output of oil and gas prediction rate is as following:

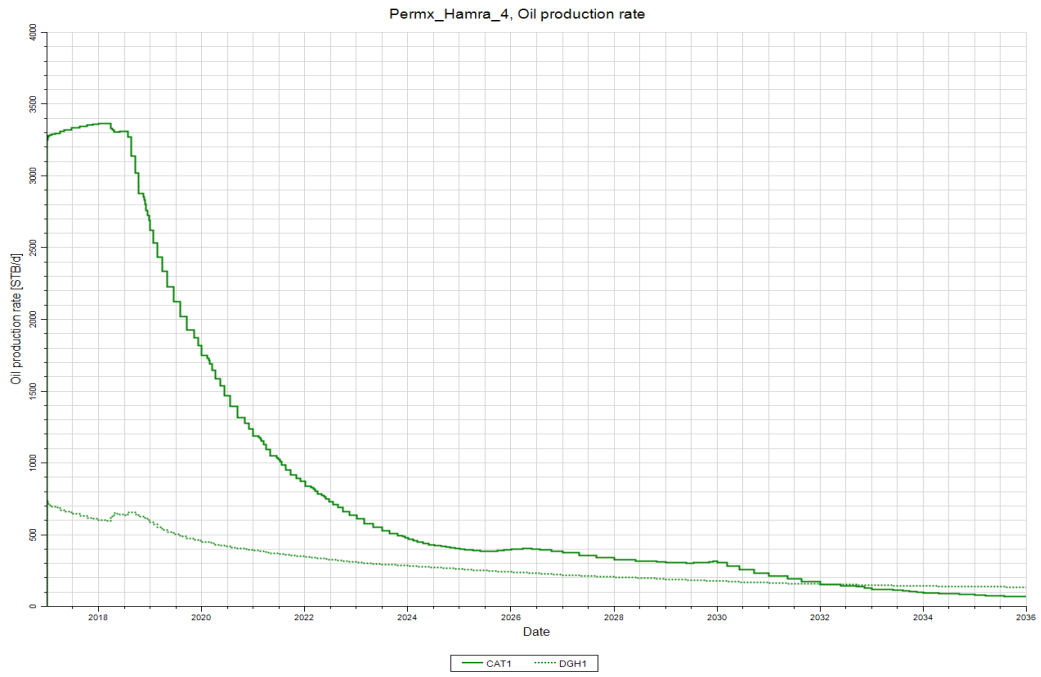


Figure 3.44- Permx ElHamra oil production rate

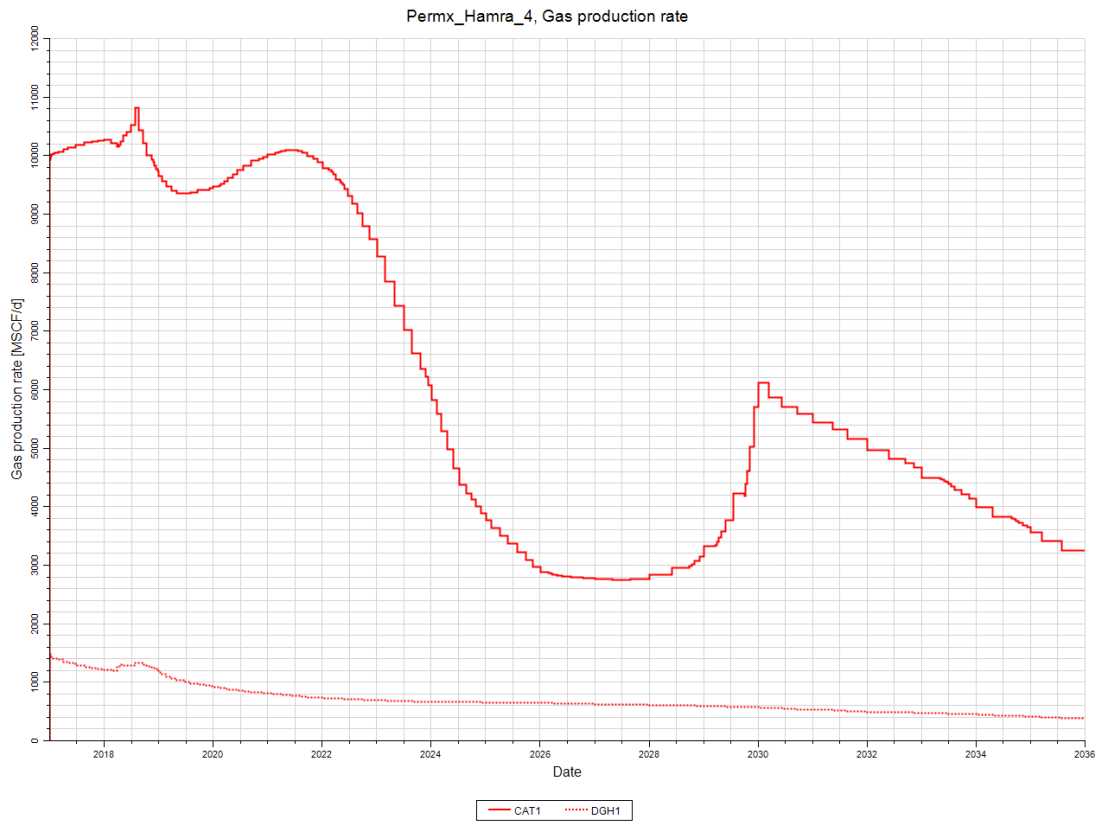


Figure 3.45- Permx E lHamra gas production rate

3.2.4.9 Permx EL Hamra_4 and skin=0

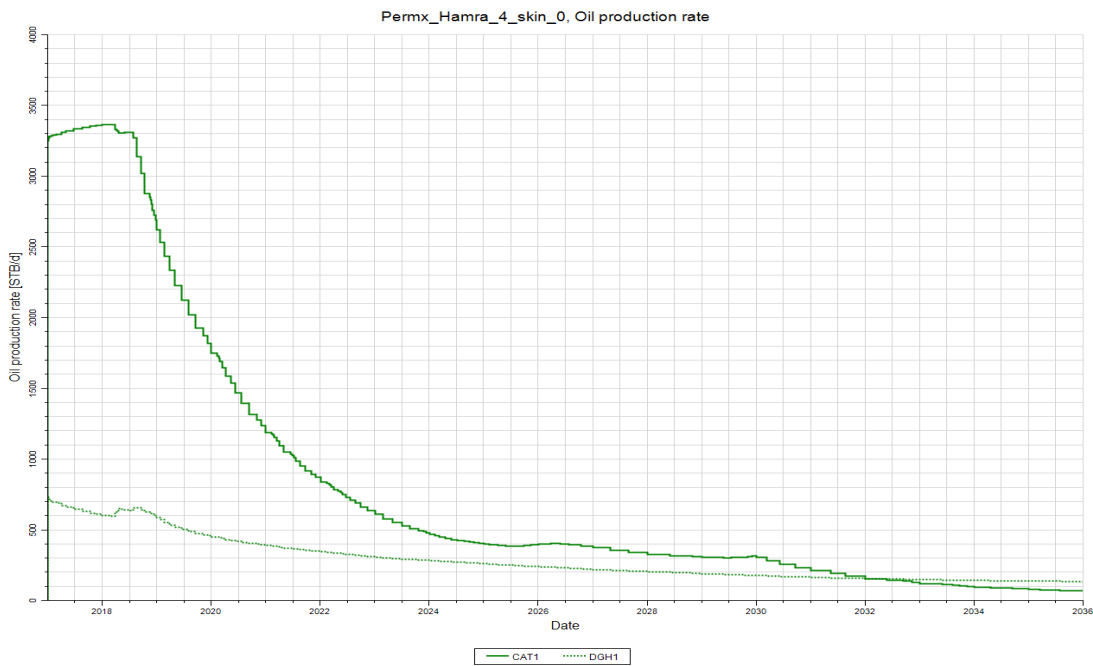


Figure 3.46- Permx El Hamra_4_skin_0 oil production rate

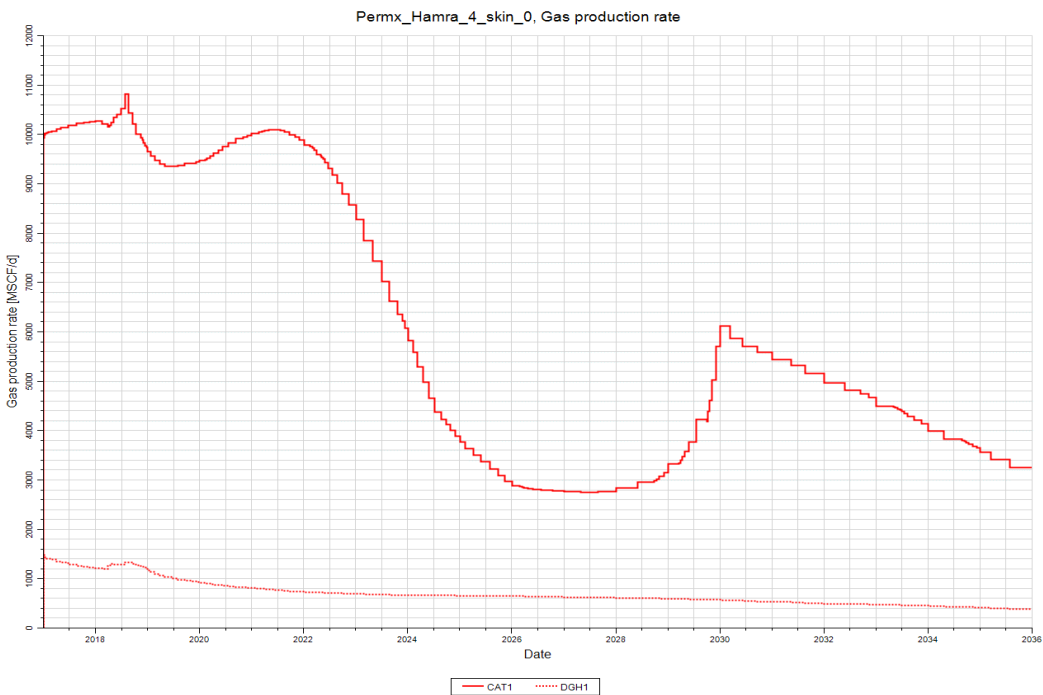


Figure 3.47- Permx El Hamra_4_skin_0 gas production rate

3.2.4.10 Oil water contact OWC=3740 ft

In this scenario, the oil water contact is estimated to be 3740 ft instead of 3760 ft which will obviously affect the original oil in place and thus the cumulative production.

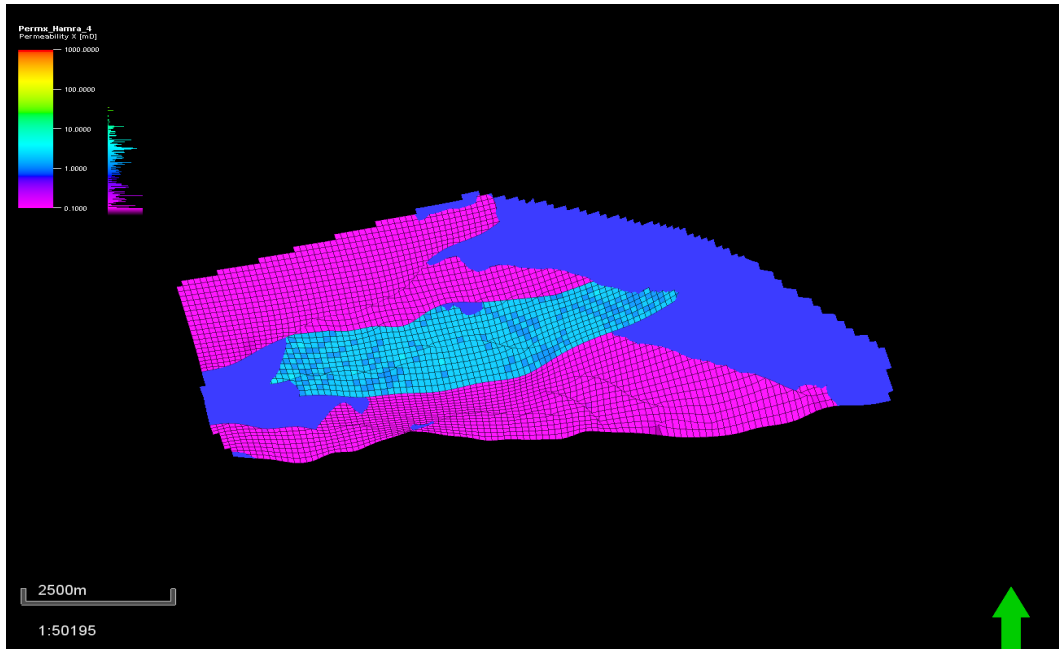


Figure 3.48- Oil water contact at 3740

The output for oil and gas prediction rate is as following:

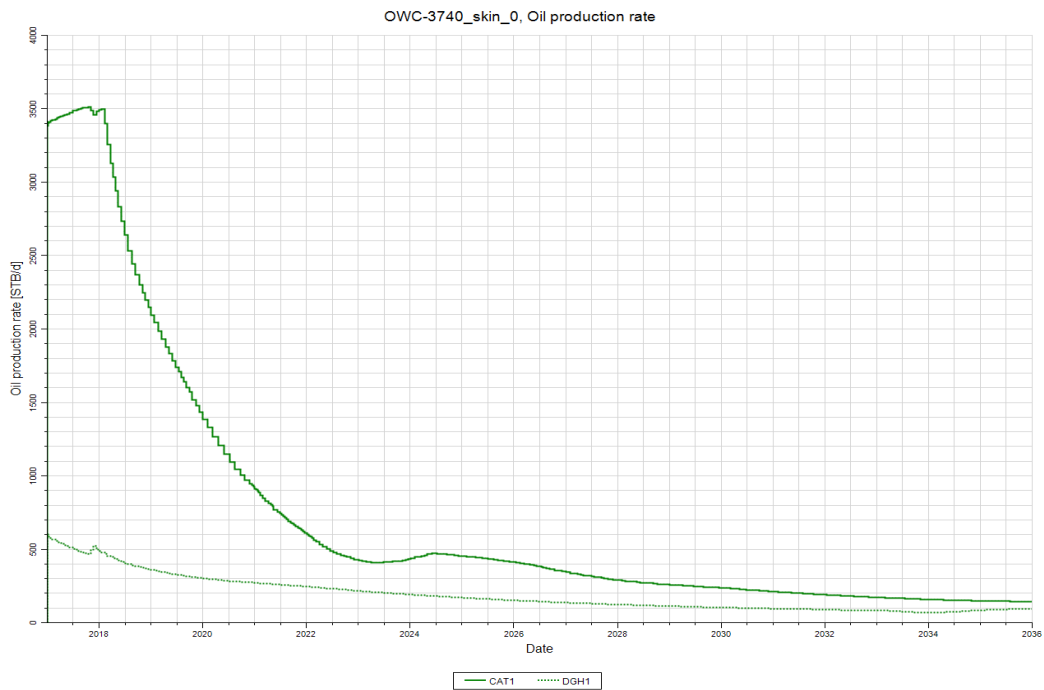


Figure 3.49- OWC_3740 oil production rate

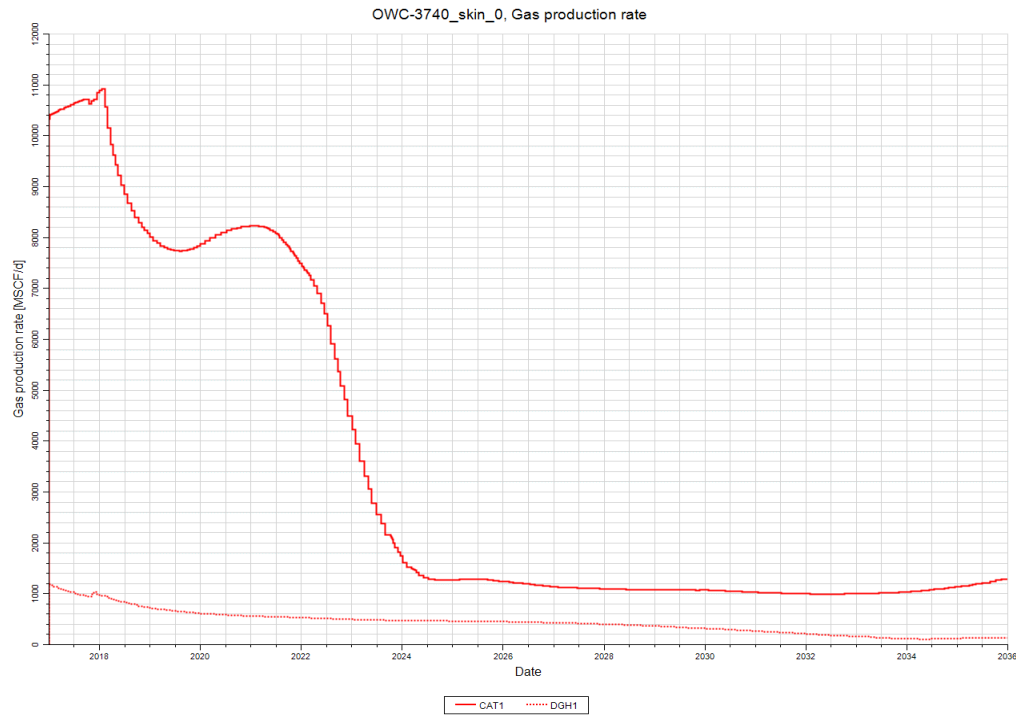


Figure 3.50- OWC_3740 gas production rate

3.2.5 Development strategies

3.2.5.1 Perenco scenario (base case prediction)

This case consists in involving another company called Perenco, which is independent Anglo-French oil, and gas Company that has its own production field in the area. The point was to keep the same input as the base case with the same constraints and the produced oil and gas is transported and stored within perenco's equipments. Therefore, this case only influences the economic level.

Obviously, the outputs of oil and gas rates are the same as the base case.

3.2.5.2 Gas injection scenario

During this scenario, by dint of its better reservoir properties, CAT-1 is converted to an injector CAT-1GI (as shown in figure3.50) starting from 2023 until 2036. Actually, CAT-1 keeps also producing from El Hamra formation since the injection process is achieved at the level of the underlying formation (El Atchane). This scenario has no impact on DGH-1 since the two wells are separated by a non-sealing fault.

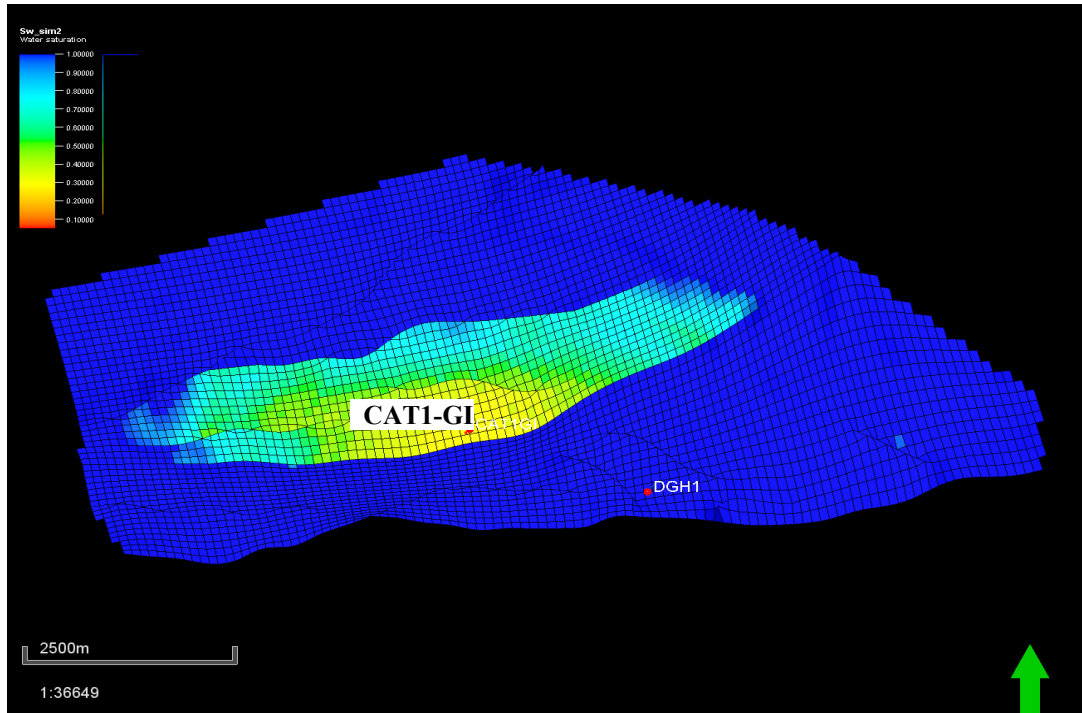


Figure 3.51- The injector CAT-1GI location

The output of the oil and gas production for both wells besides gas injection rate is shown below:

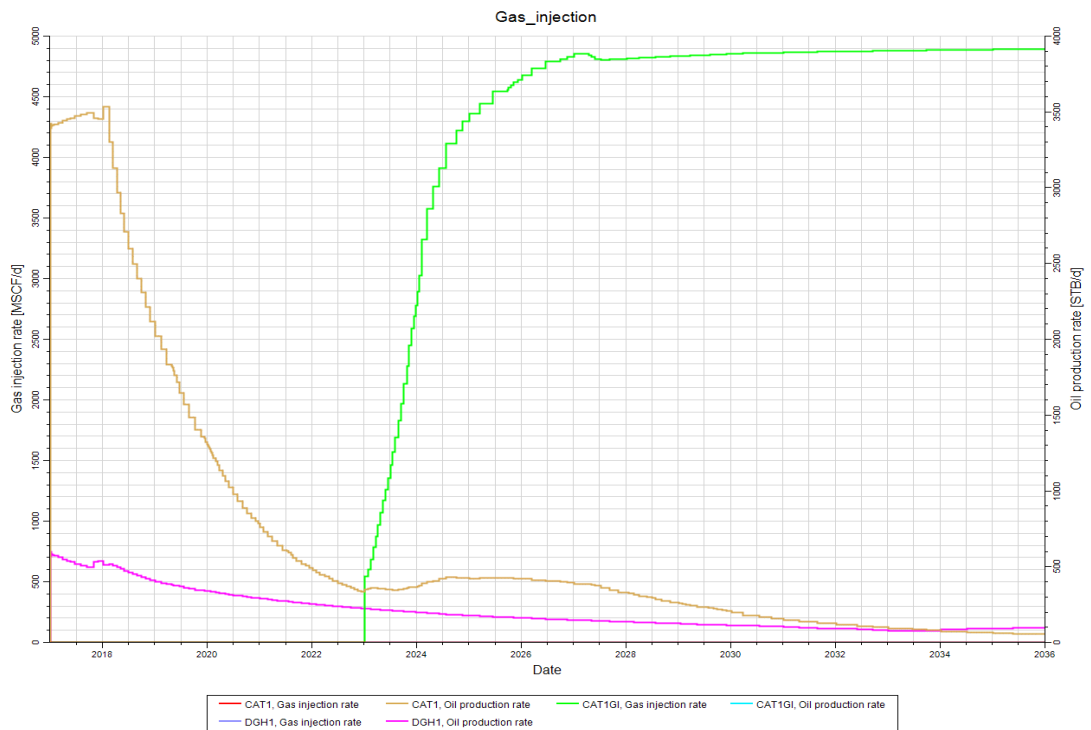


Figure 3.52- Oil production, Gas injection rate for both wells

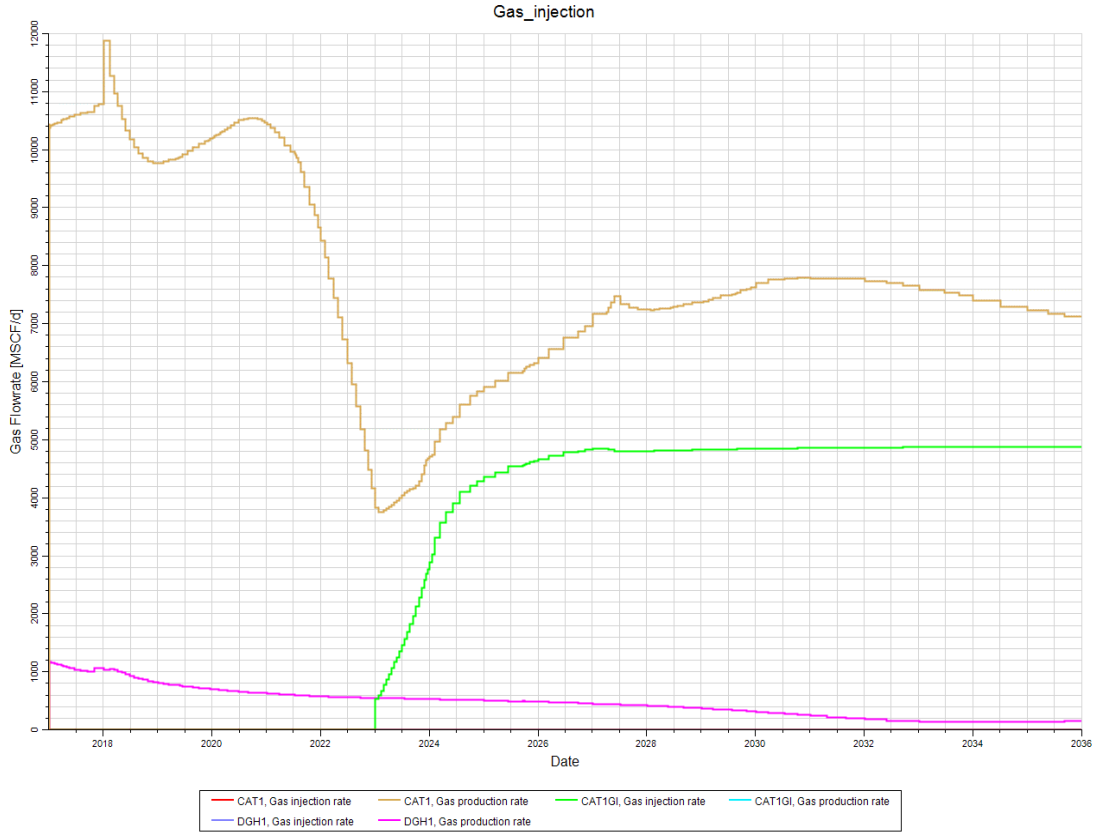


Figure 3.53- Gas flow rate, Gas injection for both wells

This table summarizes the cumulative production of oil and gas for both wells:

Table 3.12- Cumulative production of oil and gas for all cases (both wells)

Cases	Np, MMSTB	Gp, Bscf
Base case	6.35	27.48
Reference case (skin 0)	6.56	30.22
Gas injection	6.21	57.20
Skin_3	6.49	30.06
Skin_10	6.43	27.35
Skin_13	6.38	26.47
Permeability_ELAtchane_0.5	5.79	25.08
Permeability_ELAtchane_0.5_skin_0	5.81	25.34
Permeability_ELHamra_4	7.72	46.73
Permeability_Elhamra_4_skin_0	7.89	46.94
OWC_3740	6.47	27.38

Chapter 4

Results and Discussion

In the reservoir simulation section, the model is good matched with available DST data. Actually, it is suitable for production forecast and assessing further reliable development plans.

However, the sensitivity analysis has shown that the case of higher permeability (multiplied by 4) gives the most productive case (7.89MMstb) whereas the lowest productive case is the one with the lowest permeability (5.79 MMstb). For that reason, hydraulic fracturing may be a good development scenario to enhance the production but it has to be consistent with corporate factors and incorporate the time value of money.

The comparison of build-up tests conducted on both wells between the year 2015 and 2017 has shown a significant increase in skin factor, which has led to a reduced permeability and thus productivity. However, this important issue may be solved using two common methods of stimulation, which are matrix acidizing and hydraulic fracturing.

Hydraulic fracturing also known, as "fracking" is a decades-old technique that unlocks oil and natural gas from deep hydrocarbon formation. It is an efficient technique that helps in increasing the productivity of a well by allowing the trapped hydrocarbon within the rock to flow freely toward the wellbore by creating an artificial channel. In fact, the process of fracking consists in pumping under a very high pressure (high enough to overcome the rock closure stress and cause the rock failure). Moreover, fluid fracturing choice is made upon reservoir properties, the ideal fluid should be able to transfer the propping agent toward the fracture, be compatible with the formation rock and, of course, has to be cost-effective. In addition, matrix acidizing is also considered as an efficient method of stimulation when it comes to an under-productive wells. Below the reservoir fracture pressure, an acid is pumped into the well, specifically, into the pores of the formation in order to dissolve the sediments and mud solids that are lowering the

permeability and hence allowing hydrocarbons to flow easily. It is essential to know the type of formation and its composition before starting the acidizing treatment to get positive results. In our case, sandstone formations, the acid used to dissolve quartz and feldspar that are blocking pore spaces is hydrofluoric acid (HF). Two other techniques may be employed as well to reduce skin damage which are drilling a sidetracking horizontal well from the already existing vertical one in order to enhance the drainage area or simply re-perforating.

Chapter 5

Conclusion

The most significant conclusions to be drawn as a result of this thesis, is, firstly, that simulation is a bough of reservoir engineering that is more developed lately since oil and gas companies had to justify their investments. This former requires the collaboration and assistance of different specialists in order to well characterize a reservoir, determine its profitability, and allow the development phase. In this case study, a development plan of Ghrib field was executed based on a sensitivity study that was suggested besides a production forecast of different development scenarios based on a model matched with DST data on ECLIPSE 300.

Secondly, during the production phase, a significant pressure drop occurred. That is why, in the second section, we have numerically investigated well test responses on Ecrin Saphir (KAPPA) in order to understand this unexpected behavior. Although, these tests have given acceptable results it is more recommended executing a new well test because the pressure behavior during the last test was aberrant, most probable because of the flush of volatile oil into gas and thus the existence of two-phase flow inside the tubing. Besides, an update of the dynamic model and a new simulation study should be done to assess further development plan.

Chapter 6

References

Retrieved from Kappaeng: <https://www.kappaeng.com/software/saphir/overview>

Asser, m. a. (2015). *Simulation and interpretation of well test in pressure sensitive reservoir*.

Chaudhry, A. U. (2004). *Oil Well Testing Handbook*. USA .

chen, z. (2007). *reservoir simulation mathematical techniques in oi recovery* . Canada.

Clement, W. P. (2008, February 2). *Writing and Thinking Well*. Retrieved July 13, 2016, from <http://cgiss.boisestate.edu/~billc/Writing/writing.html>

ferrero, P. (2001). *pressure transient analysis*. houston.

G.Bourdarot. (2010). *Well testing interpretation methods*.

(2015). *Ghrib concession POD*. Tunis.

jelmert, T. A. (2000). Retrieved from http://www1.uis.no/Fag/Learningspace_kurs/PetBachelor/webpage/tech%5CReservoir%5CPressureTestAnalysis%5Cpressbui.pdf.

Kirmaci, H. (2014). *A reservoir engineering study for field development*.

kuiper, I. (2009). *well testing in the framework of system identification* .

M.onur, F. k. (2010). *pressure transient formation and well testing*. Netherlands.

Matthews, C. S. (1967). *Pressure Buildup and Flow Tests in Wells*.

Oliver houzé, d. v. (2008, octobre). *dynamic flow analysis*.

Pesendorfer, D. M. (2015). *Boundary response*.

rossito, d. (2003). *well test analysis*.

skin factor. (n.d.). Retrieved from test wells: <https://www.testwells.com/the-skin-factor/>

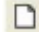
slotte, A. (2017). *Lectures note in well testing*.

Swiss Academic Software. (n.d.). *Citavi - Organize your knowledge. Reference management, knowledge organization, and task planning*. Retrieved May 24, 2016, from <https://www.citavi.com/>

Appendix A

Appendix A

A.1 Ecrin Sapphire tutorial

This is a simple tutorial explaining basic features of Saphir Ecrin while conducting a build up test. It is assumed that the software has been installed. After running Ecrin a new file must be opened by clicking on new  in the toolbar. A succession of dialogs will be displayed where you can put in values. The first one as shown in figure below allows the user to specify the test type, fluid reference, what rates are available, average porosity, thickness and well radius. We can also choose the reference time based on the given data.

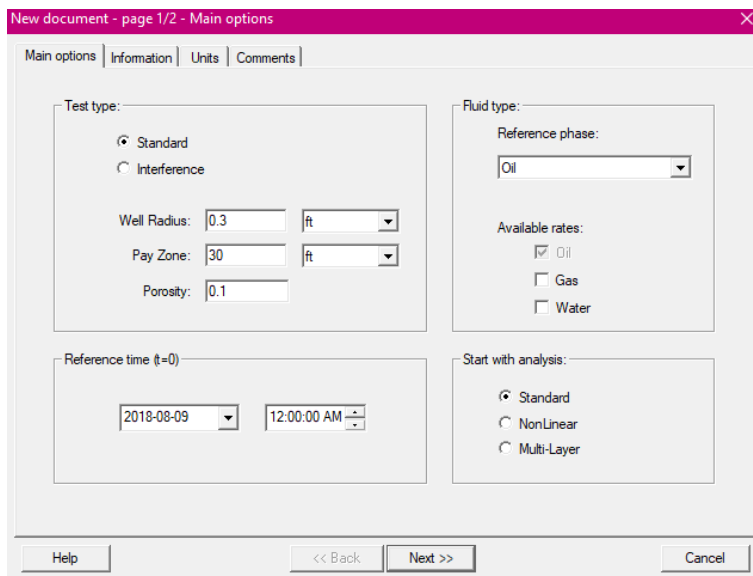
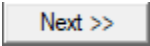


Figure 6.1- Initialization dialog 1/2

By clicking next , a second dialog is displayed which is dedicated to PVT characteristics, fluid viscosity, formation volume factor and the system compressibility.

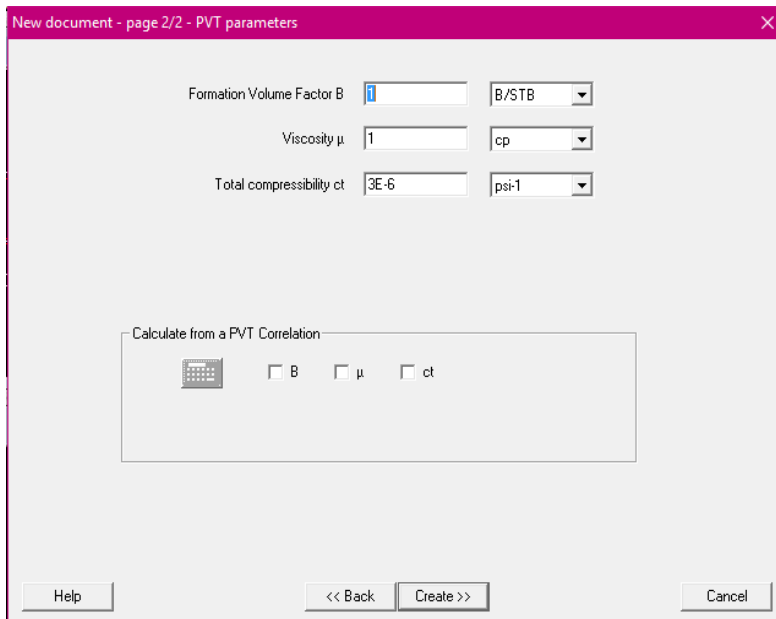





Figure 6.2- Initialization dialog 2/2

Once you click on create, a new project will be created and thus saphir main screen is displayed where you can load flow rates by pressing on  and load pressure . We first start by loading the flow rates, So window will be displayed where you upload the file that contains the data of the rate by clicking on , a preview of the data will be shown as in the figure below:

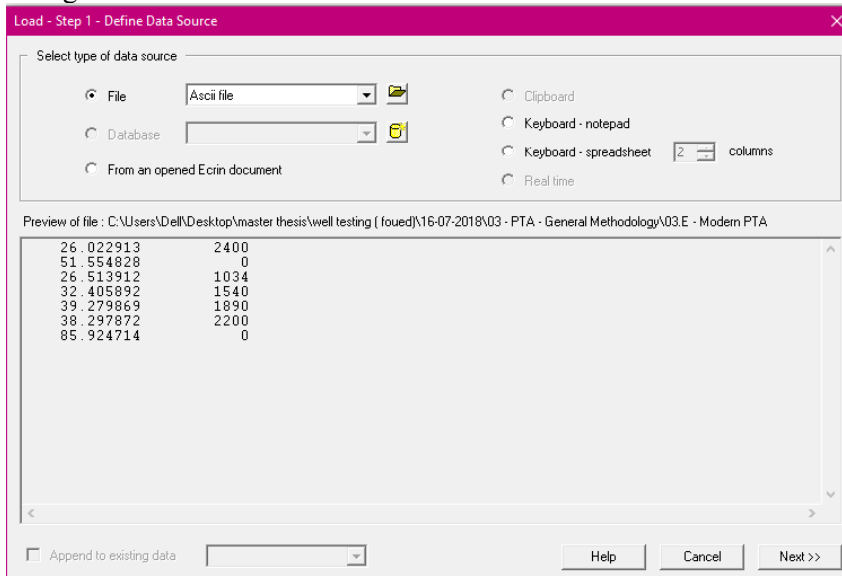


Figure 6.3- Define data source

The software has recognized the file and has automatically assigned the first column as 'decimal time' and the second as 'oil rate' with their appropriate units. You may change the format if needed.

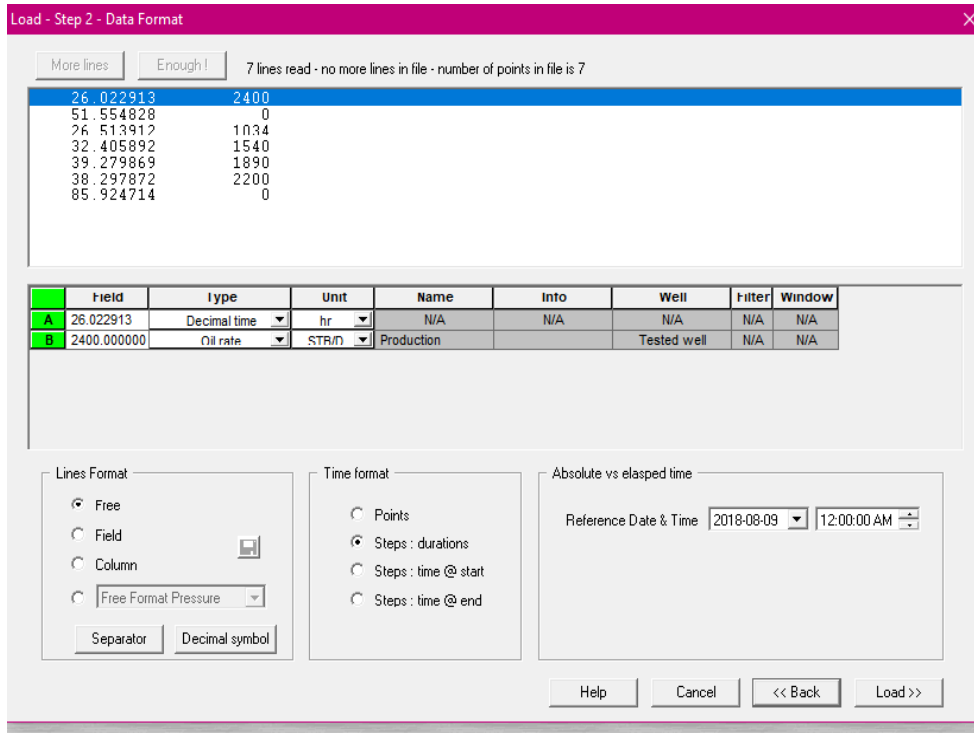


Figure 6.4- Define data format

Then a plot of flow rate is shown as follows:

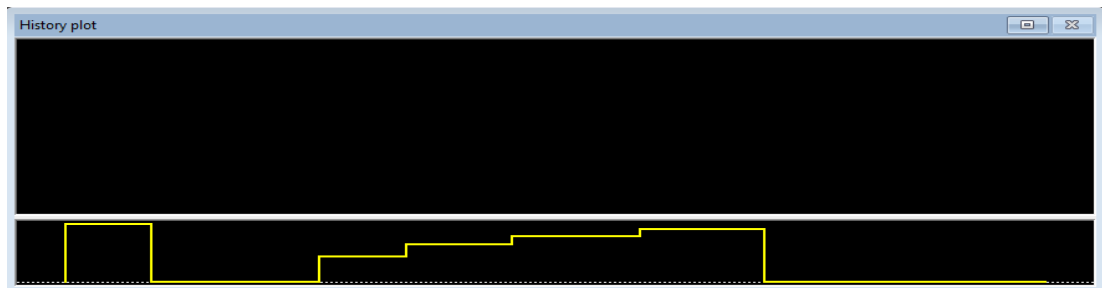


Figure 6.5- Flow rates loading

Basically the same procedure is done with the pressure loading. In other words, a dialog will be displayed exactly the same as in case of flow rates so we upload the right file of pressure and we get 2 plots displayed one describing the pressure (up) and the second describing the rate (down).

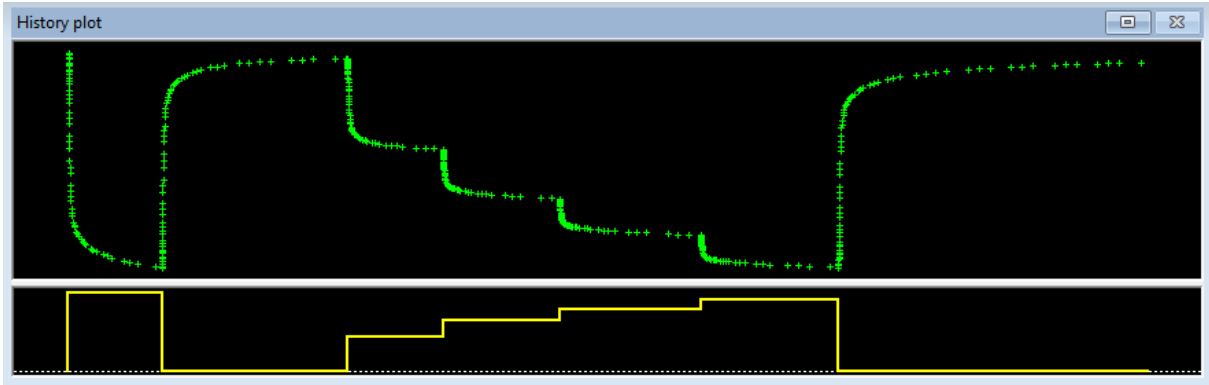
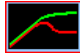


Figure 6.6- History plot

the next step, is extracting the derivative by clicking on  in order to get the reservoir geometries and properties for that reason we extract the build up period :

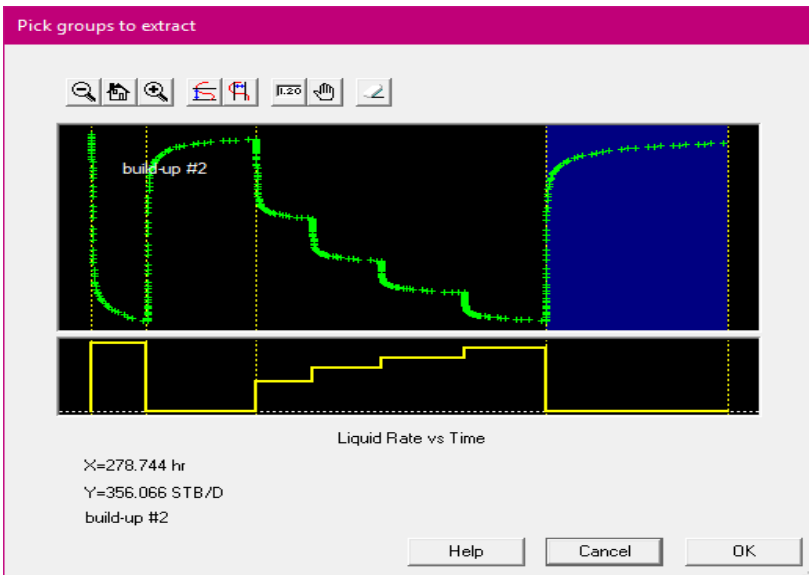


Figure 6.7- Build-up selection

Then, the computed Bourdet derivative is displayed as shown in figure together with delta P:

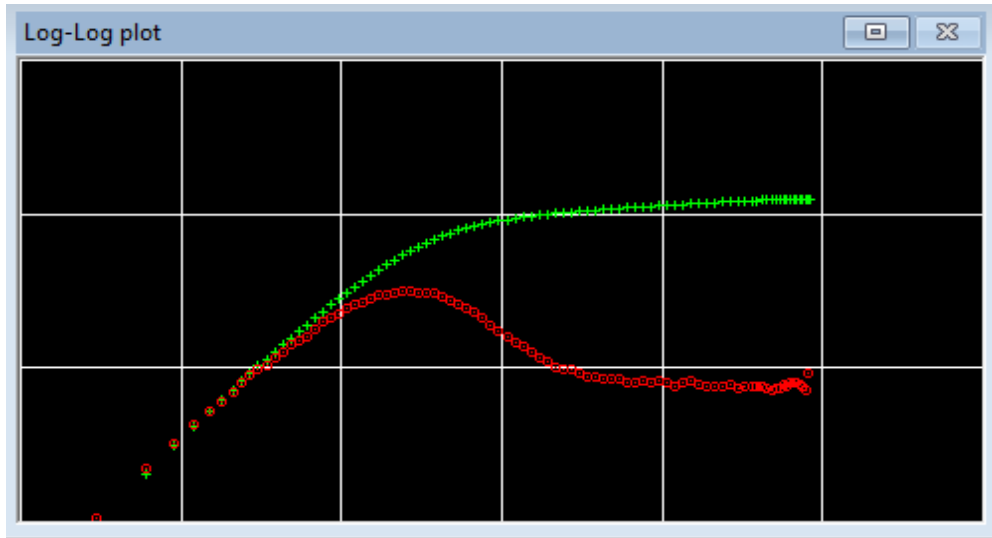
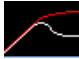


Figure 6.8- Bourdet and delta P plot

Once we got the plot, we run a model that may match the data and yield the results by pressing on . A dialog where the combination of wellbore, well, reservoir and boundary models may be selected is displayed.

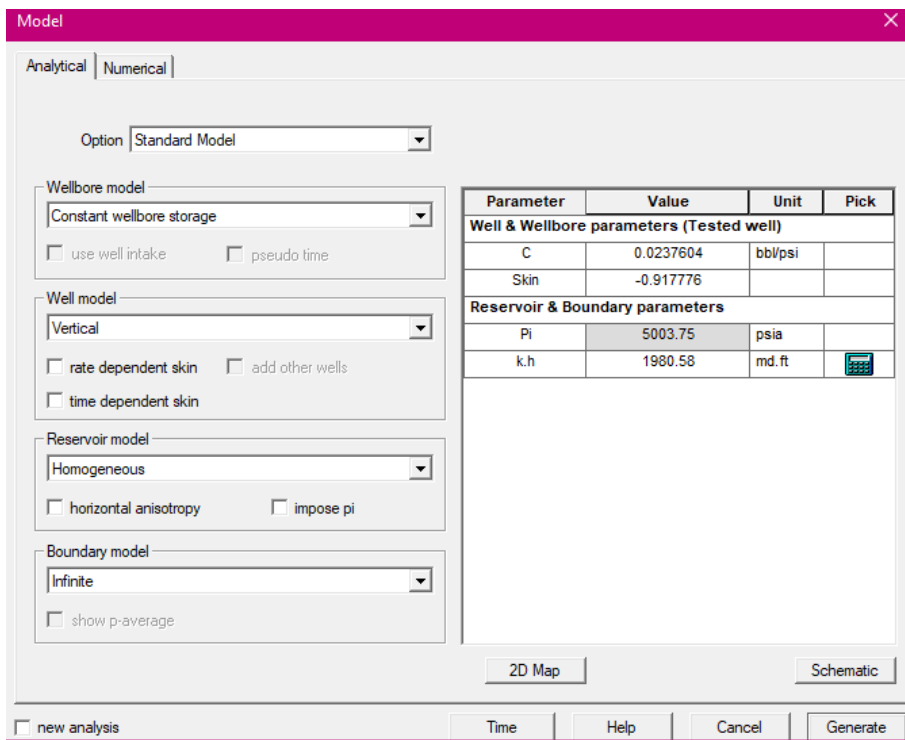
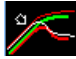


Figure 6.9- Model parameters

the default values of kh (permeability thickness product) and C wellbore storage are deduced automatically from the match made originally by the software.

The model is then generated, it could have, in some cases, an important mismatch that may be corrected by changing manually the skin or wellbore storage values using improve .

Once we realize the best possible match we get the following final plot result with the most important parameters deduced from it.

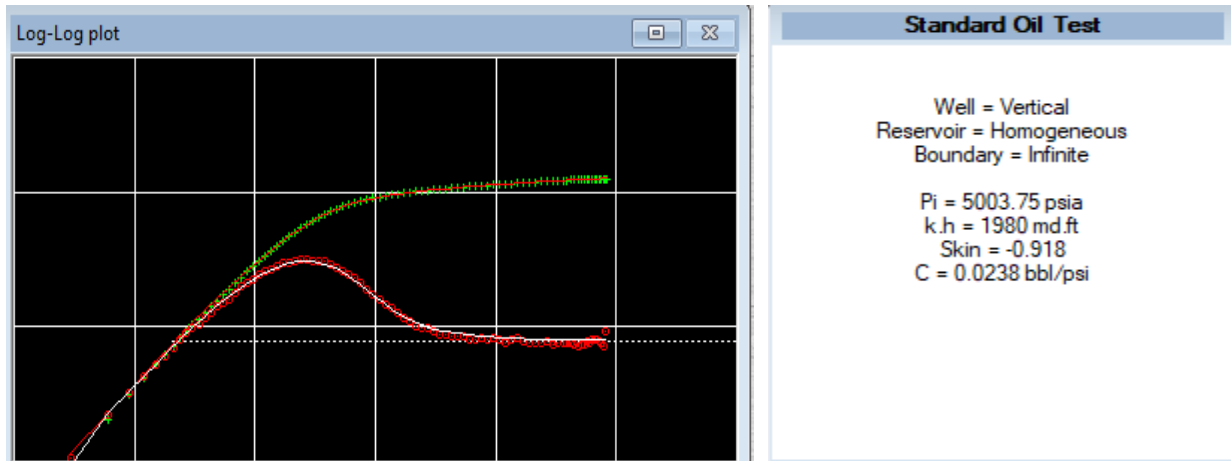
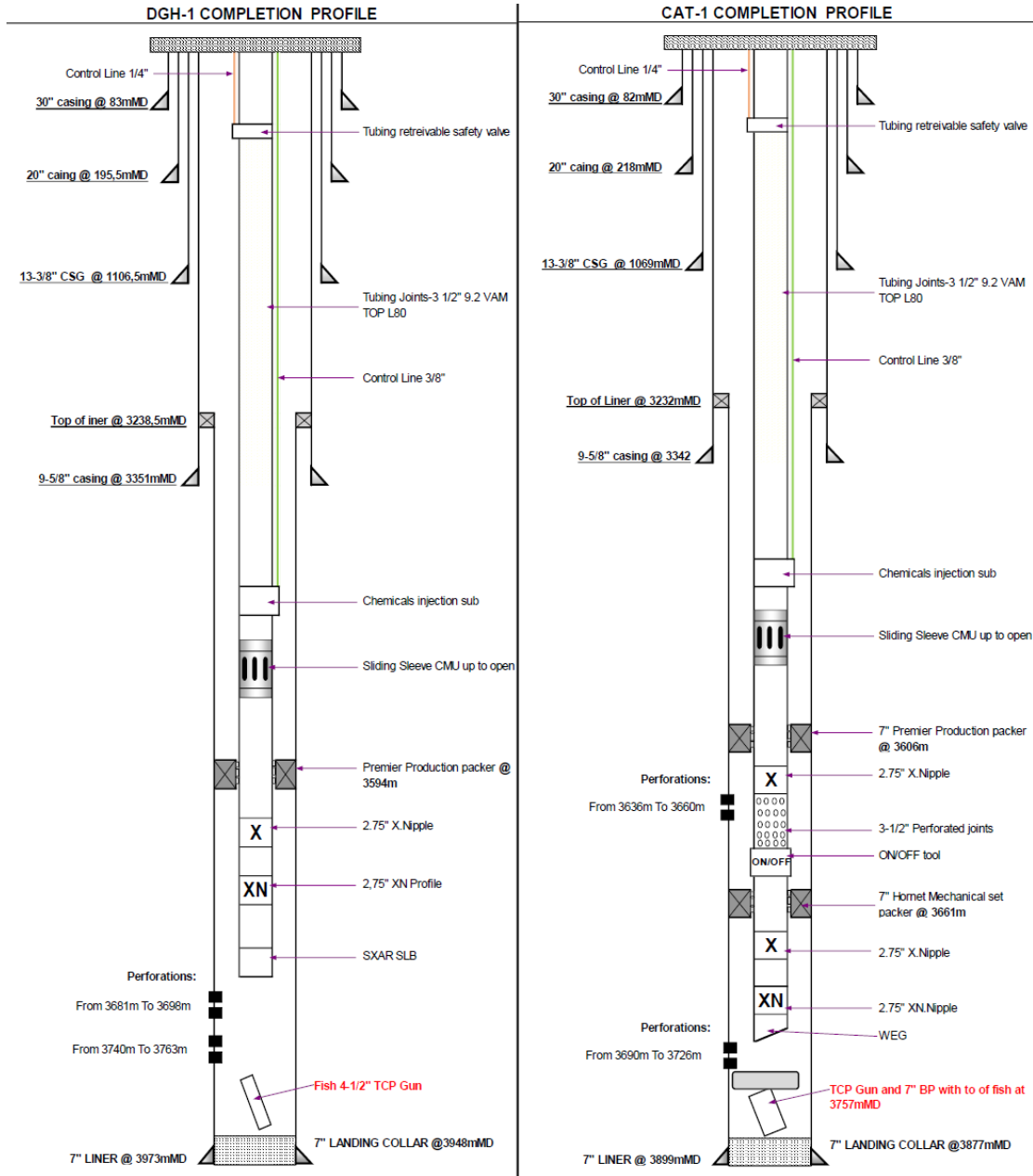


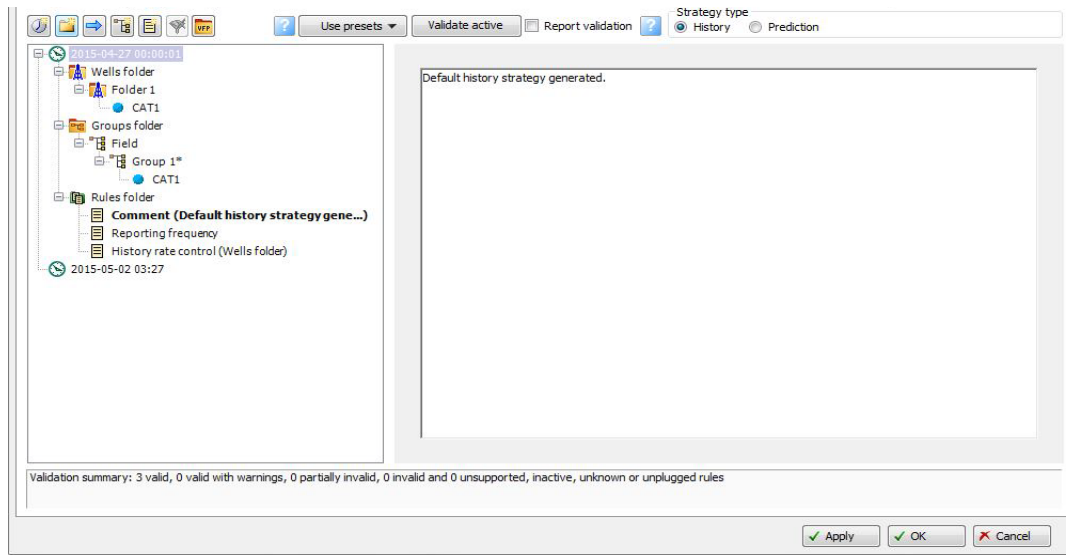
Figure 6.10- Matched model

A.2 Completion profiles



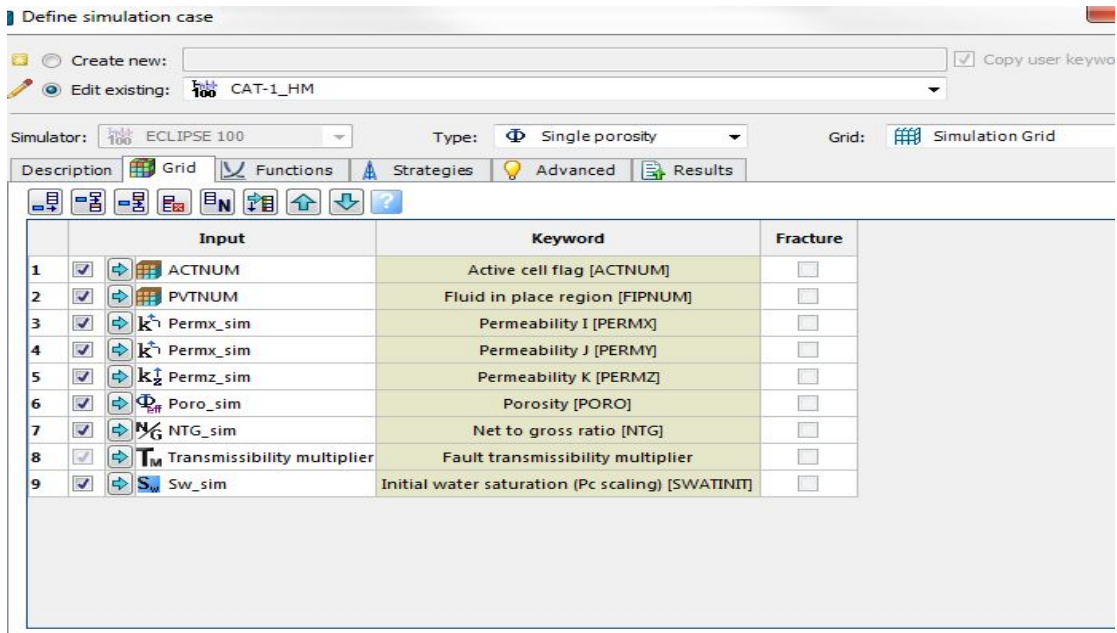
A.3 Simulation tutorial

The history matching was done by defining the start date and the end date of the new history development strategy all by determining the concerned well(s) and the rules if there is any .We start by matching the first well CAT-1 and the same procedure was done later for DGH-1.



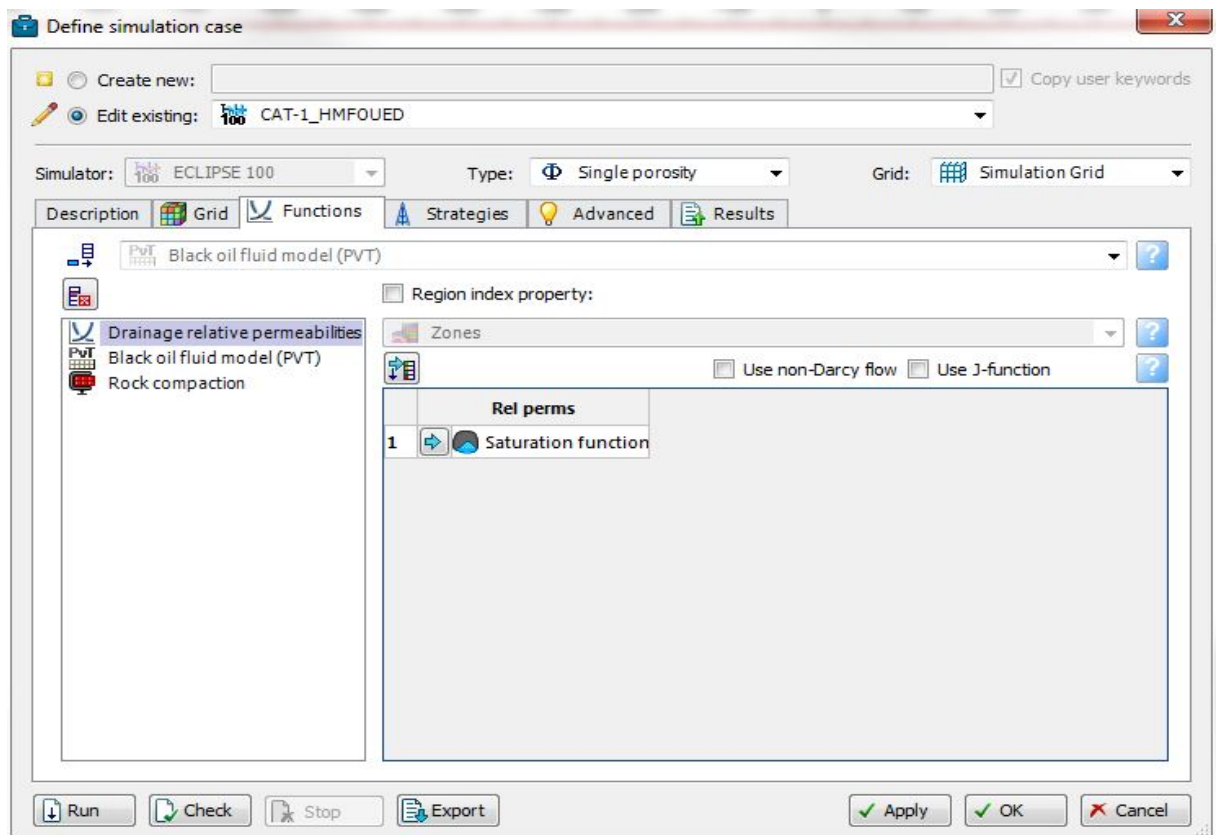
6.11 History matching step

Then we define the simulation case .So, we start by selecting simulator ECLIPSE100 and 'single porosity' for the type. Then we assign each property from the input panel of the provided dynamic model to its appropriate row in the 'grid' tab like shown in figure below.

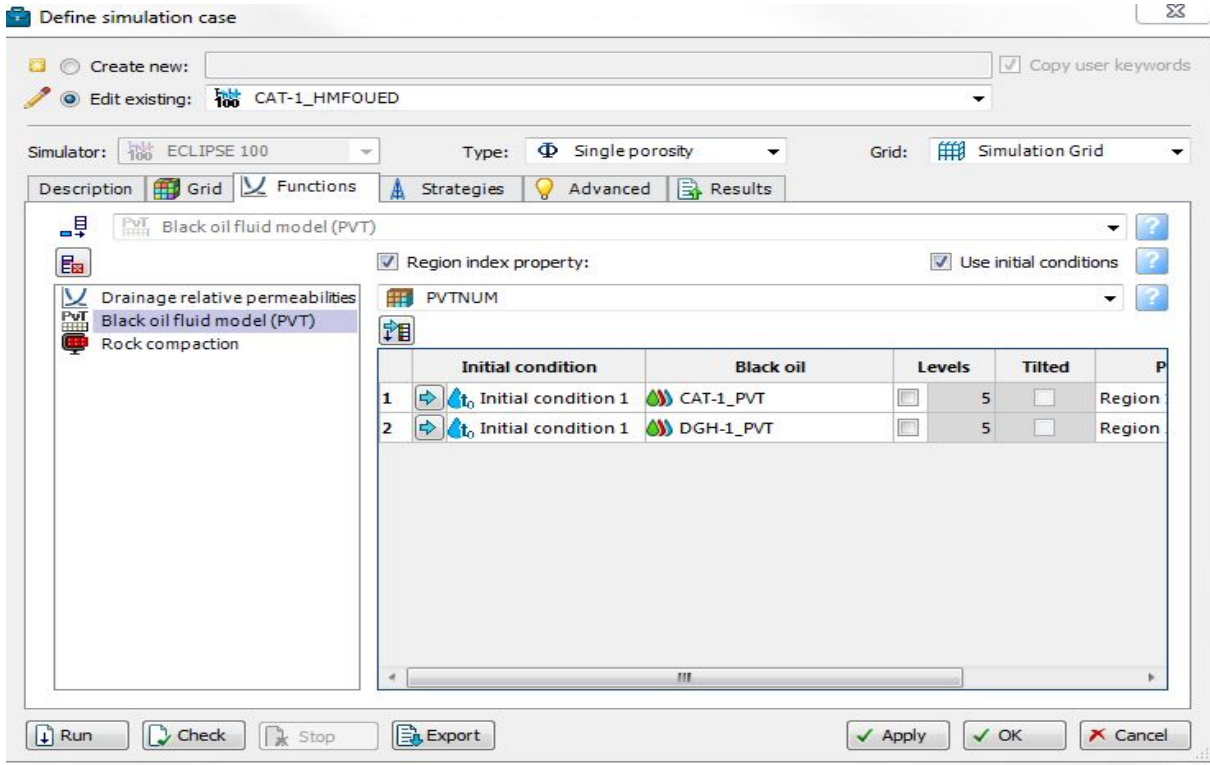


6.12- Define simulation case 1/4

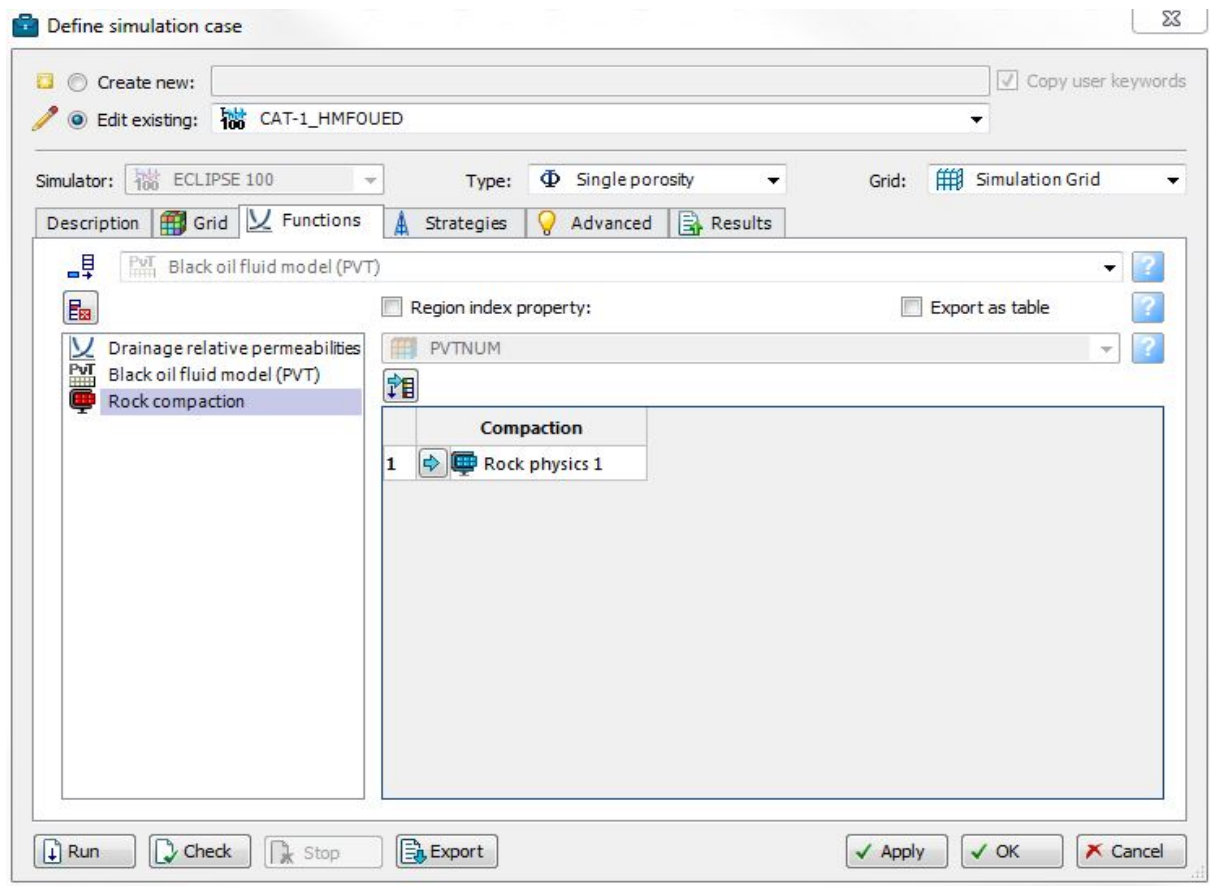
We select 'functions' in the next tab then we drop drainage relative permeabilities ,black oil fluid model (PVT) and rock compaction from the input window as shown in the three figure below.



6.13- Define simulation case 2/4



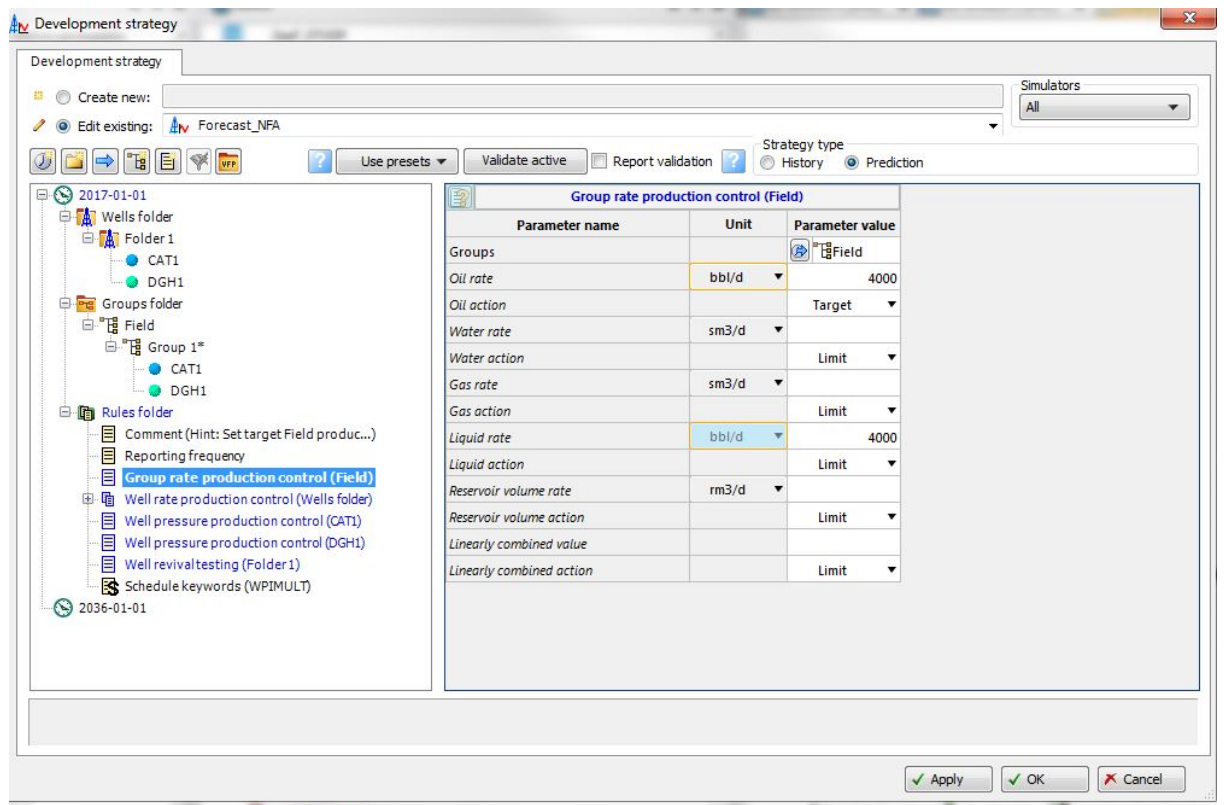
6.14- Define simulation case 3/4



6.15- Define simulation case 4/4

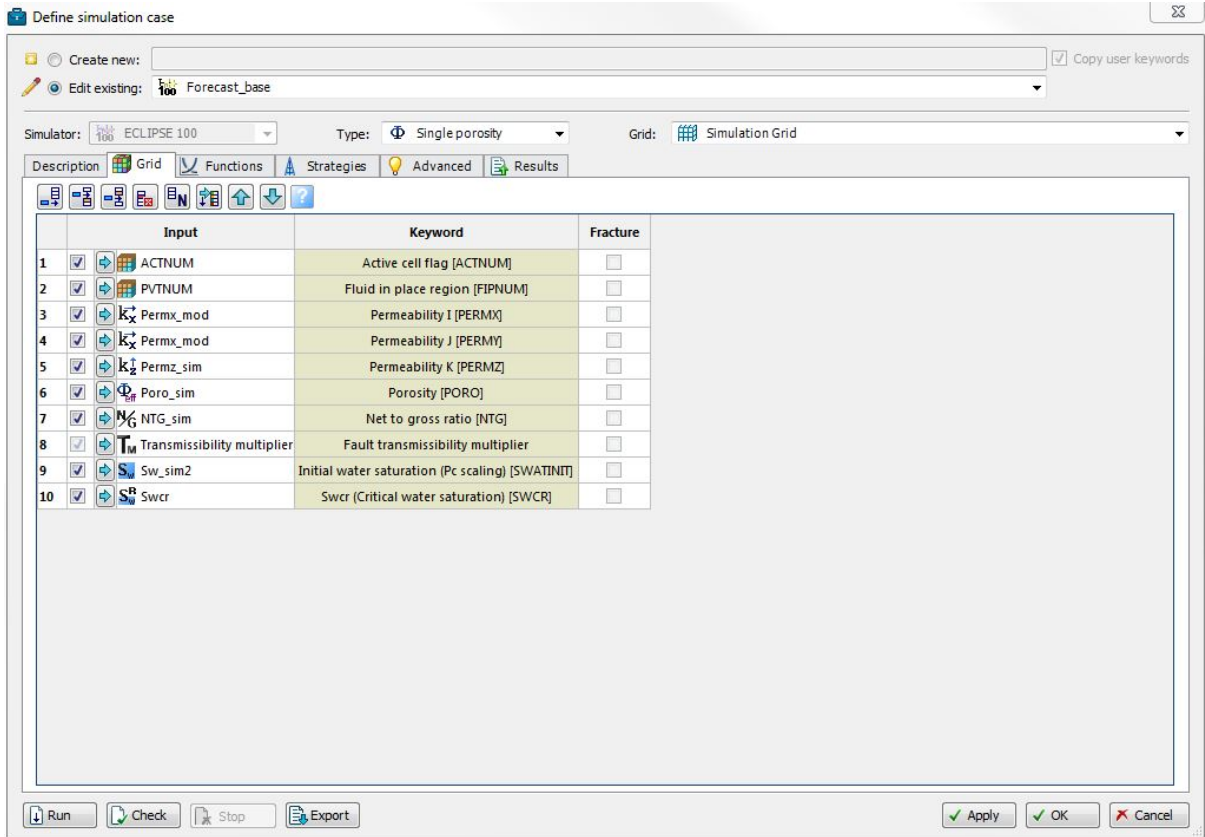
Finally, we switch to the strategies tab to drop the appropriate strategy that we already created in the development strategy.

For the base case prediction, we follow the same steps. We only check the prediction in strategy type when defining the strategy, we specify the new rules that states an oil group oil field equals to 4000 bbl/d, and head tubing pressure equals to 360 psi as shown in figure below:

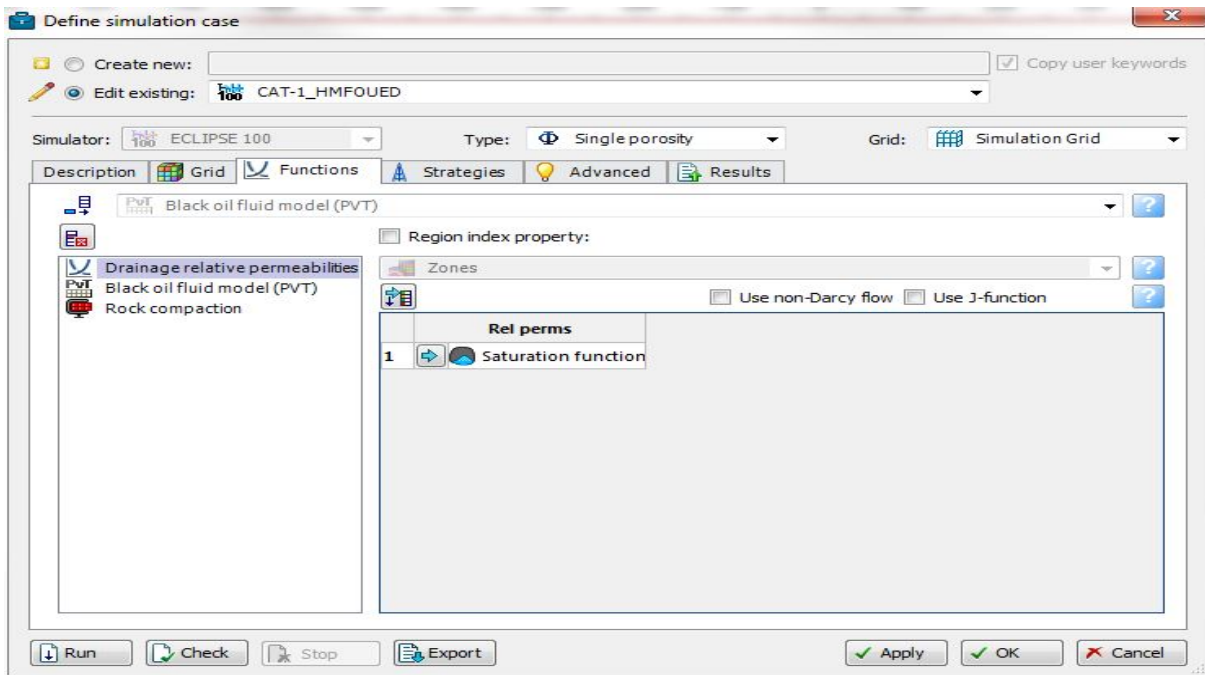


6.16- Development strategy

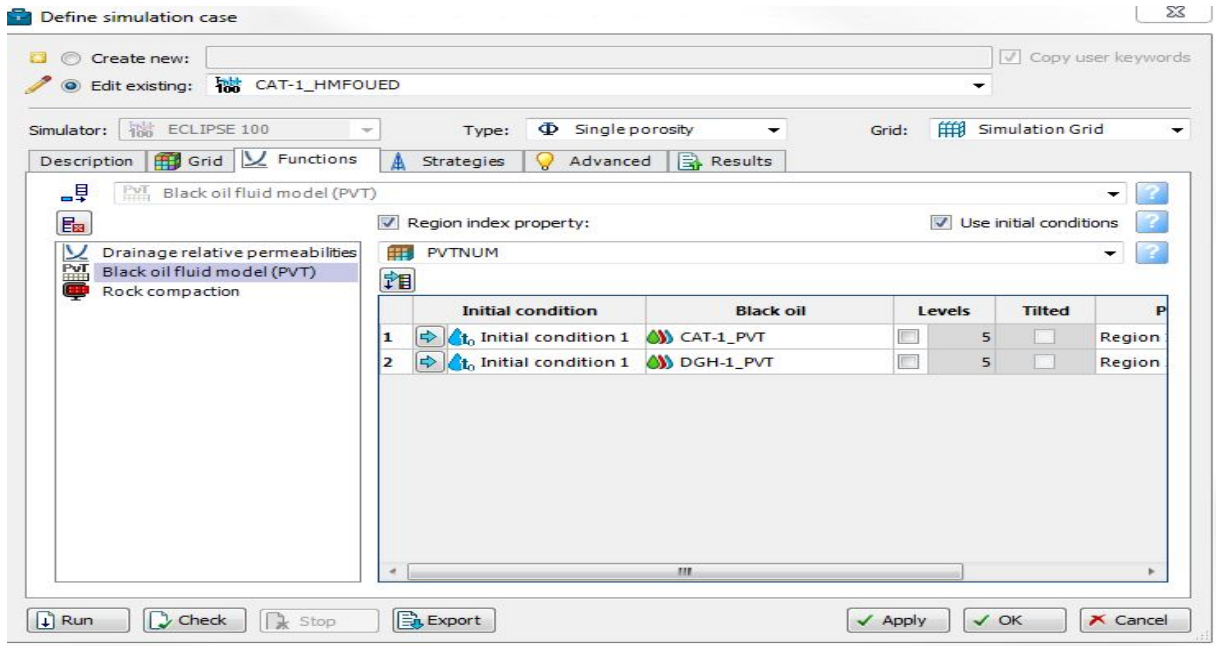
Next, to define the simulation case we enter the following properties and functions:



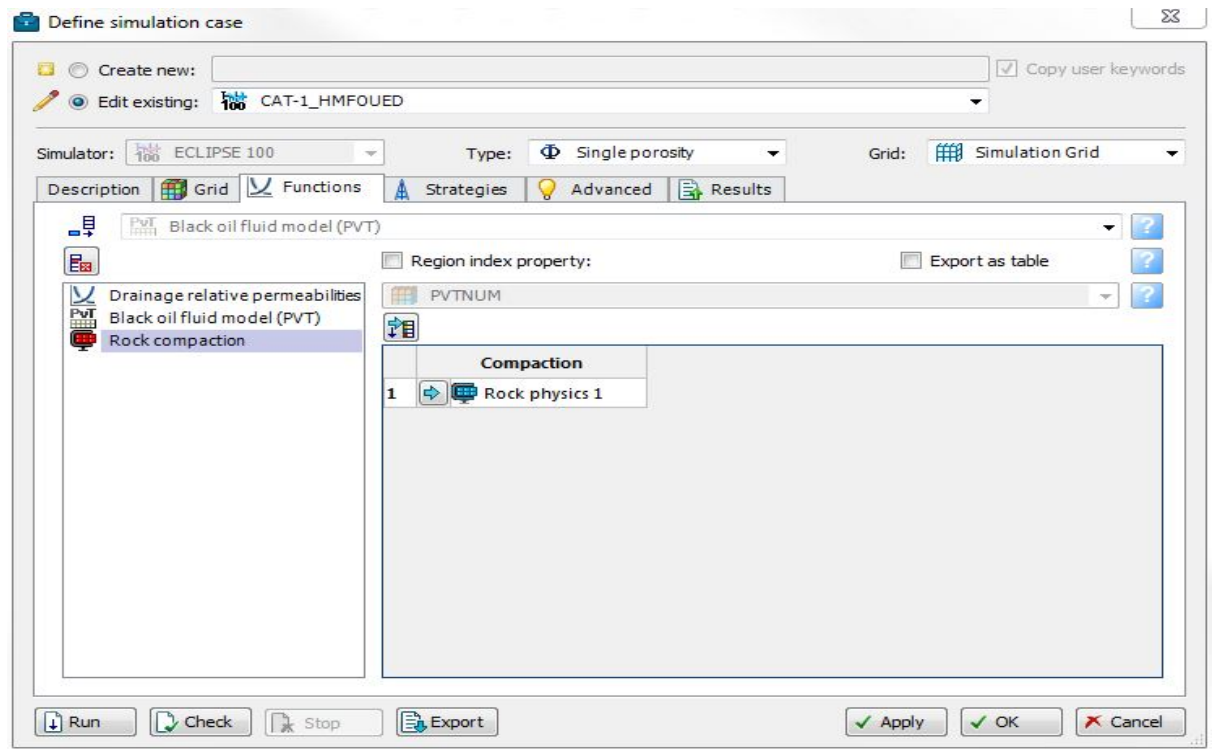
6.17- Define simulation case (forecast) 1/4



6.18- Define simulation case (forecast) 2/4



6.19- Define simulation case (forecast) 3/4



6.20- Define simulation case (forecast) 4/4